TECHNISCHE UNIVERSITÄT MÜNCHEN

Fakultät für Medizin

Lehrstuhl für klinische Chemie und Pathobiochemie
am Klinikum rechts der Isar

Consequences of CARD11(L225LI) expression in murine B lymphocytes *in vivo*

Nathalie Knies

Vollständiger Abdruck der von der Fakultät für Medizin der Technischen Universität München zur Erlangung des akademischen Grades eines Doktors der Naturwissenschaften genehmigten Dissertation.

Vorsitzender: Univ.-Prof. Dr. Christian Peschel
Prüfer der Dissertation:

1. Univ.-Prof. Dr. Jürgen Ruland
2. Univ.-Prof. Dr. Bernhard Küster

Die Dissertation wurde am 12.02.2014 bei der Technischen Universität München eingereicht und durch die Fakultät für Medizin am 07.05.2014 angenommen.

Eidesstattliche Erklärung

Ich erkläre an Eides statt, dass ich die bei der promotionsführenden Fakultät für Medizin der TUM zur Promotionsprüfung vorgelegte Arbeit mit dem Titel:

"Consequences of CARD11(L225LI) expression in murine B lymphocytes *in vivo*"

in dem Institut für klinische Chemie und Pathobiochemie unter der Anleitung und Betreuung durch Prof. Dr. Jürgen Ruland ohne sonstige Hilfe erstellt und bei der Abfassung nur die gemäß § 6 Abs. 6 und 7 Satz 2 angegebenen Hilfsmittel benutzt habe.

(x) Ich habe keine Organisation eingeschaltet, die gegen Entgelt Betreuerinnen und Betreuer für die Anfertigung von Dissertationen sucht, oder die mir obliegenden Pflichten hinsichtlich der Prüfungsleistungen für mich ganz oder teilweise erledigt.

(x) Ich habe die Dissertation in dieser oder ähnlicher Form in keinem anderen Prüfungsverfahren als Prüfungsleistung vorgelegt.

( ) Die vollständige Dissertation wurde in ..... veröffentlicht. Die promotionsführende Einrichtung..... hat der Vorveröffentlichung zugestimmt.

(x) Ich habe den angestrebten Doktorgrad **noch nicht** erworben und bin **nicht** in einem früheren Promotionsverfahren für den angestrebten Doktorgrad endgültig gescheitert.

( ) Ich habe bereits am .....bei der Fakultät für ..... der Hochschule .....unter Vorlage einer Dissertation mit dem Thema .....die Zulassung zur Promotion beantragt mit dem Ergebnis: .....

Die öffentlich zugängliche Promotionsordnung der TUM ist mir bekannt, insbesondere habe ich die Bedeutung von § 28 (Nichtigkeit der Promotion) und § 29 (Entzug des Doktorgrades) zur Kenntnis genommen. Ich bin mir der Konsequenzen einer falschen Eidesstattlichen Erklärung bewusst.

Mit der Aufnahme meiner personenbezogenen Daten in die Alumni-Datei bei der TUM bin ich

(x) einverstanden

( ) nicht einverstanden

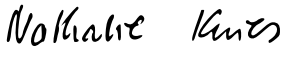

München, den Unterschrift

TABLE OF CONTENTS

1. INTRODUCTION

Our immune system is challenged with infectious microbes every day. Successful defense against these requires a coordinate and collective interaction of numerous molecules and diverse cell types. Despite the protective function of the immune system, various immunological malfunctions exist due in part to lifestyle and genetic predispositions. Those include immune responses against harmless foreign substances or defects in self-tolerance, which lead to the attack and destruction of self. Gene mutations in immune cells leading to abnormal and uncontrolled cell growth potentially cause lymphoma, which is another immunological disorder. The edge between protection of the organism against foreign pathogens and the development of immune diseases is a fine line.

In the first section, a general introduction of the immune system will be given, followed by the presentation of B lymphocyte development and antigen receptor-mediated signaling events. On this basis, different lymphoma entities and frequent mutations will be introduced. According to this background the involvement of a CARD11 mutation derived from a B cell lymphoma patient is depicted in lymphomagenesis and its molecular mechanisms will be discussed.

1.1. Immune system

The immune system operates via two branches. An early and rapid immune response is provided by the innate immune system, whereas antigen-specific long-term protection is given by the acquired immune system.
Skin and mucosal layers represent the first barrier of the innate immune system against infection by physically hindering the entry of pathogens into the organism. If these barriers are broken and the pathogen is able to invade, the second line of innate defense takes over (reviewed in (Abbas et al., 2011; Janeway, 2001)). Most bacteria that invade the body are destroyed by the complement system (Sarma and Ward, 2011). Complement proteins either lyse bacteria by forming pores in their membrane, or they

opsonize the bacteria, targeting them for phagocytic destruction within myeloid cells at the site of infection (Sarma and Ward, 2010).

Myeloid cells, such as granulocytes, macrophages, natural killer cells, mast cells and dendritic cells (DCs) are the cellular component of the innate defense. These express a repertoire of germline-encoded pattern-recognition-receptors (PRRs), which recognize evolutionary conserved pathogen-associated molecular patterns (PAMPs) (Janeway, 1989). After PRR engagement, myeloid cells initiate an inflammatory response against the pathogen by secreting chemokines and cytokines, which recruit and activate other immune cells. DCs and macrophages engulf pathogens, process them, and after migrating to secondary lymphoid organs, present parts of the pathogen to T cells, which then launch a pathogen-specific adaptive immune response (Batista and Harwood, 2009; Galli et al., 2011; Kumar et al., 2011).

The adaptive immune system protects the body against pathogens that are not eliminated by the innate immune system and provides long-term defense against re-infections termed immunological memory. The cellular mediators of adaptive immunity are T and B lymphocytes. Both arise from the common lymphoid progenitor (CLP). Before birth, hematopoiesis takes place in the fetal liver (Ottersbach et al., 2010). After birth, stem cells migrate to the thymus, where they differentiate into T cells (Rolink AG, 2006). In contrast to T cells, B cell development takes place in the bone marrow.

1.1.1. Early B cell development

In the bone marrow several B cell maturation stages exist: the pro B cell, pre B cell and the immature B cell stage (Figure 1). The immature B cell then exits the bone marrow as recirculating B cell to finish maturation in the periphery. The peripheral mature murine B cell pool is composed of two main subgroups: the mostly fetal liver-derived B-1 B cells and the bone marrow-derived B-2 B cells, whereby the latter representing the larger B cell pool including follicular (FO) B cells and marginal zone (MZ) B cells.

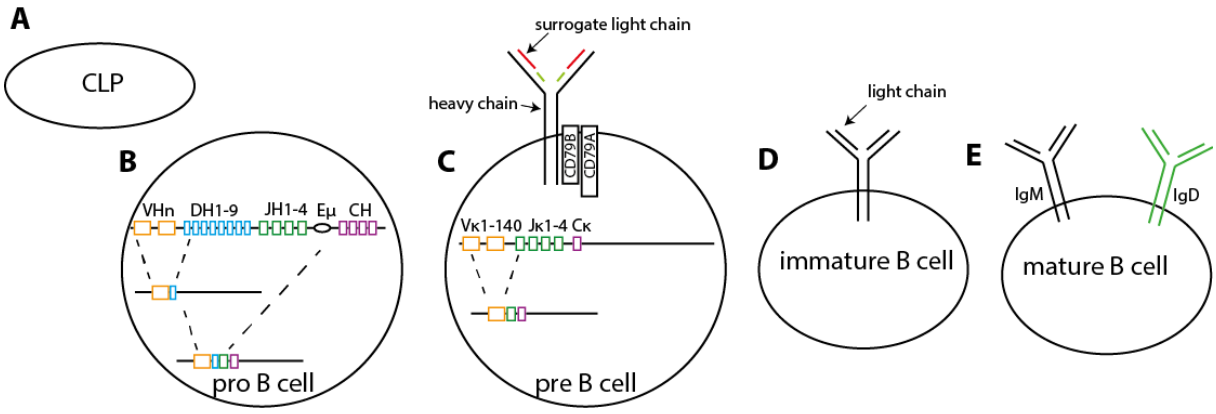

Figure 1: B cell development

A) The CLP in the bone marrow gives rise to the pro B cell. B) During the pro B cell stage the immunoglobulin (Ig) rearrangement of the heavy chain locus takes place. C) After successful rearrangement of the heavy chain, the surrogate light chain assembles to the heavy chain. Functional signaling by the pre B cell receptor (BCR) enables light chain rearrangement. D) The immature B cells expresses surface IgM. E) Recirculating immature B cells co-expressing surface-IgM and IgD are called mature B cells. Adapted from (Chaudhuri and Alt, 2004; Herzog et al., 2009).

B cell development starts with interactions between the CLP and stromal cells that secrete growth factors, most importantly stem cell factor and interleukin-7 (IL-7), which support the differentiation of the CLP into a pro B cell (Figure 1a). The subsequent steps provide the B cell with a functional BCR, which sustains its survival and enables interactions with the microenvironment. Variable-diversity-joining region (VDJ) recombination at the pro and pre B cell stage is responsible for the production of an unique BCR, composed of each two identical heavy (H) and light (L) chains, and is mediated by the enzymes recombination-activating genes 1 and 2 (RAG1 and RAG2) (Schatz and Ji, 2011). Rearrangement of the heavy chain diversity (D_H) to joining (J_H) regions in the early pro B cell is prerequisite for the rearrangement of the variable (V_H) chains to the DJ_H in the large pro B cell (Figure 1b). Successful VDJ_H joining allows the expression of the antigen receptor μ heavy chain in the pre B cell.

The VpreB and λ5 proteins pair to form the surrogate light chain and assemble with the μ heavy chain, and with CD79A and CD79B to form the pre B cell receptor, which is a major checkpoint in B cell development (Herzog et al., 2009). This step initiates the light chain rearrangement from the κ chain locus (Figure 1c). If this does not result in a functional light chain, rearrangement of the λ locus begins. Successful light chain

production allows the assembly of the light chain to the heavy chain yielding an intact B cell receptor of the immunoglobulin (Ig) M isotype (Figure 1d). These early steps in B cell development involving receptor rearrangements are important to establish receptor diversity within the mature B cell pool. It is estimated that each B cell expresses one out of 10^{15} different possible receptors, each unique and specific for one antigen.

The expression of only one antigen receptor with one specificity per B cell is ensured by the mechanism of allelic exclusion, where the receptor gene is expressed from solely one allele, as there are two IgH and some IgL loci (Herzog et al., 2009). An immature B cell whose surface IgM strongly binds to self-antigen is subjected to negative selection, either by receptor editing or by apoptosis. This avoids the maintenance of self-reactive cells. Immature B cells, also called transitional B cells, leave the bone marrow to recirculate. The first entry into peripheral follicles such as lymph nodes, spleen and gut-associated lymphoid tissues (GALT) induces the expression of surface IgD (Chen and Cerutti, 2010) (Figure 1e), so that the mature B cells expresses simultaneously IgM and IgD. The strength of the BCR signal determines whether mature B-2 B cells differentiate into either FO B cells or into MZ B cells.

1.1.2. Mature B cell subsets

The murine mature B cell pool can be divided in three B cell subsets in terms of their development and their role in immune responses: FO B cells, MZ B cells and B1-B cells. FO B cells represent the major fraction of the mature B cell pool; they recirculate between B cell follicles and mediate T cell-dependent (TD) immunity. In contrast to FO B cells MZ B cells reside between the marginal sinus and the red pulp of the spleen and are therefore part of the first line of defense for blood-borne T-independent (TI) bacterial antigens (Pillai and Cariappa, 2009).

1.1.2.1. MZ B cells

MZ B cells are permanently localized next to the marginal sinus in the spleen, which enables them to rapidly respond to blood-borne TI antigens (Pillai and Cariappa, 2009). TI antigens are antigens that induce plasma cell differentiation without the aid of helper

T cells. These antigens include polysaccharides, nucleic acids and membrane glycolipids, which efficiently cross-link the BCR on account of their repetitive structure (Abbas et al., 2011). These preferably activate innate-like B cells, such as MZ B cells, which express low-affinity BCRs and recognize mostly microbial determinants. Despite their role in TI immunity MZ B cells are able to support T-dependent humoral responses by transport and deposit of IgM-containing complexes to FDCs with their surface receptor CD21, which load the antigen and present it to T cells (Ferguson, 2004).

1.1.2.2. B-1 B cells

B-1 B cells represent the third category of peripheral mature B cells. They are generated earlier than B-2 B cells, and originate mostly from progenitors in the fetal liver and just to a small extent from bone marrow stem cells (Herzenberg, 2000). B-1 B cells are the main B cell population within the peritoneal cavity and populate to a lesser degree spleen and bone marrow. While B-2 B cells are continuously generated from the bone marrow during lifetime, de novo synthesis of B-1 B cells is restricted once the cell pool is established (Lalor et al., 1989). B-1 B cells produce IL-10 to activate a positive autocrine regulatory loop for their long-term maintenance (Gary-Gouy, 2002; O'garra et al., 1992). Dead cells are replaced by cell division so that the existing B-1 B cell pool is maintained.

B-1 B cells, which are IgM^{high}, $CD19^{high}$, $CD43^{pos}$, $CD23^{neg}$, and IgD^{low}, can be further distinguished by their CD5 expression (Baumgarth, 2011; Hayakawa et al., 1983). CD5-negative B-1b B cells were shown to provide a long-term protection against different bacterial infections and CD5-expressing B-1a B cells are the main source of natural IgM (Haas et al., 2005; Alugupalli et al., 2004). Natural IgM opsonizes pathogens and activates the complement system (Grönwall et al., 2012). All immunoglobulins derived from B-1 B cells are very similar to germline-state antibodies, as they do not undergo somatic hypermutation, and because the enzyme terminal deoxynucleotidyltransferase (TdT) is absent from these cells, nontemplated N-insertions do not occur (Li et al., 1993; Rothstein, 2002).

Despite the fact that B-1 B cells produce huge amounts of natural IgM after TI encounter, they do not undergo the germinal center reaction or somatic hypermutation (Caroll and Prodeus, 1998) (see 1.1.3.). Also class switch recombination is restricted in B-1 B cells.

While the class switch to IgA is functional, the IgG1 and IgG2a class switch recombination in B-1 B cells is defective *in vitro* (Tarlinton et al., 1995; Kaminski and Stavnezer, 2006). Besides their role as main producer of natural IgM, B-1 B cells also produce about 50% of the IgA levels found in organisms (Macpherson et al., 2008). In comparison to natural IgM, IgA eradicates toxins and pathogens without inflammation as it is not able to activate the complement system (Cerutti, 2008). Therefore B-1 B cells play a crucial role in the early immune response and should be considered as innate-like B cells.

1.1.3. The germinal center reaction

The life-long aim of a mature B cell is to encounter its cognate antigen. Therefore, the mature but naïve, antigen un-experienced, FO B cell circulates between the peripheral lymphoid organs searching the specific antigen for its surface receptor. Once the FO B cell encounters the matching antigen, the antigen bound to the BCR is internalized and processed by endosomes. The resulting peptides are loaded on the major histocompatibility complex II (MHCII). B cells, macrophages and DCs are able to present antigen this way to T cells, though macrophages and DCs employ alternative mechanisms for antigen internalization (Neefjes et al., 2011). Upon recognition of MHCII-presented antigen by the T cells receptor (TCR), T cells become activated. Similar to what occurs in B cell development, rearrangement of the TCR locus to generate an antigen-specific receptor also occurs during early thymic development of T cells. In contrast to the BCR, the TCR is not able to recognize intact or native antigens, but rather recognizes processed antigen within the context of MHC molecules.

In the follicular T cell zone the antigen-primed T cell is poised to encounter B cells presenting the matching peptide for its TCR. In this event, small extrafollicular B cell foci are formed in the T cell zone, where plasma cells secrete low affinity antibodies or differentiate to early memory B cells (MacLennan et al., 2003). Within this area, B cells are activated by a number of surface molecules on follicular helper T (T_{FH}) cells, as well as by IL-21-secreted by T_{FH} cells. The co-stimulation via CD40/CD40L and TCR-peptide-MHCII interaction are indispensable, but also engagement by the CD28 family members Inducible costimulator (ICOS), programmed cell death-1 (PD-1) and the C-X-C chemokine receptor CXCR5 are important for full interaction and hence activation

(Nutt and Tarlinton, 2011). One or few antigen-specific B cells massively proliferate forming a structure called dark zone in the germinal center (GC). These B cells are called centroblasts. Once centroblasts finish to proliferate, they are called centrocytes.

1.1.3.1. Germinal center B cells

The term germinal center B cells (GCBs) includes FO B cells entering the GC reaction, as well as massively proliferating centroblasts and centrocytes. GCBs are antigen- and T cell-activated B cells, which change their cellular program with the final aim to produce high affinity antibodies. They are characterized by expression of peanut agglutinin (PNA), CD95 (also called Fas), Gl-7 and B220 (Goetz and Baldwin, 2008).

The first steps in the transition from a naïve B cell to a GCB include the down-regulation of proliferation-inhibitory proteins, tumor and growth suppressors. Early response genes responsible for transition from G1 to S phase are up-regulated, and the cell changes from an anti-apoptotic state towards a pro-apoptotic state (Klein et al., 2003). This is mainly controlled by the transcriptional repressor B cell lymphoma 6 (Bcl-6), which down-regulates the anti-apoptotic protein Bcl-2 (Saito et al., 2009; Kondo and Yoshino, 2007) and p53 (Phan and Dalla-Favera, 2004). Bcl-6-mediated down-regulation of p53 leads to the proliferative status of GCBs (Phan and Dalla-Favera, 2004). Bcl-6 efficiently blocks the DNA damage sensors ataxia-telangiectasia-related (ATR) and checkpoint kinase 1 (CHEK1) resulting in a state of DNA damage tolerance (Ranuncolo et al., 2007; 2008). Another important target gene of Bcl-6 is the transcriptional repressor PR domain zinc finger protein 1 (*Prdm1)*, which encodes for B-lymphocyte-induced maturation protein 1 (Blimp-1). Inhibition of *Prdm1* gene expression by Bcl-6 blocks terminal differentiation into a plasma cell (Shaffer et al., 2000). The exact mechanism by which differentiation into a plasma cell or memory B cell occur are still under extensive investigation (Zotos and Tarlinton, 2012).

1.1.3.2. Biological mechanisms within the germinal center

Main events of TD antibody responses occur during the GC reaction: Heavy chain class switch, somatic hypermutation and the generation of memory B cells.

During the GC reaction centrocytes are able to switch their Ig isotype, which provides plasticity in the humoral immune response. Isotypes differ in their effector function and are defined by the nature of the pathogen/antigen (Xu et al., 2012) and by cytokines secreted from T cells. For example, in mice interferon-γ (IFN-γ) secretion mediates IgG2a class switch recombination, whereas interleukin-4 (IL-4) promotes IgG1 and IgE class switch recombination (Abbas et al., 2011).

Another process during the GC reaction is called somatic hypermutation resulting in antibody diversity. Receptor diversity raises the likelihood to have a specific antibody for the efficient eradication of any intruder and is therefore crucial for efficient immune responses. This diversity is achieved by the enzyme activation-induced-deaminase (AID), which indirectly leads to double strand breaks within the switch regions so that the rearranged VDJ segment recombines with another downstream constant region. In the next step the variable region of the BCR is somatically mutated, leading to BCR diversification. AID deaminates cytosines in the variable region to generate uracils (U), which lead to either uracil:guanine (U:G) mismatches, or to the removal of the U residues by the enzyme uracil N-glycosylase. The U:G mismatch is recognized and excised by mismatch repair mechanism and filled-up by the error-prone Polymerases Polη and Polκ (Chahwan et al., 2012; Peled et al., 2008). Mutations in the BCR accumulate in the complementary determining regions within the variable region, which is important for antigen binding ability.

After class switch and somatic hypermutation, centrocytes migrate to the less dense light zone and test the affinity of their receptor with the help of antigen-presenting follicular dendritic cells (FDC) and T_{FH} cells (Victora and Nussenzweig, 2012). Cells with low-affinity receptor are negatively selected by CD95 ligation and undergo apoptosis. The generation of high-affinity B cells, which exit the germinal center either as memory B cell or plasma cell, is called affinity maturation (Vinuesa et al., 2009).

Memory B cells are post-GC B cells, which survive for long periods without antigenic stimulation. They are able to rapidly respond to known antigens as they express a high-affinity BCR and are indispensable for immunological memory (Abbas et al., 2011).

1.1.4. Terminal differentiation into a plasma cell

Post-GCBs differentiate either into memory B cells, which feature the long-term memory to a pathogen, or into a plasma cell, which mount the humoral immune response. The terminal differentiation into a plasma cell is tightly regulated by the action of several transcription factors.

T_{FH}-mediated CD40 receptor ligation blocks the action of Bcl-6 in GCBs and leads subsequently to NF-κB activation. NF-κB regulates the expression of Interferon regulatory factor 4 (IRF4), which suppresses *Bcl-6* in a regulatory loop (Saito et al., 2007). IRF4 activation and Bcl-6 down-regulation initiate the differentiation into a plasma cell by *Prdm1* gene induction (Angelin-Duclos et al., 2000).

Blimp-1, which is encoded by *Prdm1,* is the master regulator of plasmacytic differentiation. It represses the transcription factors paired box 5 (Pax5) and Bcl-6, which are indispensable for GC formation (Shaffer et al., 2002; Lin et al., 2002). This crucial step prevents the plasma cell to return to an earlier developmental stage. At the same time, mature B cell-specific surface molecules such as CD19, B220, MHCII, CD79 and surface Ig (Oracki et al., 2010) are down-regulated and the IgH, IgL and J chain genes, which are the modules for antibody production, are expressed (Shapiro-Shelef and Calame, 2005).

The transcription factor X-box binding protein 1 (Xbp-1) which is negatively regulated by Pax5, is the main driver for cellular changes in plasma cells, including expansion of the endoplasmatic reticulum (ER), increase in cell size, rise in total protein synthesis and the secretory phenotype. Xbp-1 induces the unfolded-protein response (UPR), which increases protein folding and translocation by the ER. This can lead to ER stress and thereby a decrease in protein synthesis and apoptosis. Therefore it was suggested that plasma cells utilize a physiological UPR that antagonizes decreased protein synthesis

(Shaffer et al., 2004). Further, Blimp-1 inhibits CXCR5 expression, thereby frees B cells from retention in the B cell follicle, and simultaneously induces CXCR4 expression, which mediates homing to bone marrow niches by sensing CXCL12 secreted by stromal cells (Sciammas and Davis, 2004).

A number of factors control plasma cell survival in the bone marrow. These include CXCR4 signaling, IL-6, IL-5, tumor necrosis factor α (TNFα), ligation of the cell adhesion molecule CD44, and also B cell-activating factor (BAFF), which stimulates the plasma cell-specific B cell-maturating antigen (Shapiro-Shelef and Calame, 2005). Syndecan-1, also called CD138 is commonly used as murine and human plasma cell marker (Sanderson et al., 1989). The survival for antibody-secreting plasma cells cultured *ex vivo* is limited to a few days, whereas long-lived plasma cells are able to survive for more than one year in the bone marrow (Slifka et al., 1998).

All essential steps in B cell development and main biological functions of B cells rely on the BCR. Within the early B cell development correct production and assembly of the BCR is prerequisite for B cell survival and the exit from the bone marrow into the periphery. In the periphery, the B cell function is determined by the signal strength (MZ versus FO B cells). Upon antigen encounter the Ig effector class and somatic hypermutation of the BCR constitute the efficiency of the humoral immune response, which is mediated by plasma cells that secrete their antigen receptor.

1.2. The BCR

1.2.1. Structure of the BCR

Surface BCR expression and its ability to bind antigens are prerequisite for B cell functioning. The BCR translates receptor activation after antigen binding to intracellular signaling events. These intracellular signals determine whether a B cell differentiates, proliferates or undergoes apoptosis.

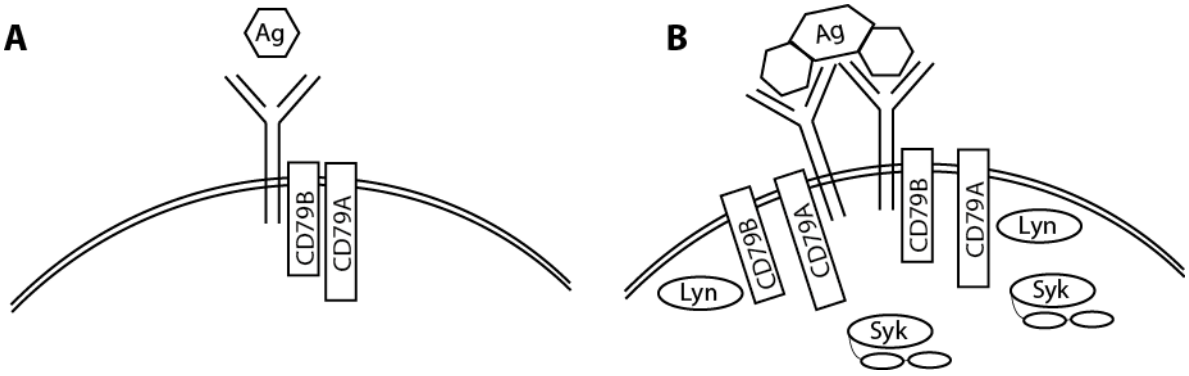

Figure 2: Structure of the BCR
A) The BCR is a membrane bound Ig, which is non-covalently bound to the CD79 heterodimer. B) Antigen-mediated crosslinking of the BCR results in receptor oligomerization and accessibility of the CD79 ITAM motifs to the receptor proximal kinases LYN and SYK due to an open conformation (Tolar et al., 2005).

The two membrane-bound heavy chains and the two light chains of the BCR are typically organized in Y shape. Upon antigen binding BCRs oligomerize and start signal transduction. Interestingly, the BCR heavy chains are not able to transduce extracellular signals to the cytoplasm due to their short cytosolic tails. Therefore the BCR assembles non-covalently with the CD79 heterodimer, consisting of CD79A and CD79B, to form the BCR complex (Figure 2a). Both of these proteins have immunoreceptor tyrosine-based activation motifs (ITAM), which consist of a conserved four amino acid sequence YxxL/I that typically repeats after six to eight amino acids (Hombach et al., 1988; Schamel and Reth, 2000). This ITAM motif couples the BCR and intracellular tyrosine kinases and is hence indispensable for all subsequent BCR signaling events.

1.2.2. BCR signaling

The expression of a functional BCR is essential for B cell development and survival in the periphery (Kitamura et al., 1991; Srinivasan et al., 2009). Engagement of the BCR initiates a multistep cascade: Adapter molecules and proteins with enzymatic activities coordinate signal transduction from BCR proximal regions to further distal areas and eventually to the nucleus. Protein modifications such as the addition of phospho-residues (phosphorylations) or ubiquitin chains result either in activation or degradation of targeted molecules (de-/ubiquitinations) and by this regulate protein activation, inhibition and turn-over.

1.2.2.1. Proximal BCR signaling

Antigen binding to the BCR leads to conformational changes, which provide accessibility of the ITAM motifs of the CD79 heterodimer to kinases. The tyrosines within the ITAM motifs are initially mainly phosphorylated by the src family kinase LYN (Gauld and Cambier, 2004). This phosphorylation builds a docking unit for the spleen tyrosine kinase (SYK) which is present in a closed conformation in resting B cells (Figure 2b) (Pao et al., 1998).

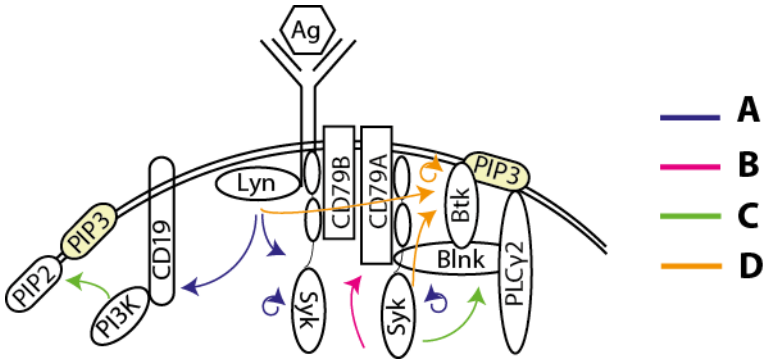

Figure 3: Proximal BCR signaling
Upon BCR engagement proximal BCR signaling is initiated. A) The addition of phospho-residues to the CD79 heterodimer builds a docking site for the tyrosine kinase SYK. B - D) Active SYK phosphorylates diverse target molecules: itself, CD79A, CD19, BLNK and BTK.

SYK is one of the most important receptor-proximal BCR kinases as it regulates many signaling pathways, and therefore needs to be tightly regulated (Koyasu, 2003; Turner

et al., 1995). An interaction between two tyrosines within the src homology (SH) 2-kinase linker region and the kinase domain leads to a closed conformation and auto-inhibition (Grädler et al., 2013). SYK-binding to the phosphorylated ITAM motif of CD79 proteins abolishes the connection between the two regions. Full activation is gained by LYN-mediated phosphorylation and auto-phosphorylation of SYK (Figure 3a) (Rowley et al., 1995), which subsequently leads to SYK-mediated phosphorylation of CD79A at the non-ITAM-tyrosine 204 (Figure 3b). B cell linker protein (BLNK) is recruited to the phospho-tyrosine in CD79A and binds to SYK (Engels et al., 2001). SYK phosphorylates BLNK and generates binding sites for Bruton's tyrosine kinase (BTK) and phospholipase Cγ2 (PLCγ2) (Figure 3c) (Fu et al., 1998). Additionally, BTK is recruited to the cell membrane, where it is phosphorylated by LYN (Rawlings et al., 1996) and SYK (Kurosaki and Kurosaki, 1997) and subsequently auto-phosphorylated (Figure 3d). These BCR proximal signaling events are essential for further downstream activation of pathways regulating fate decision of the activated B cell.

1.2.2.2. Distal BCR signaling

PI3K/AKT signaling

Constitutive basal BCR signaling, also called tonic BCR signaling, strictly depends on PI3K signaling, which is able to rescue BCR-ablated B cells from cell death (Srinivasan et al., 2009).

The initiating event for the activation of the PI3K/AKT signaling pathway is the phosphorylation of CD19 by LYN. This generates binding sites for phosphoinositide-3-kinase (PI3K) and leads to its activation (Fujimoto et al., 2000) (Figure 3a). PI3K produces phosphatidylinositol 3,4,5-triphosphate (PIP_3) by phosphorylation of phosphatidylinositol 4,5-bisphosphate (PIP_2) (Koyasu, 2003), which is a second messenger and docking unit for pleckstrin homology (PH) domain-containing proteins such as phosphoinositide-dependent protein kinase 1 (PDK-1), AKT, PLCγ2 and BTK (Figure 3d) (Salim et al., 1996). PDK-1 is recruited to the cell membrane by binding of its PH domain to PIP_3 and phosphorylates AKT (Figure 4a) (Anderson et al., 1998). Activated AKT phosphorylates forkhead box protein O (FOXO) molecules leading to their degradation, which promotes B cell growth, survival and

proliferation (Figure 4b) (Toker and Newton, 2000; Brunet et al., 1999; Burgering and Kops, 2002).

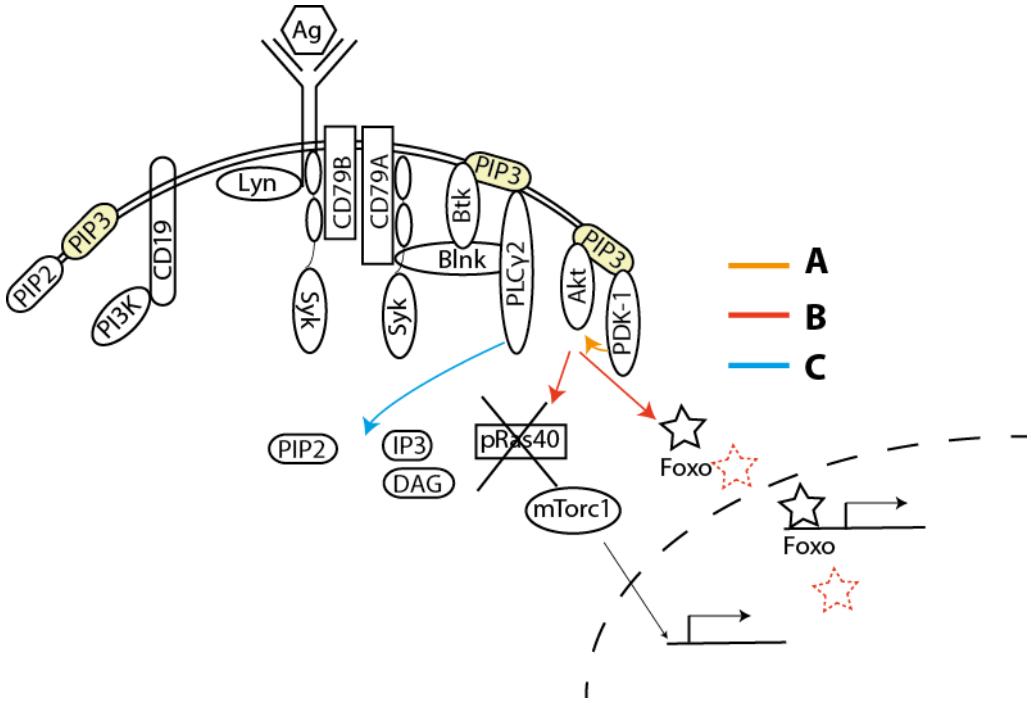

Figure 4: PI3K/AKT signaling
The PI3K/AKT signaling pathway is required for B cell survival. It is initiated with the phosphorylation of CD19, which further leads to activation of PI3K. The key molecule in PI3K signaling is the second messenger PIP_3. PI3K regulates A) AKT and via AKT the B) mTOR and FOXO pathway. C) Simultaneously it promotes Calcium mobilization by activating PLCγ2.

Another substrate of AKT is the negative regulator of the mammalian target of rapamycin 1 (mTORC1) complex proline-rich AKT substrate 40 kDa (PRAS40) (Sancak et al., 2007). PRAS40 dissociates from the mTORC1 complex after AKT-mediated phosphorylation and leads to mTORC1 activation (Newton, 1997; Fruman, 2012), which is essential for B cell metabolism and proliferation (Figure 4b).

Calcium signaling

Another effector arm of the PI3K pathway is the activation of PLCγ2, which initiates calcium (Ca^{2+}) mobilization and by this B cell proliferation. This is achieved upon membrane recruitment and activation of BTK, which directly phosphorylates PLCγ2

(Takata and Kurosaki, 1996). PLCγ2, which is also recruited to PIP_3 hydrolyses PIP_2 into the second messengers IP_3 and diacylglycerol (DAG) (Figure 4c) (Newton, 1997).

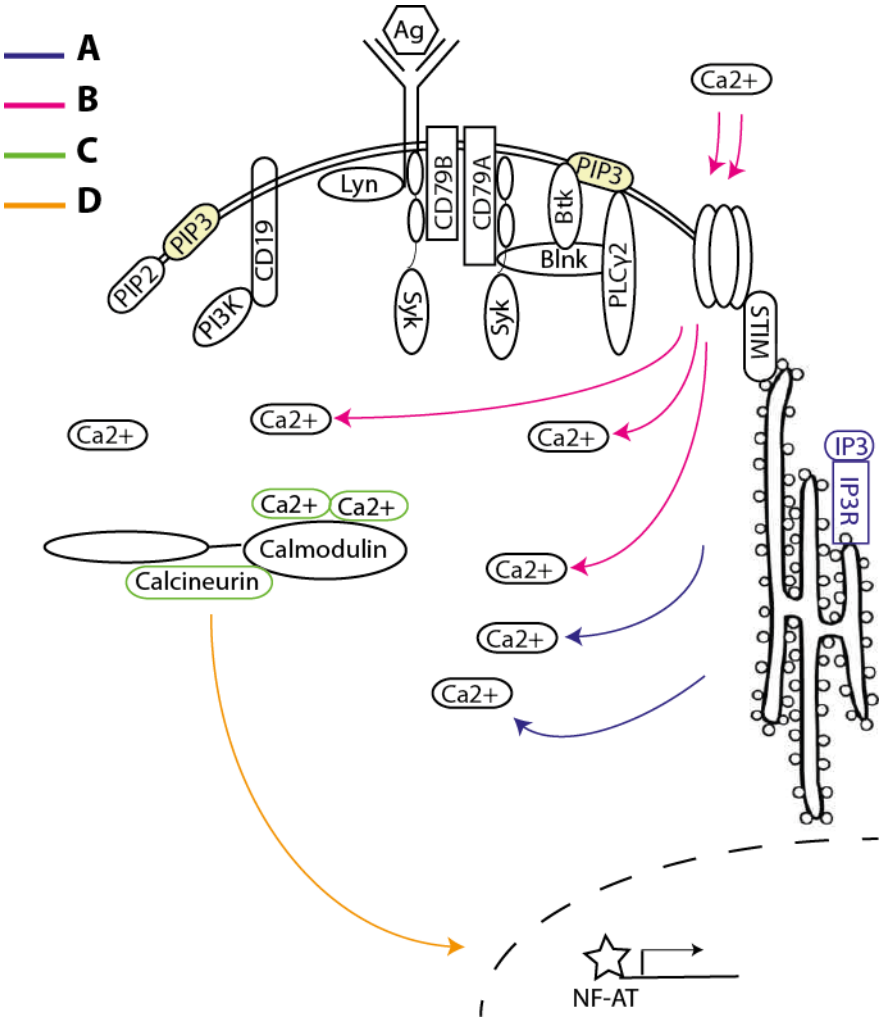

Figure 5: Calcium signaling
A) –D) show calcium influx after BCR engagement, and calcium-dependent activation of the transcription factor NF-AT (star) within the nucleus (dashed line).

The second messenger IP_3 is the key activator of Ca^{2+} signaling in B cells, which is essential for B cell function and development (Scharenberg et al., 2007). IP_3 binds to IP_3 receptors on the ER leading to Ca^{2+} release (Figure 5a). This binding enables the interaction between stromal interaction molecule (STIM) located in the membrane of the ER, and the calcium release activated channel (CRAC) (Figure 5b), which results in entry of extracellular Ca^{2+} (Roos, 2005; Vig et al., 2006). Calmodulin (CaM) binds free cytosolic Ca^{2+}, which leads to its activation due to conformational changes (Figure 5c). Interaction with CaM activates the phosphatase calcineurin, and subsequently de-phosphorylates the transcription factor nuclear factor of activated T-cells (NF-AT).

Dephosphorylated NF-AT translocates to the nucleus and induces expression of genes regulating B cell homeostasis (Figure 5d) (Hogan et al., 2003; Scharenberg et al., 2007).

ERK signaling

PLCγ2 also produces the second messenger DAG, which leads to the activation of ERK and NF-κB signaling. DAG binds to the C1 domain of protein kinase C (PKC) β, allowing PKCβ to activate RAS guanyl releasing protein (RasGRP). RasGRP catalyzes conversion of GDP-bound Ras to the active GTP-bound form by nucleotide exchange (Figure 6a), which is essential for RAF activation (Figure 6b) (Roose et al., 2005; Aiba et al., 2004). RAF phosphorylates mitogen-activated extracellular signal-regulated kinase (MEK) 1 and 2, which activate ERK1/2 leading to phosphorylation and translocation of the ETS domain-containing protein (ELK-1) transcription factor and activator protein 1 (AP-1) activating genes involved in cell cycle progression (Figure 6c) (Yasuda et al., 2008; Kurosaki, 1999; 2011; Dal Porto et al., 2004).

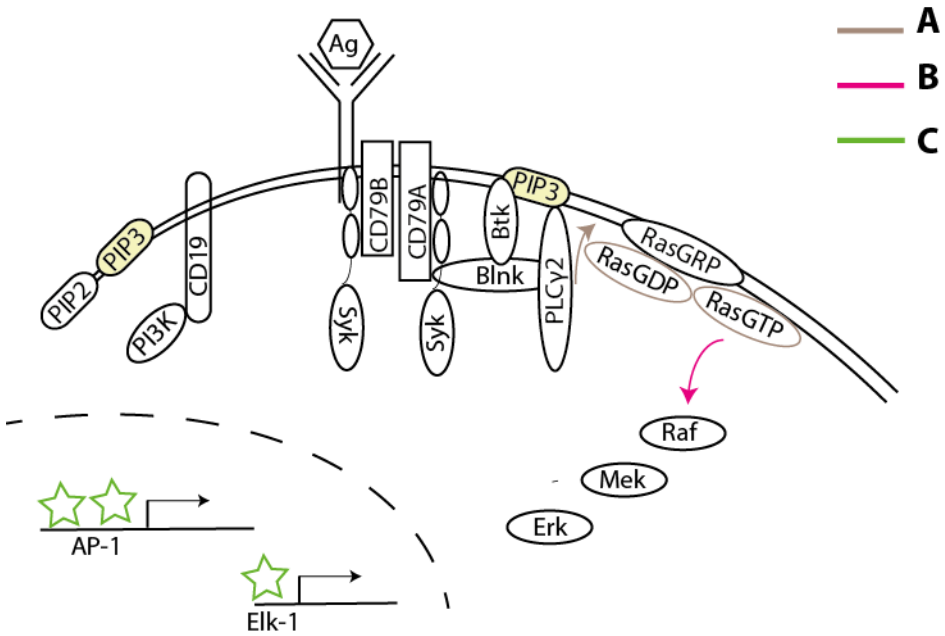

Figure 6: ERK signaling

A) PLCγ2 activates RasGRP, which provides GTP for the activation of the B) ERK signaling cascade. This pathway results in the translocation of the transcription factors AP-1 and ELK-1.

1.2.3. NF-κB signaling

The NF-κB pathway is activated by a plethora of signals. Strong inducers are antigen receptors such as the BCR, TNFα, IL-1 and signals via PRRs such as the toll-like receptors (TLRs). Cellular stress mediated by hypoxia or DNA damage also effectively activate this pathway (Perkins, 2012). The NF-κB pathway is divided in two branches: the canonical also known as the classical NF-κB, and the non-canonical or alternative pathway. Signaling through the BCR, IL-1 receptor, TLRs or TNFα receptor lead to the activation of the classical pathway. The alternative pathway can be activated by engagement of lymphotoxin-β receptor, receptor activator of NF-κB (RANK), CD40 or the BAFF receptor (Siebenlist et al., 2005).

In B cells, NF-κB signaling regulates important aspects of cell biology by controlling the expression of pro-survival genes, the secretion of cytokines, the regulation of activation markers and ensures B cell function and differentiation.

1.2.3.1. NF-κB subunits and their regulators

The NF-κB transcription factor family has five members: RelA (p65), RelB, cRel, NF-κB1 (p50) and NF-κB2 (p52) (Figure 7) (Verma et al., 1995). All possess a conserved Rel-homology-domain (RHD), which contains the DNA-binding, dimerization and the nuclear-translocation domain. The Rel proteins (RelA, RelB, cRel) enhance target gene expression via their C-terminal transactivation domain (TAD). The other two Rel proteins (p50, p52) have to be processed from their precursor molecules p105 and p100, respectively, before nuclear translocation (Ghosh et al., 1998). This happens via proteolytical removal of the ankyrin repeat motif, which abolishes the interaction with their inhibitory molecules. In absence of stimulus, the NF-κB proteins are inhibited and retained in the cytosol by molecules known as inhibitors of NF-κB (IκBs). Those also contain ankyrin repeats, which bind the ankyrin repeats in the Rel molecules. IκB-bound, inactivated NF-κB proteins shuttle from the cytosol to the nucleus and back directed by the nuclear-localization signal and the nuclear-export signal (Hayden and Ghosh, 2012).

There are different IκBs: IκBα, IκBβ, IκBε, IκBNS, IκBζ and Bcl-3 (Figure 7) (Ghosh and Hayden, 2008). IκBNS, IκBζ and Bcl-3 have an exceptional role as atypical IκB molecules. Bcl-3 for example contains a TAD and is located in the nucleus. There it binds to p50 and p52 homodimers and, dependent on the post-translational modification, it activates or inhibits NF-κB target gene transcription. IκBζ lacks a TAD, but is nonetheless able to activate gene transcription when bound to p50 homodimers (Motoyama, 2004).

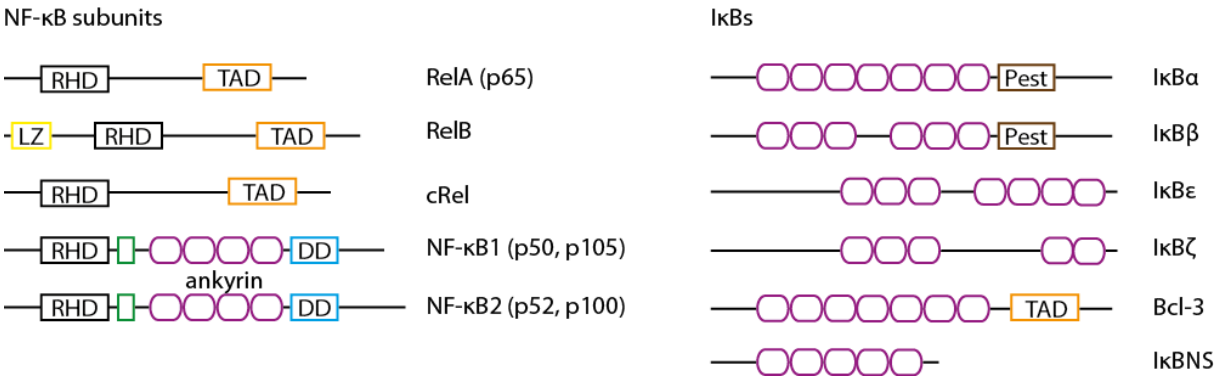

Figure 7: NF-κB subunits and regulators
RHD = Rel-homology domain; TAD = transactivation domain; LZ = leucine zipper; DD = death domain; PEST = Proline- (P), glutamic acid (E), serine (S), and threonine (T) rich domain. Figure adapted from (Ghosh and Hayden, 2008).

The IκB kinase (IKK) complex regulates the dissociation of NF-κB from the IκB molecules. Three subunits of the IKK complex have been identified: The regulatory subunit NF-κB essential modulator (NEMO), which facilitates protein interactions and lacks intrinsic catalytic activity and the two kinases IKKα and IKKβ, which phosphorylate the proto-typical IκB molecules and hence release the NF-κB factors to the nucleus (Li and Verma, 2002; Henkel et al., 1993).

NF-kB is able to negatively regulate itself, as IκBα is a target gene of NF-kB and is resynthesized when NF-kB is transcriptional active. Newly synthesized IκBα enters the nucleus and dissociates bound NF-κB dimers from the DNA-κB sites within promoters and enhancers of target genes, yielding in a negative feedback loop that shuts down NF-κB signaling.

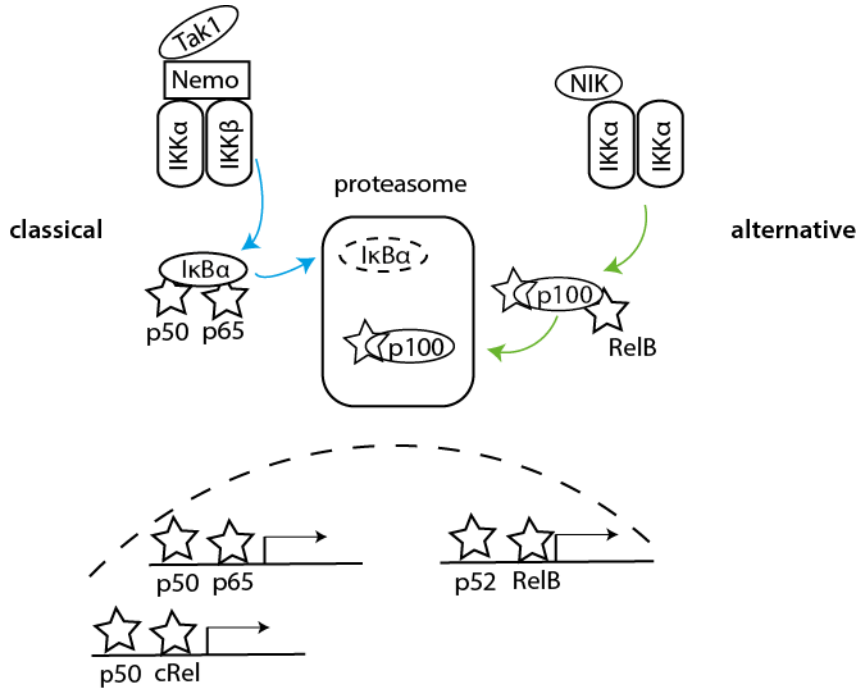

Figure 8: The canonical and alternative NF-κB pathway
Canonical pathway: The IKK complex consisting of NEMO, IKKα and IKKβ phosphorylates IκBα and marks it for proteasomal degradation causing the release of NF-κB dimers to the nucleus.
Alternative pathway: Stabilization and auto-activation of NIK activates IKKα, which phosphorylates and targets p100 for proteasomal conversion to p52. P52 subsequently translocates predominantly with RelB to the nucleus (Brown et al., 2008). Scheme adapted from (Rickert et al., 2011).

1.2.3.2. BCR-mediated NF-κB activation

One of the most important events after BCR engagement is the activation of NF-κB. For this the formation of the CARD11-BCL10-MALT1 (CBM) complex is crucial. It assembles key signaling molecules and builds a scaffold for the recruitment of NEMO. This leads to the activation of the IKK complex, which targets the NF-κB-retaining IκB molecules for degradation.

In resting cells, the scaffolding molecule CARD domain-containing membrane-associated guanylate kinase (MAGUK) 1 (CARD11) exists in a closed conformation. This auto-inhibition is regulated by interaction of the linker region with the coiled-coil domain. PKCβ-mediated phosphorylation at the linker region abolishes this connection and leads to opening of the molecule (Figure 9a) (Sommer et al., 2005). This allows the

assembly of the CBM complex. BCL10 interacts with CARD11 via its CARD domain (Bertin, 2001; Gaide et al., 2001), whereas mucosa-associated lymphoid tissue translocation gene 1 (MALT1) binds to the coiled-coil domain of CARD11 (Che et al., 2004). The ubiquitin-ligase TNFα receptor-associated factor 6 (TRAF6) and MALT1 associate and oligomerize (not shown in Figure 9) (Sun et al., 2004; Noels et al., 2007). The active E3-ubiquitin ligase TRAF6 adds K63-linked poly-ubiquitin chains to itself and to NEMO. TAK1-binding protein 2 (TAB2) senses these ubiquitin chains by its zinc fingers (ZF) and recruits transforming growth factor (TGF) β-activated kinase 1 (TAK1) to the CBM complex (Figure 9b) (Kanayama et al., 2004).

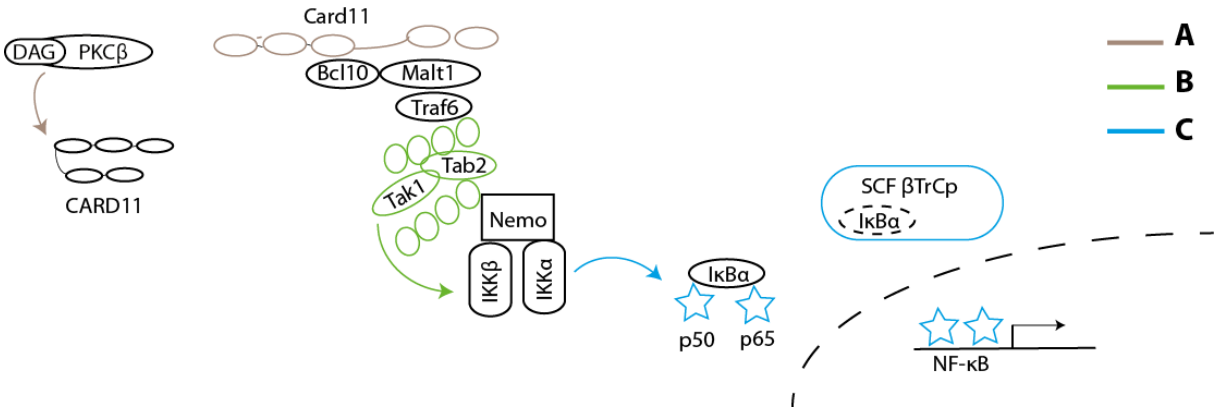

Figure 9: BCR-mediated activation of the CBM complex
BCR stimulation leads to A) the formation of the CBM complex to which B) TRAF6 and TAK1 assemble. TAK1 activates the IKK complex, which C) triggers the release of the NF-κB subunits from their inhibitors.

TAK1 phosphorylates IKKβ in its activation loop resulting in its catalytical activity (Wang et al., 2001) (Figure 9c). The Skpl, Cull, the F-box protein β-transducin repeat containing (SCF β-TrCP) E3 ligase distinguishes un-phosphorylated from phosphorylated IκBα, which is then ubiquitinylated and degraded. This leads to the release of the NF-κB subunits from inhibition by IκBα, and to their translocation to the nucleus (Figure 9c). In the nucleus, NF-κB binds to specific sequences and controls expression of genes essential for proliferation, survival and immune responses (Zandi, 1998).

1.2.3.3. The CARD11-BCL10-MALT1 complex

BCR triggering mounts a signaling cascade, which evokes the assembly of the CBM complex. Already the deficiency in one of the CBM complex molecules impairs full lymphocytic effector function and survival upon activation and thus underlines its importance (Ruland et al., 2001; 2003; Hara et al., 2003).

CARD11 is a member of the MAGUK family, which contains several regions that allow interaction with other molecules or the localization proximal to signaling clusters. These proteins harbor PDZ (postsynaptic density 95, disc large and zonula occludens 1), SH3, and guanylate kinase (GUK) domains. The latter has no kinase activity instead it interacts with the SH3 domain, leading to one of the present closed conformations of CARD11 (McGee et al., 2001; Tavares et al., 2001). How relief of this auto-inhibitory conformation is achieved is unknown. However, disruption of the SH3-GUK interaction is important for CARD11 translocation to the plasma membrane via PDZ domain interactions. CARD11 also contains a serine-rich region, which links the SH3 domain to the coiled-coil domain. An intramolecular interaction between this linker, coiled-coil and the CARD domain results in the second auto-inhibitory conformation of CARD11. Antigen-receptor stimulation evokes PKC activation, which phosphorylates the CARD11 linker region and abolishes this interaction. This event triggers conformational opening, and is the initiating step for CBM complex formation (Sommer et al., 2005): Coiled-coil domain-mediated oligomerization, MALT1 binding and the accessibility of the CARD domain to BCL10 are crucial for NF-κB activation (Lucas et al., 2001; Langel et al., 2008; Thome et al., 2010; Tanner et al., 2007). A negative feedback-loop after NF-κB activation leads to K-48 ubiquitination of the SH3 and the GUK domain, which marks CARD11 for proteasomal degradation (Moreno-Garcia et al., 2010).

The second member of the CBM complex, BCL10, consists of a CARD domain, which is necessary for CARD11 (Bertin, 2001) and MALT1 binding (Langel et al., 2008; Lucas et al., 2001). The serine/threonine rich carboxyterminus of BCL10 is phosphorylated by different kinases and ubiquitinated by E3 ligases, these posttranslational modifications lead to different cellular outcomes. For example, phosphorylation by IKKβ diminishes the interaction between BCL10 and MALT1 leading to decrease in NEMO ubiquitination and therefore attenuation of NF-κB signaling (Wegener et al., 2006). BCL10 also plays a

role in JNK signaling as it acts as c-Jun N-terminal kinase (JNK)-interacting-protein (JIP)-like protein allowing CBM complex-mediated activation of the JNK pathway upon TCR engagement (Blonska et al., 2007).

MALT1 acts as scaffold molecule and contains a death domain (DD) with two adjacent Ig-like domains, which are necessary for BCL10 binding (Lucas et al., 2001). A protease site followed by a third Ig-like domain is found at the C-terminus of the protein. After CBM complex formation, TRAF6 is recruited to MALT1, and carries out critical ubiquitination steps for further activation of the IKK complex. The E3 ubiquitin ligase of TRAF6 ubiquitinates BCL10 (Wu and Ashwell, 2008), MALT1 (Oeckinghaus et al., 2007), NEMO (Staudt, 2010) and itself (Sun et al., 2004). The ubiquitin chains serve as platform for recruitment of the IKK complex and the kinase TAK1 (Shinohara et al., 2007). The MALT1 protease activity is dependent on MALT1 oligomerization and unique due to its caspase-like activity (Kirchhofer and Vucic, 2012). The cleavage occurs after a positively-charged arginine residue in the substrate molecules (Rebeaud et al., 2008). This is different from caspases, which cleave after negatively charged aspartate residues. The substrates of MALT1 that have been identified to date are BCL10 (Rebeaud et al., 2008), A20 (Coornaert et al., 2008), CYLD (Staal et al., 2011a), RelB (Hailfinger et al., 2009) and Regnase1 (Uehata et al., 2013). Cleavage of A20 and RelB enhances NF-κB signaling. Removal of the C-terminal ZF domains from the ubiquitin-editing protein A20 disrupts binding of A20 to ubiquitinated NEMO and deubiquitination of NEMO by the N-terminal ovarian tumor (OTU) domain of A20 is abolished. Therefore, the IKK complex remains active and supports the release of NF-κB from the IκB proteins.

RelB overexpression was found to inhibit the target gene expression of the classical NF-κB pathway. Therefore, active MALT1 cleaves the NF-κB subunit RelB enhancing DNA-binding of cRel and RelA-containing NF-κB complexes.

Interestingly, the cleavage of BCL10 is not crucial for full NF-κB activation, but it is important for T cell adhesion by integrins (McAllister-Lucas et al., 2011). MALT1 substrate cleavage is also important for mitogen-activated protein kinase (MAPK) signaling. MALT1-mediated cylindromatosis (CYLD) cleavage leads to JNK and AP-1 activation, whereas a non-cleavable CYLD molecule inhibits JNK activation after TCR stimulation (Staal et al., 2011b).

Besides NF-κB and JNK activation, MALT1 paracaspase was also found to influence mRNA stability by cleavage of RNA-destabilizing molecules such as the RNAse

Regnase-1 (Uehata et al., 2013). This finding widens the area of influences of CBM-mediated paracaspase function enormously.

1.2.4. AP-1 signaling

BCR engagement triggers the activation of transcription factors, which regulate cell fate decisions in the context of B cell activation. Key transcriptional factors besides mTOR, FOXO and NF-AT are AP-1 and NF-κB. These factors regulate gene expression important for B cell function.

1.2.4.1. Transcription factor AP-1

AP-1 transcription factors consist of different homo- and heterodimers composed of Jun, Finkel-Biskis-Jinkins murine osteogenic sarcoma (Fos), musculoaponeurotic fibrosarcoma oncogene homolog (Maf) and the Atf family (Figure 10) (Shaulian and Karin, 2002). The AP-1 transcription factors regulate important cellular processes such as cell cycle progression and apoptosis (Shaulian and Karin, 2002). Binding of AP-1 to the cyclin D1 promoter leads to enhanced expression of cyclin D1 (*Ccnd1*), cell cycle entry and proliferation (Bakiri et al., 2000). On the other hand, absence of c-Jun leads to the accumulation of p53 and its target genes, which induce cell cycle arrest and apoptosis (Schreiber et al., 1999).

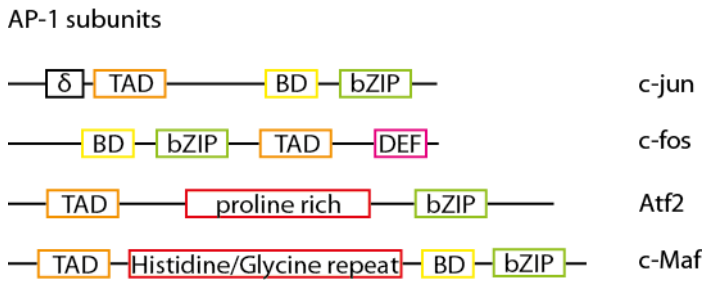

Figure 10: AP-1 subunits
Representatives for each subunit family, which can dimerize to form the AP-1 factors, are illustrated. δ domain for JNK binding; TAD = transactivation domain; BD = basic domain; bZIP = leucine zipper; DEF = docking site for ERK; Figure adapted from (Hess et al., 2004; Bhoumik et al., 2005; Blank, 2008).

C-Jun is the best-known JNK target and is the major component of the AP-1 complex. In the steady-state c-Jun has a short half-life as it is continuously ubiquitinated and

degraded by the proteasome. The phosphorylation of c-Jun at its serine residues 63 and 73 in the activation domain lead to its stabilization and transcriptional activity (Musti et al., 1997; Pulverer et al., 1991). Phosphorylated c-Jun and Atf2 heterodimerize to form an AP-1 transcription factor dimer. The c-Jun promoter itself contains AP-1 binding sites, so that once c-Jun is activated it sustains its expression levels in auto-regulatory-manner (Angel et al., 1988). This mechanism could be involved in its role as oncogene.

1.2.4.2. Ligand-induced AP-1 activation

Ligand binding to the BCR evokes a signaling cascade that results in the activation of kinases and recruitment of scaffold molecules to the BCR complex. One of these kinases recruited to the CARD11 scaffold is the MAPK JNK. There are three JNK genes, which encode up to ten different isoforms: JNK1 and JNK2 are ubiquitously expressed, whereas JNK3 is expressed in brain, testis and heart and will not be discussed in detail (Gupta et al., 1996). The full-length transcripts of JNK1 and 2 encode JNK1α2, JNK1β2, JNK2α2, JNK2β2, which are 55 kDa, whereas shorter splice variants encode JNK1α1, JNK1β1, JNK2α1, JNK2β1, which encode 46 kDa isoforms and lack the C-terminal part. The biological role of these different isoforms is so far not known. JNK is also known as stress-activated MAP kinase (SAPK). This is because JNK is not solely activated after antigen receptor stimulation but also by osmotic or redox-dependent stress and radiation (Ip and Davis, 1998). It regulates key cellular responses with antagonistic effects such as proliferation and apoptosis. JNK molecules are able to induce on the one hand apoptosis by phosphorylation of c-myc (Noguchi et al., 1999) and support cell growth by cell cycle regulation via c-Jun on the other.

TAK1 is recruited and activated at the CBM complex where it activates the IKK complex. Besides activation of the IKK complex, TAK1 also triggers the MAP kinase kinases (MAPKK or MKK) cascade, which activates JNK (Wang et al., 2001; Shinohara et al., 2005; Shinohara and Kurosaki, 2009) and subsequently AP-1 by phosphorylating the target substrates c-Jun and Atf2 (Gupta et al., 1995; Hibi et al., 1993; Davis, 2000).

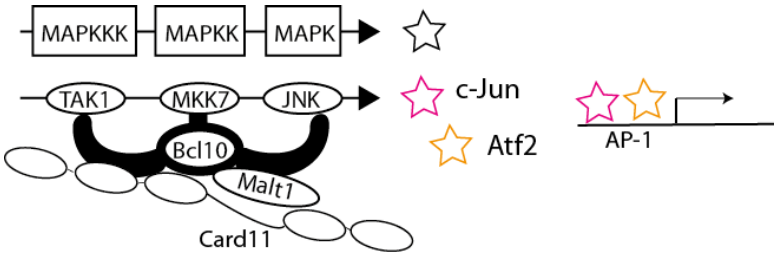

Figure 11: CBM-dependent AP-1 activation
Assembly of the CBM complex activates TAK1, which is the upstream MAPKKK of MKK7. MKK7 in turn phosphorylates JNK, which activates its targets c-Jun and Atf2.

Similar to ligand-mediated AP-1 activation after TCR stimulation, it is thought that it occurs upon BCR engagement. Generally, JNK is activated within a cascade of several kinases. First, the MAP kinase kinase kinases (MAPKKK) phosphorylate and activate the MAPKKs, which then in turn phosphorylate JNK at threonine and tyrosine residues to fully activate the kinase function of JNK.
After CD3/CD28 TCR-mediated JNK activation, BCL10 acts as JIP-like protein and assembles the MAPKKK TAK1, the MAPKK MKK7 and selectively the MAPK JNK2 leading to activation of downstream molecules such as c-Jun and Atf2. Surprisingly, JNK1 kinase activation is independent of the CBM complex as it is still functional in CARD11-deficient cells (Blonska et al., 2007). So far this was shown in detail exclusively in T cells. However, TAK1-deficient B cells are not able to activate JNK and show that TAK1 is bound to BCL10 after BCR stimulation. This could indicate a similar mechanism of BCL10 acting as a JIP-like protein (Figure 11) (Sato et al., 2005).

BCR engagement is the key event for the induction of gene expression regulated by NF-κB and AP-1. Both are crucial for B cell differentiation, survival, proliferation and even apoptosis. The central scaffold for these factors to be activated is the assembly of the CBM complex. Therefore, it is not surprising that certain lymphoma subsets need the activity of this complex for their survival (Ferch et al., 2009). The subsequent section will focus on B cell-derived lymphoma and frequently occurring mutations within different subsets.

1.3. Lymphoma

Lymphoma are neoplastic transformations of lymphoid cells and tissues, which arise from malignant natural killer cells, B or T lymphocytes. According to the World Health Organization more than 50 lymphoma subsets exist, which are categorized in three main classifications according to the cell of origin: Mature B cell neoplasms, Hodgkin´s lymphoma, mature T cell neoplasms and post-transplantation lymphoproliferative disorders (Matasar and Word, 2012). The two most prevalent lymphoma entities are follicular lymphoma and diffuse large B cell lymphoma (DLBCL).

1.3.1. B cell lymphoma

Mature B cell lymphoma are broadly divided into two main categories: Hodgkin's lymphoma (HL) and the Non-Hodgkin's lymphoma (NHL).
The tumor cells within the HL B cell lymphoma are termed Hodgkin and Reed Sternberg cells (HRS). These cells have lost their B cell phenotype, and express atypical surface markers of different hematopoietic cells (Küppers et al., 2012). NHL can arise from both B and T cells. The most common B cell lymphoma of the NHL category are DLBCL (Lenz and Staudt, 2010). The name of this lymphoma entity is based on the fact that malignant large B cells grow diffusely throughout the lymph node without a specific pattern.

DLBCL are divided in three main subtypes: primary-mediastinal B cell lymphoma (PMBL), activated B cell-like (ABC) lymphoma, and germinal center B cell-like (GCB) lymphoma. Currently, chemotherapy is the standard treatment of DLBCL resulting in different survival outcomes. PMBL and GCB type DLBCL have a favorable prognosis with 60% survival rate (Rosenwald et al., 2003; Martelli et al., 2008), whereas the survival rate for ABC type is about 30% (Joos et al., 1996; Rosenwald et al., 2003). The combination of chemotherapy with the B cell-depleting antibody rituximab improved the overall survival of ABC-DLBCL to 44%, however with the limitation that about one third of the patients relapse (Coiffier et al., 2010; Gisselbrecht et al., 2010; Chiappella and Vitolo, 2012). The modest prognosis especially for ABC type patients after standard treatment urges the need for new therapeutic strategies. To achieve this goal, a better understanding of these lymphoma entities is needed.

1.3.1.1. Primary-mediastinal diffuse large B cell lymphoma

PMBL are distinct from the ABC and GCB lymphomas in that they arise from rare thymic B cells, whose gene expression signature resembles HRS cells (Savage, 2006). However they maintain their B cell identity, and express Bcl-6 as well as signaling molecules downstream of the BCR such as SYK and PLCγ (Marafioti et al., 2005). The frequent amplification of chromosome 9 in PMBL leads to enhanced expression of PD-ligand 1/2- causing T cell anergy as well as augmented janus kinase 2 (Jak2) and activated STAT signaling (Rosenwald et al., 2003). Also the chromosomal region containing cRel is often amplified, which leads to NF-κB activation in PMBL (Joos et al., 1996).

1.3.1.2. Germinal center B cell-like diffuse large lymphoma

As described earlier in the germinal center B cells chapter, GCBs are in a highly proliferative, pro-apoptotic and DNA damage-tolerant state that allows somatic hypermutation of the variable regions and the removal of B cells with low affinity antibodies. However, this state also predisposes GCBs to aberrant chromosomal translocation of the immunoglobulin loci, and also to the action of the somatic hypermutation machinery by AID on non-Ig loci, which can result in malignant transformation and other pathologies (Klein and Dalla-Favera, 2008).

Therefore, it is not surprising that mutation-prone GCBs give rise to various B cell lymphoma: Burkitt´s lymphoma, Follicular lymphoma and GCB-DLBCL (Lenz and Staudt, 2010). Herein we will focus on GCB-DLBCL, which retain their B cell identity and express GCB-associated genes. Little NF-κB activity is found in these cells, yet, more than 25% of GCB patients have amplifications of the cRel locus (Rosenwald et al., 2002). However, NF-κB inhibition does not impair cell survival, which indicates that the accumulation of cRel may have a different molecular function in GCB lymphoma than NF-κB activation (Davis et al., 2001a). Another common translocation in GCB lymphoma involves Bcl-2 inhibiting apoptosis of these cells (Iqbal et al., 2004).

1.3.1.3. Activated B cell-like diffuse large B cell lymphoma

The ABC subtype has high NF-κB activation in contrast to GCB lymphoma and the malignant cells in ABC-DLBCL resemble *in vitro*-activated B cells (Alizadeh et al., 2000). The cell of origin is not clearly defined, but some evidence suggests it may be a post-GC plasmablast (Lenz and Staudt, 2010). ABC-DLBCL cells express a number of genes that are important for plasma cells, such as the Pax-5 regulated factor Xbp1 and the direct NF-κB target gene *Irf4*. Xbp1 regulates the gene expression of components of the ER and golgi system, and leads thereby to an expansion of the secretory apparatus (Wright et al., 2003; Shaffer et al., 2004). Tumor cells escape complete terminal plasma cell differentiation by harboring inactivating and truncating mutations in Blimp-1 (Pasqualucci et al., 2006).

This allows the malignant cell to keep its activated phenotype without arrest in cell cycle, which is acquired in terminal differentiation. This is supported by other somatic mutations found in ABC tumor samples and patients, which further feed into the activation of these cells. For instance, the signaling molecules CD79A/B and CARD11, which are involved in downstream signaling of the BCR, are mutated in more than 20% and 10%, respectively, of ABC patients (Davis et al., 2010; Lenz et al., 2008).

Frequent mutations in ABC-DLBCL

Mutations in CD79A or CD79B affect the ITAM motif, which is important for signal transduction after BCR cross-linking (Figure 12a). The most common CD79 mutation (occurring in about 6% of total ABC samples) encodes a version of CD79B in which the first ITAM tyrosine is replaced by a histidine. It is known that in the initial phase of BCR signaling, LYN phosphorylates the CD79 heterodimer facilitating downstream signaling. Afterwards LYN attenuates BCR signaling by various mechanisms such as phosphorylation of CD22 and subsequent recruitment of SHP-1, which initiates BCR complex de-phosphorylation (Gauld and Cambier, 2004; Xu et al., 2005). Therefore, the authors proposed a mechanism by which ITAM mutations negatively influence LYN, abolishing its role as negative regulator in later phases of BCR signaling so that BCR downstream signaling pathways are constitutively activated (ERK, AKT, NF-AT, NF-κB) when CD79 is mutated (Davis et al., 2010). However, the mechanism how CD79 mutations achieve this is still vague. Constitutive BCR signaling due to CD79 mutations

was termed chronic active BCR signaling, and in contrast to tonic BCR signaling, which signals via PI3K, it is CBM complex-dependent and needs BCR surface clustering (Srinivasan et al., 2009).

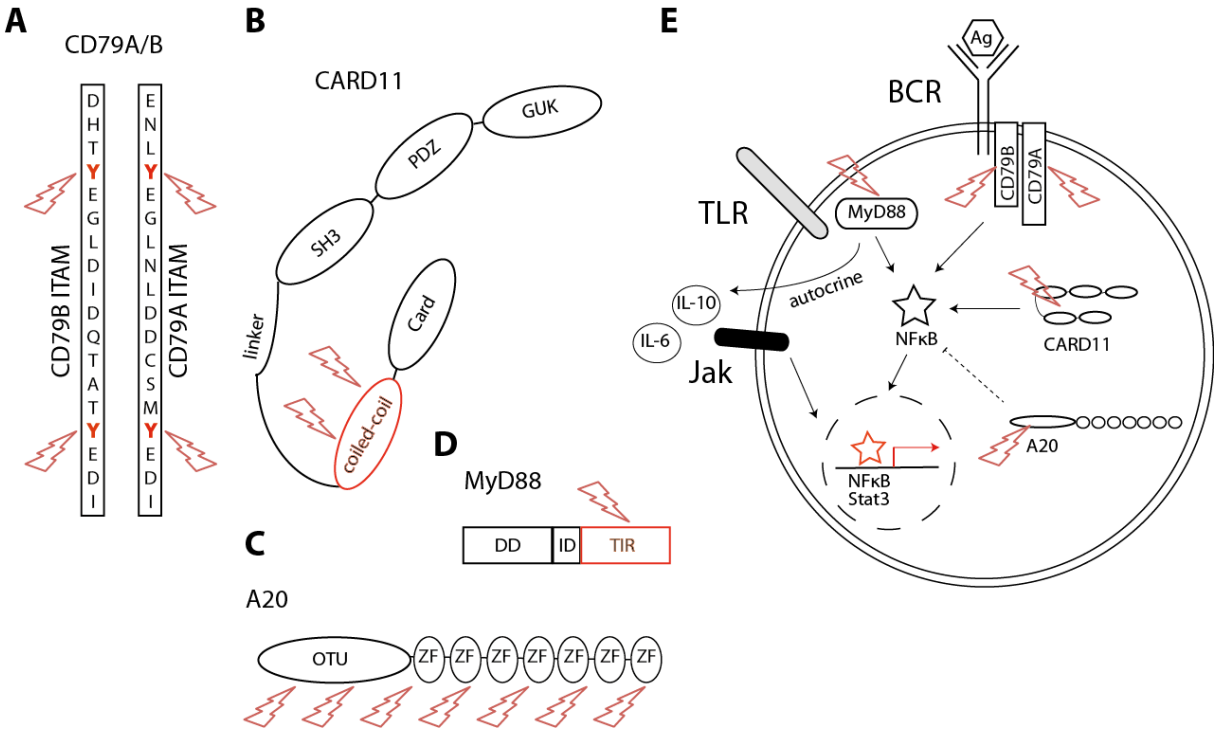

Figure 12: Mutated signaling molecules found in ABC-DLBCL
Red lightning bolts represent somatic mutations. A) ITAM motif of CD79A and B, mutated tyrosines are depicted in red. B) Schematic drawing of CARD11 domains: GUK = guanylate kinase; PDZ = PSD95, DLG and ZO1 homology; SH3 = Src homology 3; CARD = caspase-recruitment domain; C) Schematic drawing of A20 domains: OTU = ovarian tumour; ZF = zinc finger; D) Schematic drawing of MyD88 domains: DD = death domain; ID = intermediary domain; TIR = Toll/interleukin-1 receptor; E) Mutations in context; Red stars displays active transcription. For details refer to text. Adapted from (Jeelall and Horikawa, 2011).

Another frequently mutated protein is CARD11 (Figure 12b) (Lenz et al., 2008). Mutations affect the coiled-coil domain and abolish the auto-inhibitory conformation of CARD11 so that BCL10 is constitutively recruited leading to constitutive NF-κB activation (Lamason et al., 2010). Mutated CARD11 accumulates in large aggregates in the cytosol, which further enhance NF-κB signaling. Those mutations have been shown *in vitro* experiments to strongly activate NF-κB signaling in a BCL10-dependent way (Lamason et al., 2010).

Inactivating or truncating mutations in the negative regulator A20 were also found in about 30% of tumor samples (Figure 12c) (Kato et al., 2009; Compagno et al., 2009). They are most-likely bystander mutations, which support the NF-κB activation in lymphoma entities with CARD11- and CD79-mutations (Staudt, 2010). The NF-κB target gene *A20* is expressed after BCR engagement, to negatively regulate NF-κB signaling. Truncating mutations in A20 impair deubiquitination and lead to the constitutive presence of K63-linked ubiquitin chains on NEMO and hinder its degradation (Hymowitz and Wertz, 2010).

Surprisingly the adaptor molecule MyD88, which is important for TLR and IL-1 receptor signaling, is mutated in about 40% DLBCL patient samples (Figure 12d) (Ngo et al., 2010). Mutations in MyD88 lead to constitutive complex formation of MyD88 with IRAK1 and IRAK4, causing constitutive NF-κB activation and Jak-Stat3 signaling (Figure 12e) (Jeelall and Horikawa, 2011).

2. PURPOSE OF THIS STUDY

The CBM complex and the downstream activation of NF-κB are crucial for differentiation, activation and apoptosis (Siebenlist et al., 2005; Karin and Lin, 2002). As NF-κB activation mediated by the CBM complex plays a central role in lymphocyte biology it is perhaps not surprising that the CBM complex has been implicated in tumor and lymphoma development and maintenance (Lim et al., 2012; Nishikori, 2005; Packham, 2008; Pacifico and Leonardi, 2006). This is achieved by NF-κB-mediated acquirement of the seven hallmarks of cancer: inflammation, resistance to cell death, the induction of angiogenesis, proliferation paired with replicatory immortality, invasive properties and metastasis and finally evading growth suppressors (Hanahan and Weinberg, 2011).
The intriguing role of the CBM complex in cancer was shown more than one decade ago in MALT lymphoma, where NF-κB activating BCL10 and MALT1 translocations were found (Lucas et al., 2001). Previous studies showed, that the MALT1 paracaspase activity is crucial for the survival of ABC-DLBCL cell lines *in vitro* (Ferch et al., 2009), which triggered the investigation of the MALT1 paracaspase domain as potential target for the treatment of DLBCL (Fontan et al., 2012; Nagel et al., 2012).

Therefore, the aim of my PhD thesis was to examine the role of hyperactive CBM signaling utilizing CARD11 mutations found in DLBCL patients material (Lenz et al., 2008). Different questions could be addressed by the generation of a conditional knock-in mouse model expressing CARD11 with the insertion of an isoleucine at amino acid position 225 after the leucine, namely CARD11(L225LI).

Specifically:

- is the expression of mutated CARD11 *in vivo* sufficient for the pathogenesis of a lymphoid malignancy?
- does the disease resemble morphologically the human phenotype?
- is signaling affected by expression of mutated CARD11?
- does this study help to find new therapeutic strategies for treatment of the very aggressive DLBCL?

3. RESULTS

3.1. *In vitro* examination of lymphoma-derived CARD11 mutations

In human B cell lymphoma, mutations that render CARD11 constitutively active are frequently observed (Lenz et al., 2008). To study the role of these mutations *in vitro*, we expressed one of these mutations, CARD11(L225LI), in the mature B cell lymphoma line Bal-17 and assessed B cell activation (Figure 13). For this purpose, the cDNAs of *Card11(L225LI), Card11(Δlinker)* or wild type (WT) *Card11* were cloned into the retroviral vector pMIG (plasmid MSCV promoter, internal-ribosomal-entry site (IRES) combined to a green fluorescent protein (GFP)) allowing GFP tracking for transgene expression. This specific mutant, CARD11(L225LI), was used because it has been shown in previous studies to result in stronger NF-κB activation than other patient-derived or biochemically generated CARD11 mutants such as the CARD11(Δlinker), in which the linker region between coiled-coil and SH3 domains was removed resulting in spontaneous NF-κB activation *in vitro* (Lenz et al., 2008; Lamason et al., 2010; Sommer et al., 2005).

Compared to untransfected cells and cells that expressed WT CARD11 or CARD11(Δlinker), CARD11(L225LI)-expressing cells exhibited a strong up-regulation of CD80 and down-regulation of IgM, both indicating B cell activation (Figure 13a). Western blotting of nuclear lysates also revealed a constitutive nuclear translocation of the canonical NF-κB subunits RelA, cRel and p50 (Figure 13b). In line with these results, electrophoretic mobility shift assay (EMSA) demonstrated that CARD11(L225LI) expression resulted in an increased NF-κB DNA-binding which was comparable to NF-κB activation in BCR stimulated cells. BCR ligation was able to additionally enhance NF-κB DNA-binding activity (Figure 13c). Together, these first results are consistent with published data (Lamason et al., 2010) and confirm that in contrast to overexpression of WT CARD11 or CARD11(Δlinker), overexpression of CARD11(L225LI) leads to constitutively NF-κB signaling and thereby to B cell activation.

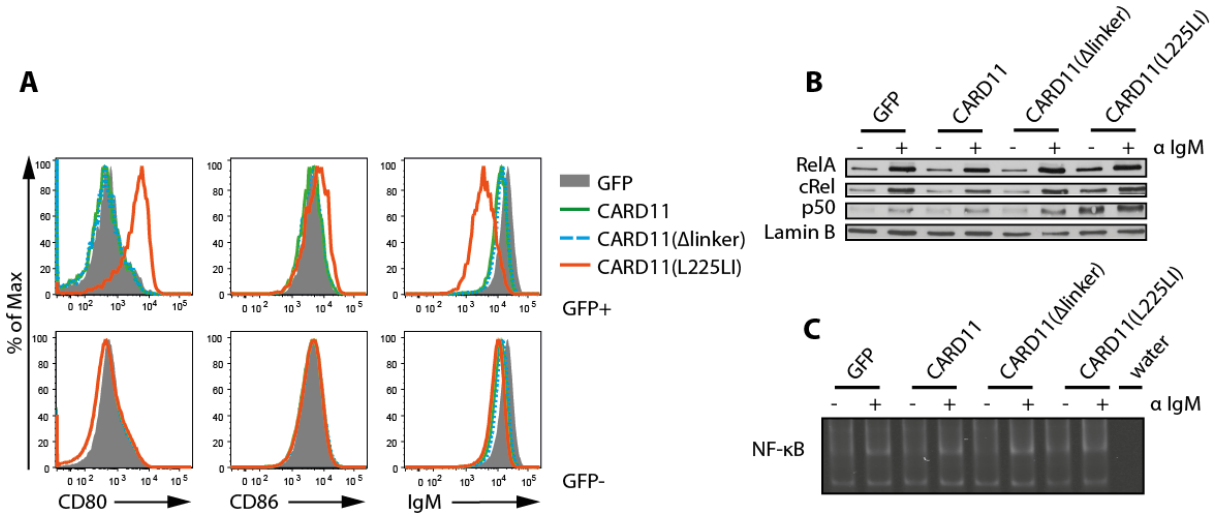

Figure 13: Mutated CARD11 activates the murine B cell lymphoma line Bal-17
A) Flow cytometric analysis of Bal-17 cells transfected with different retroviral constructs. Upper row shows gate on live GFP+, the lower row live GFP-cells. Surface expression of the activation marker CD80, CD86 and the down-regulation of surface IgM were examined. B) GFP+ sorted cells were left untreated or stimulated for 90 minutes with α-IgM. Nuclear lysates were analyzed by Western blot detecting different NF-κB subunits (RelA, cRel, p50). Equal loading was verified by Lamin B probing. C) The same nuclear lysates were subjected to a NF-κB-electrophoretic mobility shift assay (EMSA). Data shown are representative of at least two independent experiments.

3.2. Generation of a CARD11(L225LI)$^{stop FL}$ transgenic knock-in mouse

In order to examine the role of DLBCL patient-derived CARD11 mutation 10 (CARD11(L225LI)) *in vivo*, we generated a mouse model. We decided to use the human *Card11* cDNA for this purpose, since the murine (uniprot ID: Q8CIS0) and human (Q9BXL7) protein sequences are more than 90% identical. The sequence for the coiled-coil domain 1, where the mutation is located, is even 100% identical to the murine amino acid sequence.

To do so, the human *Card11(L225LI)* cDNA combined to an HA tag preceded by a *loxP*-flanked (FL) transcriptional and translational STOP cassette was inserted into the ubiquitously expressed *ROSA26* locus (Figure 14a) (Sasaki et al., 2006; Friedrich and Soriano, 1991). The *loxP*-flanked STOP cassette consists of polyA repeats shutting off transcription before the CARD11(L225LI) reading frame begins.

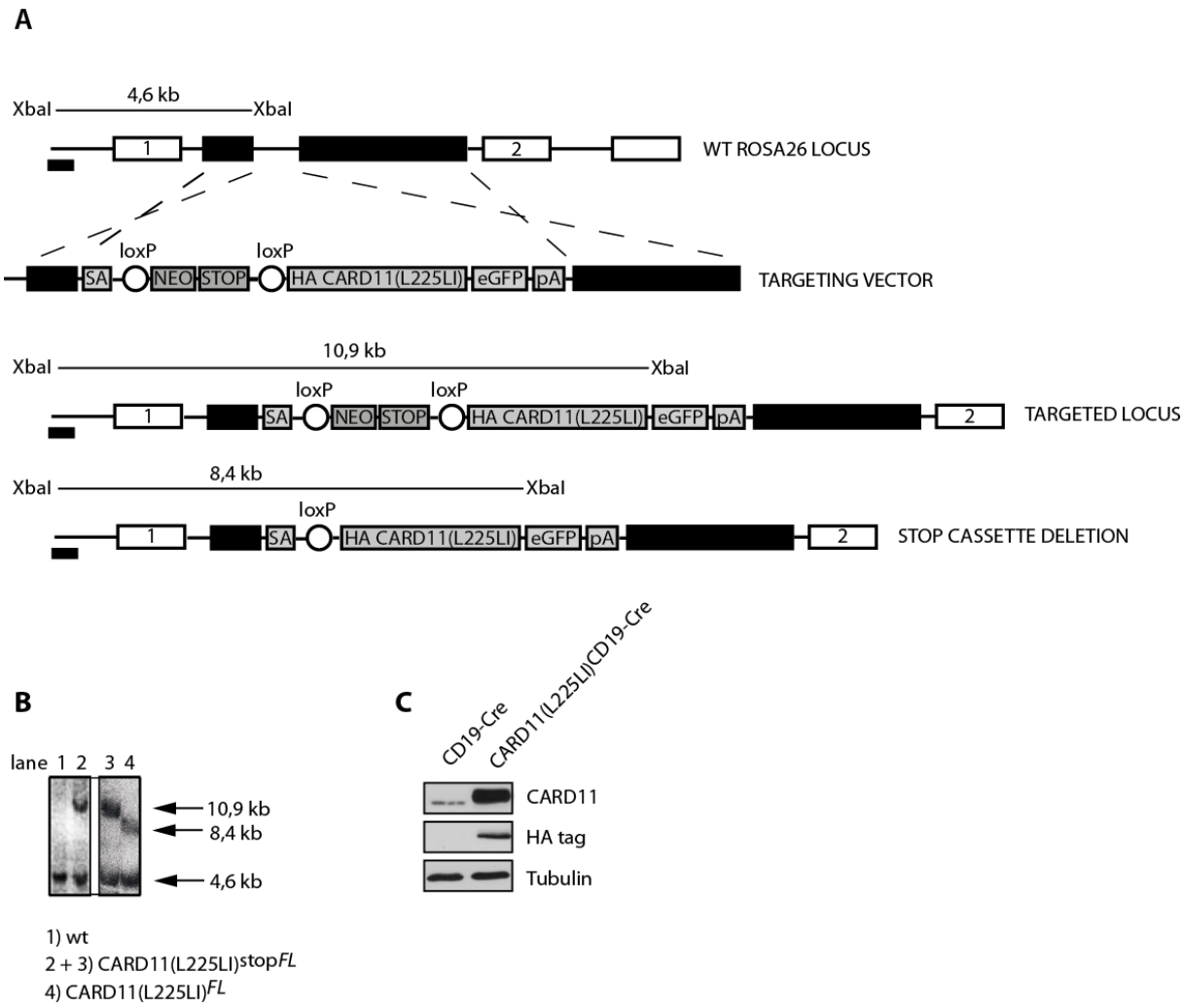

Figure 14: Generation of the CARD11(L225LI)$^{stop FL}$ mouse

A) The WT *ROSA26* locus is shown with the targeting vector below. Black bars connected by dashed lines show homology arms. Bars indicate the sites for the restriction enzyme XbaI for Southern blot verification. The probe is located 5´prime of the first *ROSA26* exon. 1 = Exon 1; 2 = Exon 2; SA = splice acceptor; IRES = internal-ribosomal-entry site; eGFP = enhanced green fluorescent protein; pA = polyA; B) Lane 1 and 2 gDNA from embryonic stem cells: First lane shows the WT ROSA26 locus (4,6kb), the second and third lane show the successfully recombined ROSA26 locus called CARD11(L225LI)$^{stop FL}$ (4,6kb and 10,9kb) and the fourth lane represents Cre-mediated removal of the STOP cassette termed CARD11(L225LI)^{FL} (8,4kb) (lane 3 and 4 gDNA from MACS-purified CARD11(L225LI)$^{CD19\text{-}Cre}$ B cells). C) Western blot of cytosolic lysates of MACS-purified CARD11(L225LI)$^{CD19\text{-}Cre}$ B cells verifying transgene expression by detection of the HA tag.

Breeding of CARD11(L225LI)$^{stop FL}$ mice to Cre transgenic animals results in the excision of the *loxP*-flanked STOP cassette and in the subsequent bicistronic expression of CARD11(L225LI) together with enhanced GFP (eGFP) (Figure 14a), which allows to identify CARD11(L225LI)-expressing cells by flow cytometry. Southern blots verified

the correct transgene insertion in the *ROSA26* locus of embryonic stem cells and functional Cre-mediated STOP cassette removal in primary B cells (Figure 14b). The addition of a N-terminal HA tag facilitates transgene detection by Western blot analysis. Lysates from primary CARD11(L225LI)$^{CD19\text{-}Cre}$ B cells verified the expression of mutant CARD11 by detection of the HA tag (Figure 14c).

For simplicity, we refer to the CD19-Cre and CARD11(L225LI)$^{stop\mathit{FL}}$ double transgenic mice throughout this study as CARD11(L225LI)$^{CD19\text{-}Cre}$ mice. This breeding allows Cre-mediated transgene expression from the pre B cell stage onwards throughout all B cell subsets (Rickert et al., 1997).

3.3. Effect of CARD11(L225LI) expression in early B cell development

3.3.1. CARD11(L225LI) expression rapidly leads to B cell expansion and cytokine production

Consequences of CARD11(L225LI) expression from early B cell development were analyzed in breedings to the CD19-Cre strain. Interestingly, we never obtained any CARD11(L225LI)$^{CD19\text{-}Cre}$ pups at weaning age (3-4 weeks after birth). When we looked at earlier time points, we discovered that all CARD11(L225LI)$^{CD19\text{-}Cre}$ mice died within the first six days after birth. To examine whether these mice were already born with an outgrowth of transgenic cells, we sacrificed mice at different time points. Since the fetal liver is the site for early hematopoiesis, we examined this organ within the first 72 hours after birth. On day 2 until day 5 after birth, we also analyzed the spleen.

The expression of eGFP revealed that CARD11(L225LI) was expressed already shortly after birth from few cells in the neonatal liver (Figure 15a). The amount of eGFP-expressing cells increased drastically from day 3 to 4 in the spleen, reaching with around 60 million cells on day 5 comparable cell counts to spleens of adult mice.

Already on the first day after birth, eGFP-positive B cells were highly activated as indicated by up-regulation of CD80. On day 5, all B cells showed high surface expression of CD80 (Figure 15b).

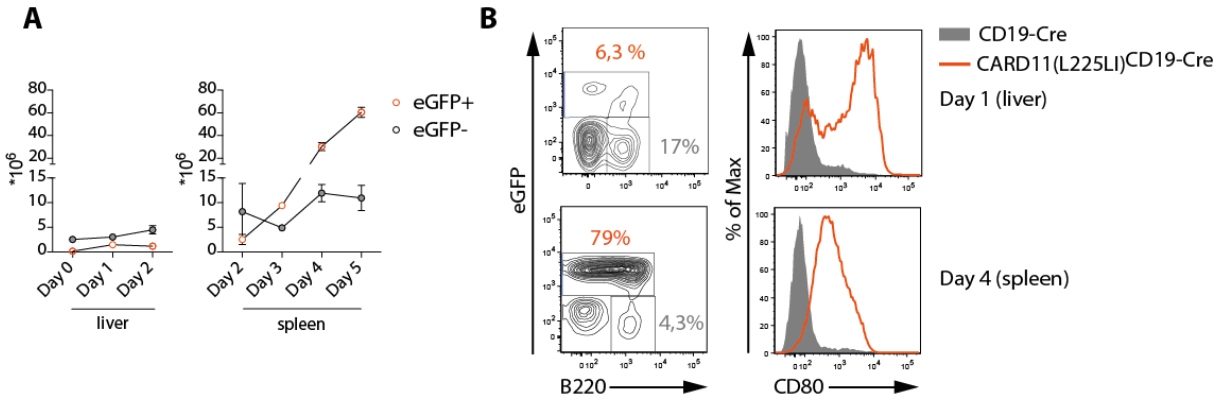

Figure 15: Proportion of eGFP-expressing cells over time

A) Newborn CARD11(L225LI)$^{CD19\text{-}Cre}$ mice (birth is defined as day 0) were sacrificed at the given time points after birth. Liver and/or spleen cells were counted, and eGFP-expressing (eGFP+) cells were determined by flow cytometry. B) Upper row shows the total cell gate in the liver from a 1-day-old transgenic mouse gated on eGFP and B220. eGFP-expressing and B220-positive eGFP-negative (eGFP-) cells were further gated on the activation marker CD80. Lower row shows the total cell gate in the spleen from a 4-day-old transgenic mouse. Data are presented as mean or mean ± SEM of n ≥ 3 per genotype.

Intracellular analysis by flow cytometry revealed that transgenic cells produced inflammatory cytokines such as IFN-γ, IL-6 and TNFα already early (day 1, top), whose levels increased over time (day 4, bottom) (Figure 16a). Sera obtained from 5-day-old animals were tested for the presence of these and additional cytokines. Indeed, elevated amounts of the inflammatory cytokines IL-1α and TNFα were measured in sera from CARD11(L225LI)$^{CD19\text{-}Cre}$, but not from CD19-Cre controls (Figure 16b). Moreover, sera from CARD11(L225LI)$^{CD19\text{-}Cre}$ mice exhibited high concentrations of IL-10 and IL-6, which are cytokines that are also autonomously produced by ABC-DLBCL cells and which sustain their proliferation (Lam et al., 2008; Ferch et al., 2009).

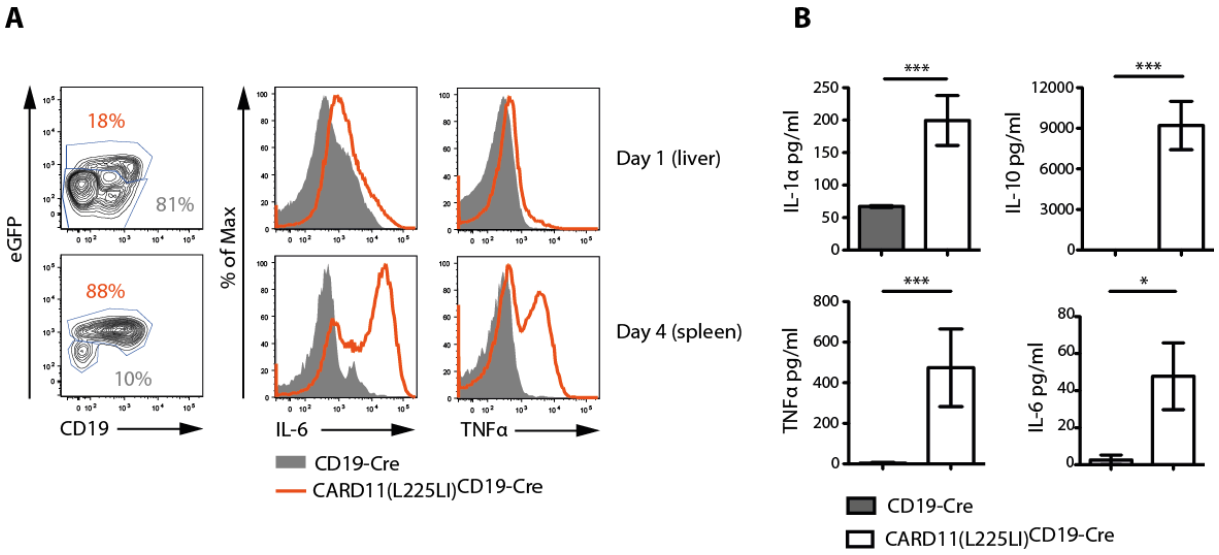

Figure 16: Cytokine measurements

A) The upper row shows the total live cell gate in the liver from a 1-day-old CARD11(L225LI)$^{CD19\text{-}Cre}$ mouse gated on eGFP and CD19. eGFP-positive and eGFP-negative cells were further gated intracellular on the cytokine IL-6 and TNFα. Lower row shows the total cell gate in the spleen from a 4-day-old CARD11(L225LI)$^{CD19\text{-}Cre}$ mouse. Data are presented as mean of n ≥ 3 per genotype. B) Sera from at least 20 animals per genotype (CD19-Cre and CARD11(L225LI)$^{CD19\text{-}Cre}$) were subjected to Th1/Th2 FlowCytomix multiplex assay. Data are shown as mean ± SEM.

3.3.2. CARD11(L225LI) induces terminal plasma cell differentiation

Due to the fact that CARD11(L225LI)$^{CD19\text{-}Cre}$ animals died mostly between day 5 and day 6, control and moribund transgenic animals were analyzed 5 days after birth. CD19-Cre littermates were used as control animals.

CARD11(L225LI)$^{CD19\text{-}Cre}$ animals appeared smaller in size and displayed hepatosplenomegaly (Figure 17a, b). They exhibit massive splenomegaly with a high increase in the frequency as well as the total number of CD19-expressing B lymphocytes, which were more than 96% GFP-positive (Figure 17c), whereas other cell populations such as TCRβ-positive T cells remained unchanged.

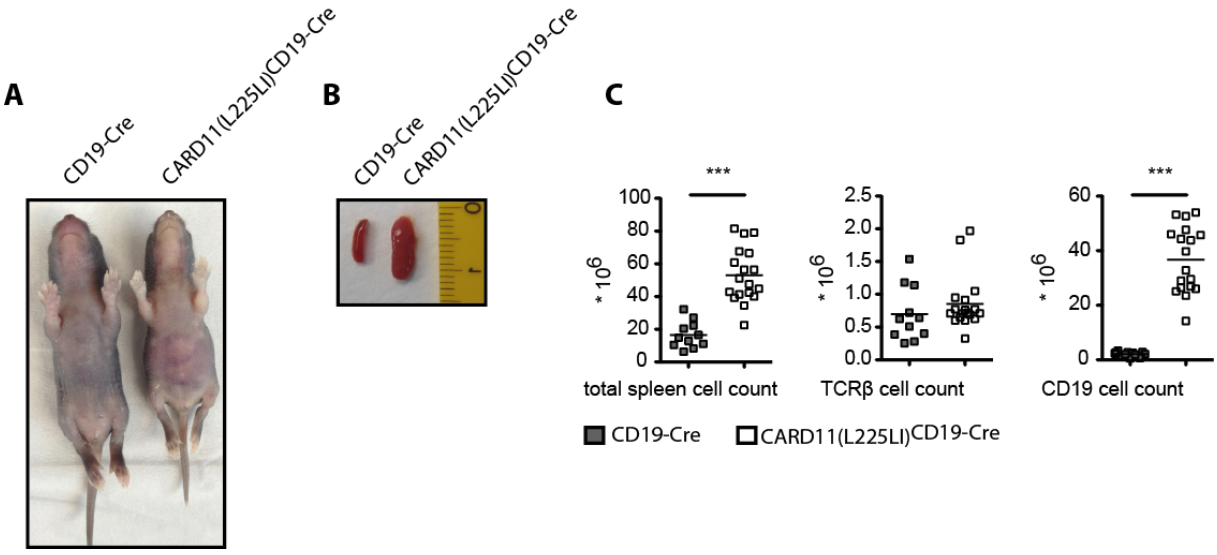

Figure 17: CARD11(L225LI)$^{CD19\text{-}Cre}$ animals develop splenomegaly
A) 5-day-old CARD11(L225LI)$^{CD19\text{-}Cre}$ and control animal. B) Spleens from 5-day-old transgenic and control animals. C) Splenic cell counts from 5-day-old animals.

Histological examination of transgenic spleens showed a monotonous population of large cells with prominent nucleoli featuring a high proliferation index of more that 75%, as assayed by Ki-67 staining. These blastoid cells infiltrated solid organs such as the liver and thus show pathohistological signs of a high-grade lymphoma (data not shown).

Control bone marrow showed normal early B cell development with clear pre (B220+IgM-CD25+) and pro B cell populations (B220+IgM-ckit+) and few immature and recirculating B cells (B220+ IgM+). It appeared that CARD11(L225LI)$^{CD19\text{-}Cre}$ peripheral B cells infiltrated the bone marrow. B cells present in the bone marrow of CARD11(L225LI)$^{CD19\text{-}Cre}$ mice also showed elevated expression of c-kit (Figure 18a left panel).

We observed in the spleens of WT mice the expected frequencies of CD5 and IgM-positive fetal liver-derived B1-B cells (Figure 18 right panel) (Zhang et al., 2012; 2007; Hayakawa et al., 1983; Baumgarth, 2011; Godin et al., 1993). The splenic B cell compartment of perinatal mice has been shown to be composed to a big extend of fetal liver-derived B1-B cells, whose percentage declines in favor of B2-B cells during the life. Control animals showed normal peripheral B cell maturation measured as surface

co-expression of IgM and IgD, whereas CARD11(L225LI)-expressing cells showed arrested maturation as the IgD-positive B cell population was reduced.

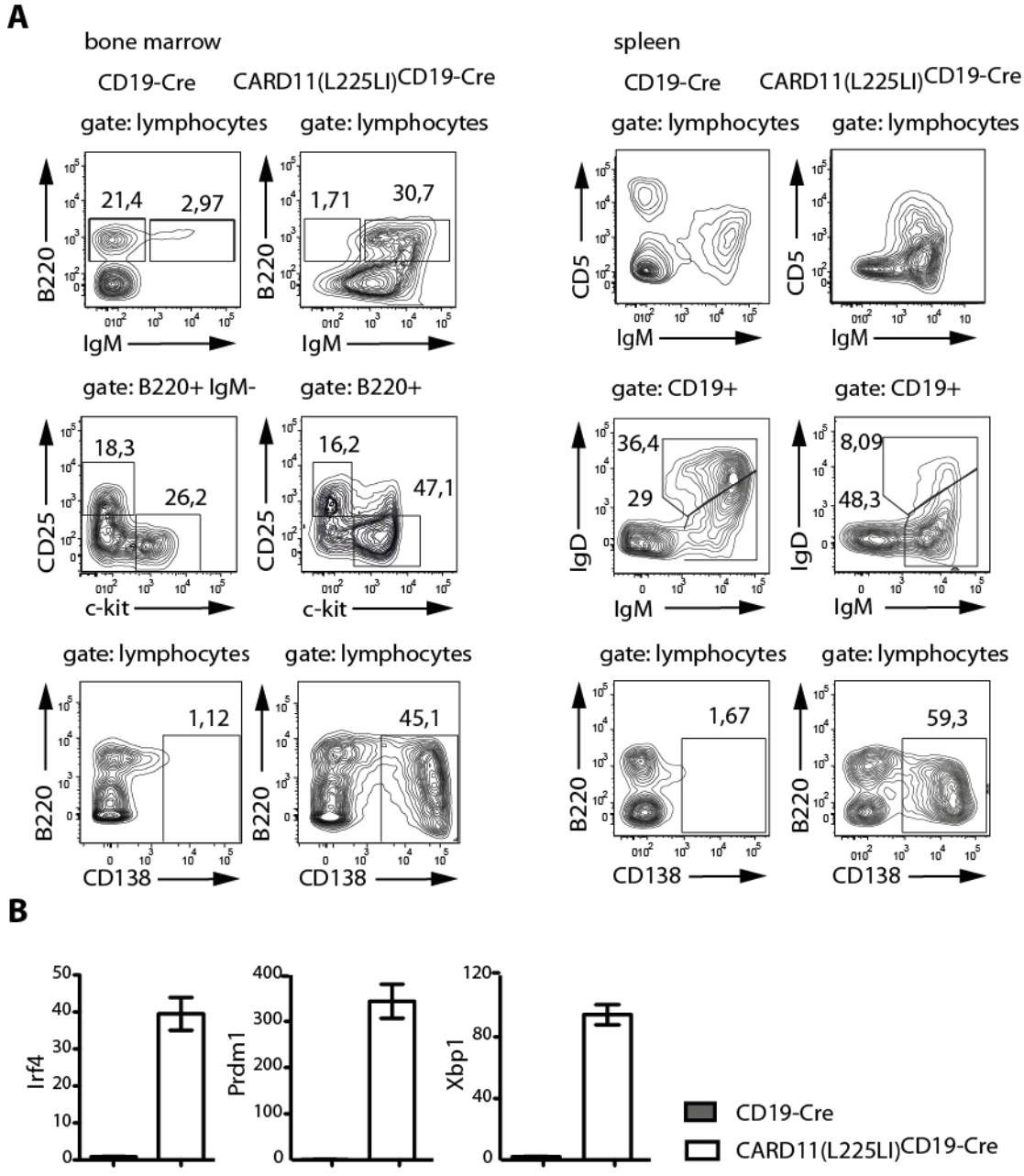

Figure 18: CARD11(L225LI) induces plasma cell differentiation

Flow cytometric analysis of bone marrow and spleen of 5-day-old animals. Bone marrow was analyzed for B220, IgM, CD25, c-kit and CD138; Pre/pro B cells: B220+ IgM-; Pre B cells: B220+ IgM- CD25+; Pro B cells: B220+ IgM- ckit+; Recirulating B cells: B220+ IgM+; Plasmablasts: B220 intermediate or low CD138+; Plasma cells: B220- CD138+; Spleens were analyzed for eGFP, CD5, IgD, IgM, B220 and CD138. B) Relative transcript level in MACS-purified B cells for *Irf4, Prdm1* and *Xbp1* were examined by real time PCR, results were normalized to the housekeeping gene *Hrpt1*. Data are presented as mean or mean ± SEM of n ≥ 4 per genotype.

Both the bone marrow and spleen of CARD11(L225LI) transgenic animals were infiltrated with a high percentage of eGFP expressing CD138-positive B cells that show low B220 expression indicating that these are plasmablasts ($B220^{int}CD138^{+}$) and plasma cells ($B220^{low}CD138^{+}$). Indeed, qRT-PCR analysis of *Irf4, Prdm1* and *Xbp1* expression demonstrated that these markers of plasma cell differentiation were also highly expressed in these CARD11(L225LI)-expressing B cells (Figure 18b).

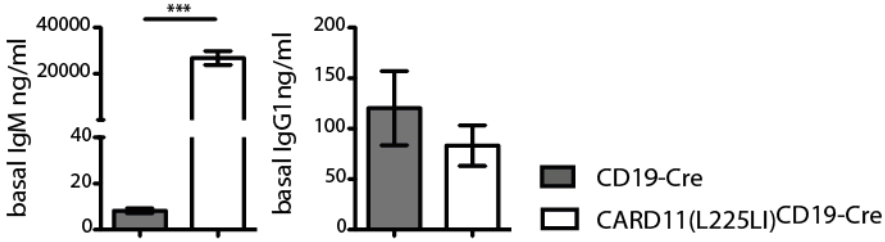

Figure 19: Plasma cells in CARD11(L225LI)$^{CD19\text{-}Cre}$ animals secrete IgM
A) Basal immunoglobulin levels of IgM (n = 11 mice per genotype) and IgG1 (n ≥ 8 mice per genotype) in sera from 5-day-old animals.

The characterization of CARD11(L225LI)$^{CD19\text{-}Cre}$ cells suggested that transgenic cells were terminally differentiated, antibody-secreting plasma cells with high inflammatory and proliferative potential. To test whether the plasma cells produce antibodies, sera were analyzed for the presence of IgM and class-switched IgG1 (Figure 19). Although comparable concentrations of IgG1 were found in both genotypes, highly increased concentrations of IgM were observed in the sera from CARD11(L225LI)$^{CD19\text{-}Cre}$ mice indicating autonomous antibody production.

3.3.3. Roles of BCL10 and MALT1 in CARD11(L225LI)-mediated lymphomagenesis

Next, we investigated whether the assembly of the CBM complex is causative for the lethal lymphoproliferation. Therefore, we crossed CARD11(L225LI)$^{CD19\text{-}Cre}$ transgenic mice onto BCL10- or MALT1-deficient or MALT1 paracaspase mutant (PM) backgrounds (CARD11(L225LI)$^{CD19\text{-}Cre}$;BCL10-/-, CARD11(L225LI)$^{CD19\text{-}Cre}$;MALT1-/-, CARD11(L225LI)$^{CD19\text{-}Cre}$;PM/-).

The PM mouse strain harbors a point mutation (C464A) within the paracaspase domain of MALT1, which results in a paracaspase loss-of-function mutant (Gewies, A. and Gorka, O., unpublished) with the biological consequence that paracaspase target molecules such as CYLD, RelB and A20 are not cleaved upon receptor engagement. PM/- mice express on one allele the paracaspase deficient version of MALT1 and harbor on the other one a targeted disruption of MALT1. The MALT1 protein levels expressed by PM/- cells are comparable to MALT1 WT cells. Upon antigen receptor engagement PM/- expressing B and T lymphocytes show normal MAPK and IKK activation (unpublished data). In contrast to PM/- lymphocytes, BCL10- or MALT1-deficient T and B lymphocytes show defective IKK activation and fail to activate NF-κB. Receptor-proximal tyrosine phosphorylations and ERK activation are normal in BCL10-/- or MALT1-/- lymphocytes after antigen receptor stimulation (Ruland et al., 2001; 2003).

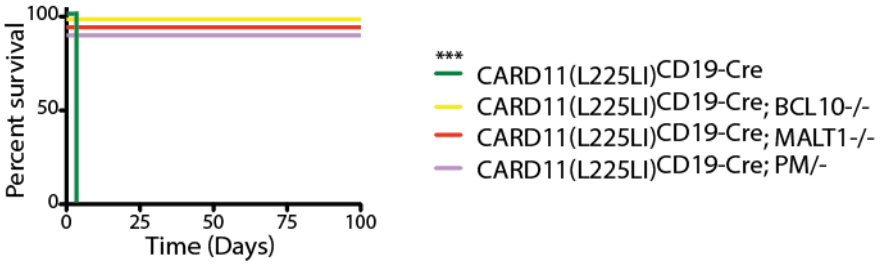

Figure 20: CARD11(L225LI)$^{CD19\text{-}Cre}$;BCL10-/-, CARD11(L225LI)$^{CD19\text{-}Cre}$;MALT1-/-, CARD11(L225LI)$^{CD19\text{-}Cre}$;PM/- mice survive longer than 6 days

Kaplan-Meier curves for CARD11(L225LI)$^{CD19\text{-}Cre}$ mice on different genetic backgrounds: CARD11(L225LI)$^{CD19\text{-}Cre}$;BCL10-/-, CARD11(L225LI)$^{CD19\text{-}Cre}$; MALT1-/-, CARD11(L225LI)$^{CD19\text{-}Cre}$;PM/-; each genotype n ≥ 5

BCL10 and MALT1 heterozygous CARD11(L225LI)$^{CD19\text{-}Cre}$ mice succumbed similar to CARD11(L225LI)$^{CD19\text{-}Cre}$ mice six days after birth (data not shown), whereas the complete absence of BCL10 and MALT1 rescued the mice from early lethality (Figure 20). Interestingly, the presence of MALT1 as scaffolding molecule without paracaspase function also rescued the CARD11(L225LI)$^{CD19\text{-}Cre}$ animals from perinatal death. This indicated that the presence of the CBM complex per se and the paracaspase function of MALT1 are essential for CARD11(L225LI)-mediated activation of downstream pathways, which lead to pathogenesis. Thus, the constitutive and functional assembly of CBM complexes triggered by CARD11(L225LI) is solely responsible for the B cell

activation and lethality *in vivo* excluding important CBM independent functions of CARD11(L225LI) for pathogenesis.

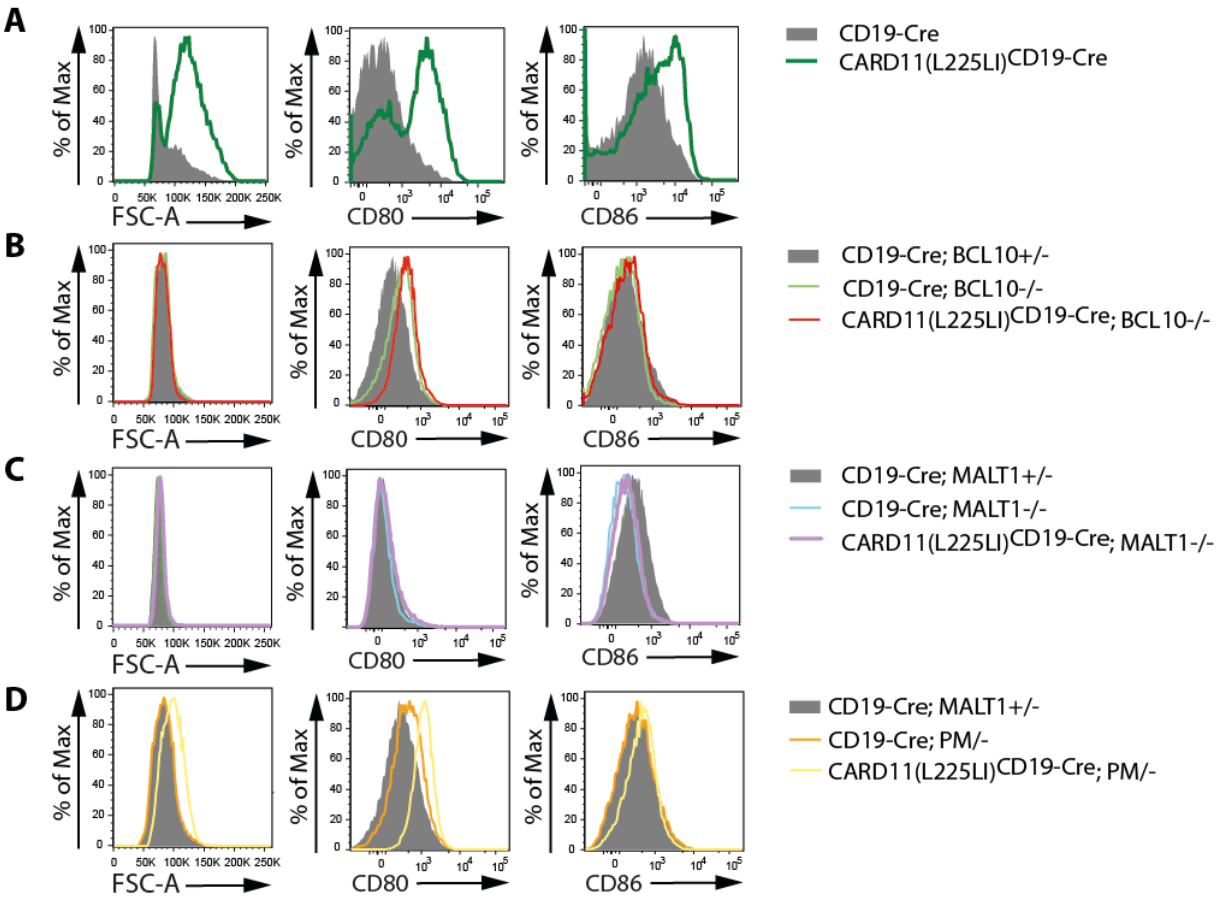

Figure 21: CARD11(L225LI)-mediated B cell activation is dependent on BCL10 and MALT1

The expression of activation markers on splenic B cells from different genotypes was assessed by flow cytometry using Forward-scatter-area (FSC-A) for cell size, CD80 and CD86 as activation marker. Animals were analyzed between two and three months of age, n ≥ 4 per genotype. A) Histograms of CD19-Cre and CARD11(L225LI)$^{CD19\text{-}Cre}$ B cells. B) Histograms of CD19-Cre;MALT1+/-, CD19-Cre;MALT1-/- and CARD11(L225LI)$^{CD19\text{-}Cre}$;MALT1-/- B cells. C) Histograms of CD19-Cre;BCL10+/-, CD19-Cre;BCL10-/- and CARD11(L225LI)$^{CD19\text{-}Cre}$;BCL10-/-. D) Histograms of CD19-Cre;MALT1+/-, CD19-Cre;PM/- and CARD11(L225LI)$^{CD19\text{-}Cre}$;PM/- B cells.

The B cell compartment of CARD11(L225LI)$^{CD19\text{-}Cre}$ animals is severely increased and is composed of strongly enlarged and activated cells (Figure 17c, 21a). Interestingly, on a BCL10- or MALT1-deficient background splenic CARD11(L225LI)-expressing B cells showed neither an increase in cell size nor surface expression of the activation markers CD80 and CD86 (Figure 21b, c). Although CARD11(L225LI)$^{CD19\text{-}Cre}$;PM/- mice did not die

prematurely, CARD11(L225LI)-expressing paracaspase-deficient B cells were bigger and up-regulated CD80 when compared to control B cells (Figure 21c).

To identify changes in lymphoid cell compartments, total cell counts from various organs were compared between BCL10-, MALT1- or paracaspase function-deficient CARD11(L225LI)-expressing mice. It is known that BCL10-/- and MALT1-/- mice lose their T_{FH} cells and GCBs within PPs due to defective NF-κB activation. As expected T_{FH} cells and GCBs were almost absent within the PPs of CARD11(L225LI)$^{CD19\text{-}Cre}$;BCL10-/- and CARD11(L225LI)$^{CD19\text{-}Cre}$;MALT1-/- and decreased in CARD11(L225LI)$^{CD19\text{-}Cre}$;PM/- mice (data not shown).

Surprisingly, we found elevated total cell counts in PPs from CARD11(L225LI)$^{CD19\text{-}Cre}$;MALT1-/- mice, which were due to elevated numbers of CD19-positive non-GCBs (Figure 22a). In contrast to MALT1-deficient CARD11(L225LI)-expressing animals, PPs were barely detectable in mice expressing CARD11(L225LI) together with the paracaspase-deficient version of MALT1, which was due to a total decline in B cell levels.

Total splenocyte counts also varied between the different genotypes. CARD11(L225LI)$^{CD19\text{-}Cre}$;BCL10-/- counts were decreased by trend, whereas CARD11(L225LI)$^{CD19\text{-}Cre}$;PM/- and CARD11(L225LI)$^{CD19\text{-}Cre}$;MALT1-/- counts were elevated (Figure 22b). Changes in splenocyte counts were consistent with alterations in mature B cell counts within the different CARD11(L225LI)-expressing genotypes, whereas T cell counts were mostly unaffected (Figure 22b).

Consistent with previous studies of BCL10 and MALT1 knock-out mice, the B-1 B cell population was absent or diminished in the peritoneal cavity of BCL10-, MALT1- or paracaspase function-deficient CARD11(L225LI)-expressing animals (data not shown). Interestingly, peritoneal cavities of CARD11(L225LI)$^{CD19\text{-}Cre}$;PM/- mice showed a decrease in B2-B cells in behalf of an increase in T cells (Figure 22c).

Ultimately, the deficiency in BCL10-, MALT1- or paracaspase function rescued CARD11(L225LI)$^{CD19\text{-}Cre}$ animals from perinatal death. Although B cells from BCL10 and MALT1-deficient animals were of normal size and not activated, it is noteworthy that

CARD11(L225LI) expression has an influence on the size of the B cell population. Interestingly, paracaspase-deficient CARD11(L225LI)$^{CD19\text{-}Cre}$ animals showed slightly activated and enlarged B cells and strong changes in different B cell compartments within examined organs.

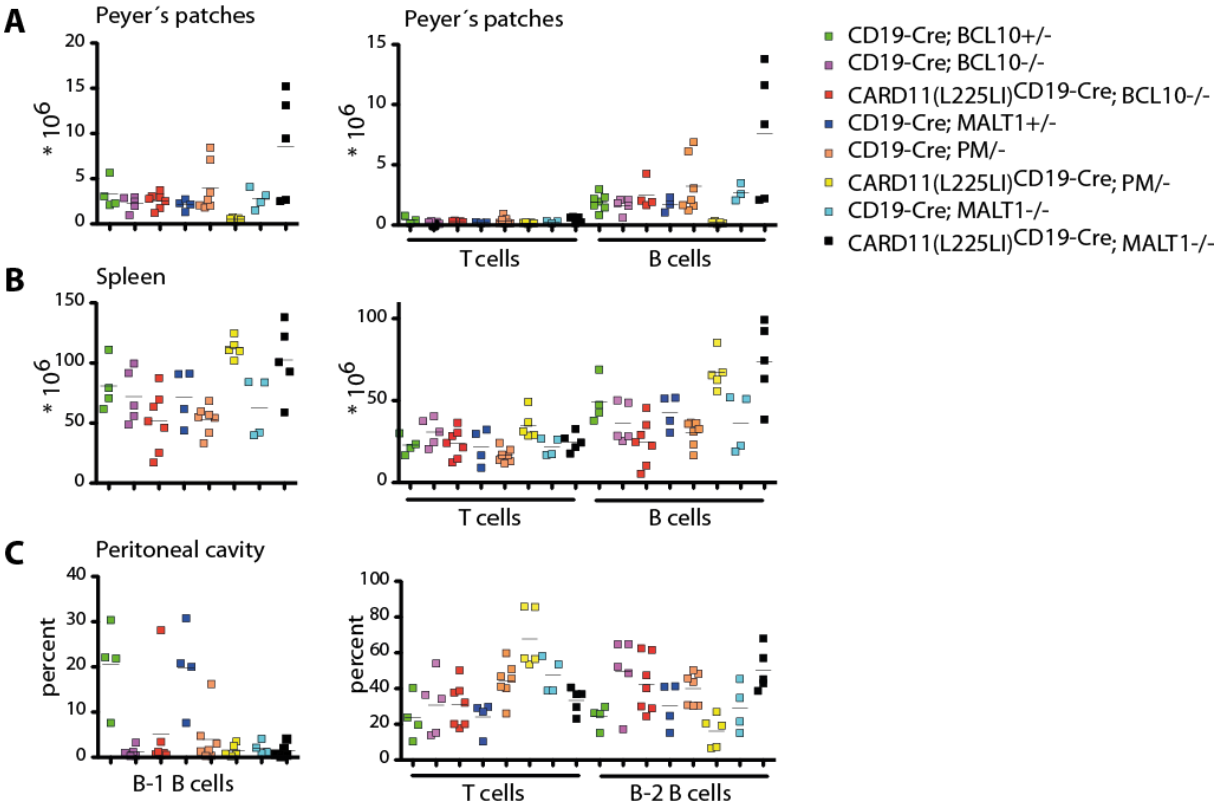

Figure 22: Distribution of lymphoid populations in various organs from different genotypes

A) Total cell counts in PPs; CD4-positive and CD19-positive cell counts and percentages of T_{FH} cells and GCBs within the CD4-positive or respectively the CD19-positive compartment in PPs. T_{FH} cells were gated as CD4+ICOS+PD-1+; GCBs were gated as CD19+CD38-Fas+. B) Total splenic cell counts; total cell counts for FO B cells (B220+AA4.1-CD23+) and splenic IgM- and IgD-expressing B cells; total cell counts for TCRβ+ CD4 and CD8 T cells C) B-1 B cell (CD19+B220^{low}CD5+) counts in peritoneal cavity as well as B-2 (CD19^{high}B220^{high}CD5-) and T cell counts (CD5+) for indicated genotypes.

3.3.4. CARD11(L225LI) expression in B cells simultaneously activates NF-κB and AP-1

CARD11 together with BCL10 and MALT1 are essential for canonical antigen receptor-induced activation of NF-κB by transducing the receptor signal through the IKK

complex. Interestingly, a mouse model expressing a constitutive active mutant of IKKβ (ca-IKKβ) in B cells showed a milder phenotype compared to mice expressing CARD11(L225LI) in the B cell lineage (Sasaki et al., 2006). Although a very comparable approach was used to express the constitutive active signaling molecule in the B cell lineage, animals did not die prematurely. Thus, CARD11(L225LI) must trigger parallel additional pathways besides NF-κB that are important for the activation and expansion of the transgenic lymphocytes.

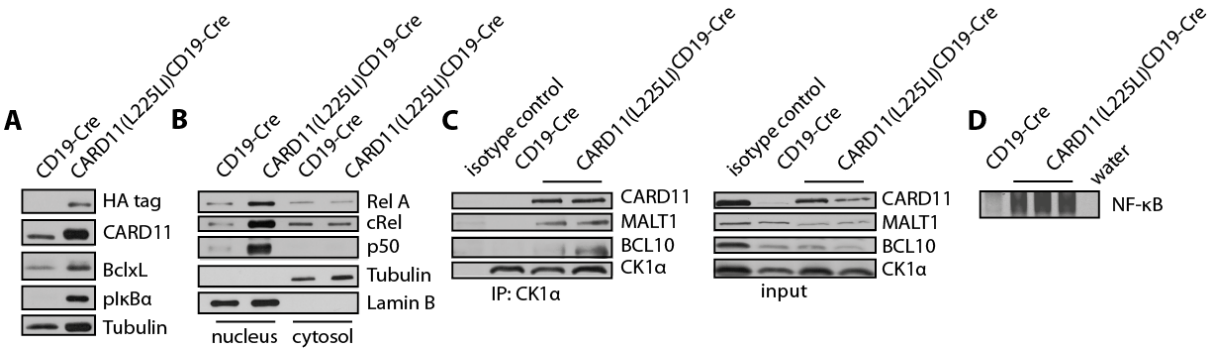

Figure 23: CARD11(L225LI)$^{CD19\text{-}Cre}$ B cells show NF-κB activation

A) Splenic B cells from 5-day-old animals of the indicated genotypes were MACS-purified (pooled) and cytosolic cell lysates were subjected to Western blot analysis. Examination of CBM protein expression (HA tag, CARD11), NF-κB activation (Bcl_{xL}, pIκBα); equal loading was verified by Tubulin. B) Nuclear lysates were prepared from samples from A), nuclear translocation of NF-κB subunits (RelA, cRel, p50) was examined; equal loading was controlled in nuclear extracts by Lamin B and in cytosolic fractions by Tubulin. C) Lysates from B cells from 5-day-old animals were immunoprecipitated with anti-CK1α and immunocomplexes were analyzed for the presence for CARD11, BCL10, MALT1 or CK1α by immunoblotting. D) Nuclear extracts from B) were subjected to EMSA for NF-κB DNA-binding activity. Western blot lysates and immunoprecipitations were obtained from at least 3 independent experiments.

Since CBM signaling is also involved in antigen receptor induced IKK activation, we speculated that CARD11(L225LI) triggers spontaneous NF-κB signaling. Indeed, constitutive IκBα phosphorylation was found in the cytosol of transgenic B cells, which is the result of IKK complex activity. To investigate the nuclear consequences of these cytosolic signaling events, we performed cell fractionations. In line with constitutive active IKK signaling, we detected high levels of the NF-κB subunits RelA, cRel and p50 in the nucleus of primary B cells from CARD11(L225LI)$^{CD19\text{-}Cre}$ animals (Figure 23b).

Subsequent IκBα degradation leads to the release of NF-κB subunits, which induce expression of NF-κB target genes. One of these target genes is Bcl_{xL}, which was found in the cytosol of transgenic B cells (Figure 23a).

As indicated above, antigen-induced BCR signaling triggers an inducible association of CARD11 with BCL10 and MALT1 and the formation of the CBM complex that recruits further factors including casein kinase 1 α (CK1α) into the signalosome for downstream signaling (Bidère et al., 2009; Thome et al., 2010). To test whether mutant CARD11(L225LI) expression would induce a constitutive assembly of CBM complexes *in vivo*, we immunoprecipitated CK1α from CARD11(L225LI)$^{CD19\text{-}Cre}$ transgenic or WT B cells and tested the association with CARD11, BCL10 and MALT1. Western blotting revealed that indeed CBM complexes are constitutively assembled in CARD11(L225LI)$^{CD19\text{-}Cre}$ transgenic B cells (Figure 23c). The DNA-binding ability of translocated NF-κB subunits was examined by EMSA and verified strong NF-κB DNA-binding within CARD11(L225LI)$^{CD19\text{-}Cre}$ samples (Figure 23d).

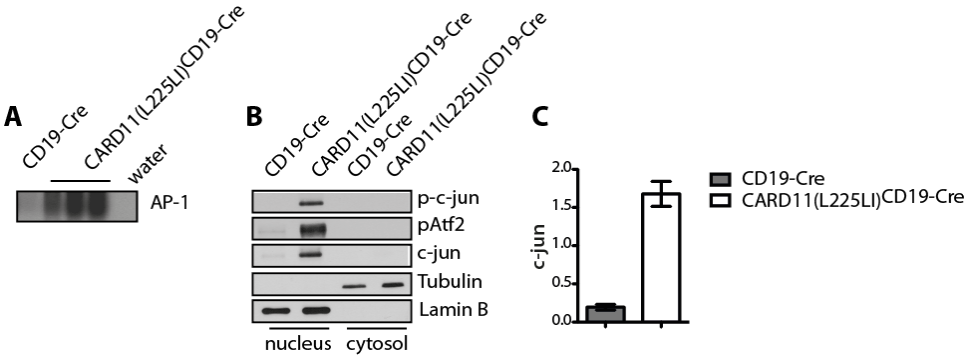

Figure 24: CARD11(L225LI)$^{CD19\text{-}Cre}$ B cells show AP-1 activation

A) Nuclear extracts from Figure 23 were subjected to EMSA for AP-1 DNA-binding activity. B) Nuclear translocation of AP-1 transcription factor subunits (pAtf2, p-c-Jun, c-Jun); equal loading was controlled in nuclear extracts by Lamin B and in cytosolic fractions by Tubulin. C) Relative expression levels of *c-Jun* within CD19-Cre and CARD11(L225LI)$^{CD19\text{-}Cre}$ MACS-purified splenic B cells from 5-day-old animals. The expression levels were normalized to the housekeeping gene *Hrpt1* (n = 4). Western blot lysates were obtained from at least 3 independent experiments.

As it is known that CARD11 is able to transduce signals, which are important for AP-1 activation, nuclear lysates were tested also with an AP-1 probe (Blonska et al., 2007). EMSA revealed strong binding of AP-1 subunits to the respective binding motif (Figure 24a). We examined the translocation of the well-known AP-1 subunits Atf2 and c-Jun.

Indeed, those were found to be phosphorylated and translocated to the nuclei of CARD11(L225LI)$^{CD19\text{-}Cre}$ cells (Figure 24b). According to nuclear translocation and DNA-binding activity, we found high transcript levels of *c-Jun*. C-Jun is known to sustain its expression levels in auto-regulatory-manner (Figure 24c).

In summary, we could demonstrate that enforced CARD11-BCL10-MALT1 signaling in CARD11(L225LI)-expressing cells activates NF-κB and JNK pathways simultaneously. This combined activation of JNK and NF-κB signaling is presumably a reason for the fundamentally different phenotypes of ca-IKKβ and ca-CARD11 transgenic mice and causative for the rapidly lethal phenotype triggered by CARD11(L225LI) expression in B cells *in vivo*.

3.3.5. Constitutive JNK and IKK activation triggered by CARD11(L225LI) depends on the presence of BCL10 and MALT1

Since normal CBM signaling is also involved in antigen receptor induced JNK activation (Hara et al., 2003), we speculated that CARD11(L225LI) triggers NF-κB and JNK signaling in BCL10 and MALT1-dependent manner *in vivo*. To test this hypothesis, we performed western blot analysis of cytosolic extracts from CARD11(L225LI)-expressing cells in a WT, BCL10-/-, MALT1-/- or PM/- background.

CARD11(L225LI)$^{CD19\text{-}Cre}$ B cells showed NF-κB and JNK activation (see Figure 23, 24). Basal phosphorylation levels of AKT at Serine 473 (strong exposure) were decreased within the CARD11(L225LI)$^{CD19\text{-}Cre}$ B cells compared to other genotypes. BCL10 and MALT1 deficiency abolished NF-κB and JNK activation, as IκBα and JNK phosphorylation were absent and Bcl_{xL} and c-Jun were not present in the cytosol (Figure 25a, b). Interestingly, the expression of paracaspase-deficient MALT1 ablated constitutive NF-κB activation and decreased AKT phosphorylation. Yet, JNK activation and c-Jun stabilization were maintained (Figure 25c).

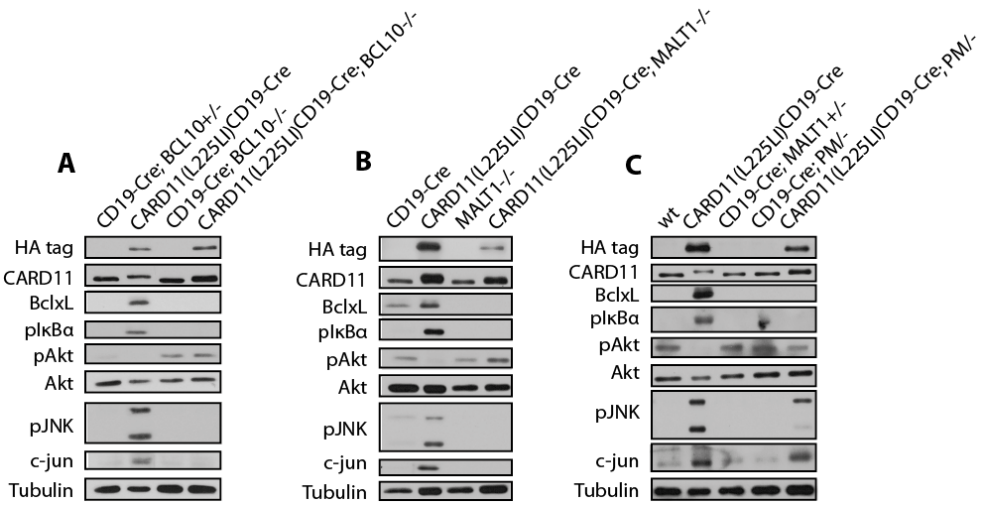

Figure 25: Role of BCL10 and MALT1 in CARD11(L225LI)-triggered signaling
A) – C) CD19-Cre and CARD11(L225LI)$^{CD19\text{-}Cre}$ samples were prepared from MACS-purified B cells (pooled) from spleens from 5-day-old mice. Other genotypes were sacrificed at ages between 6 and 12 weeks and splenic B cells were MACS-purified. Cytosolic extracts were prepared and analyzed for CBM protein expression (HA tag, CARD11), NF-κB activation (Bcl_{xL}, pIκBα), AKT signaling (pAKT, AKT), JNK pathway activation (pJNK, c-Jun); equal loading was verified by Tubulin. Western blot lysates were obtained from at least 3 independent experiments.

Next, lysates were tested for the presence of cleavage fragments of known paracaspase targets such as RelB and CYLD in CARD11(L225LI)$^{CD19\text{-}Cre}$ cells, and further whether these cleavage products were absent in CARD11(L225LI)$^{CD19\text{-}Cre}$;PM/- or CARD11(L225LI)$^{CD19\text{-}Cre}$;MALT1-/- and CARD11(L225LI)$^{CD19\text{-}Cre}$;BCL10-/- B cells (Figure 26). Indeed cleavage products were present without additional receptor stimulation in CARD11(L225LI)$^{CD19\text{-}Cre}$ cells and as expected absent in BCL10- and MALT1-deficient or PM cells.

Since both the constitutive IκBα phosphorylation as well as the constitutive JNK phosphorylation were not observed in CARD11(L225LI)-expressing B cells that are deficient for BCL10 or MALT1, we conclude that CARD11(L225LI) activates both IKK and JNK signaling simultaneously through BCL10 and MALT1 engagement. Besides, we found that MALT1 as scaffolding molecule is essential for JNK activation and that paracaspase activity is necessary for complete NF-κB activation.

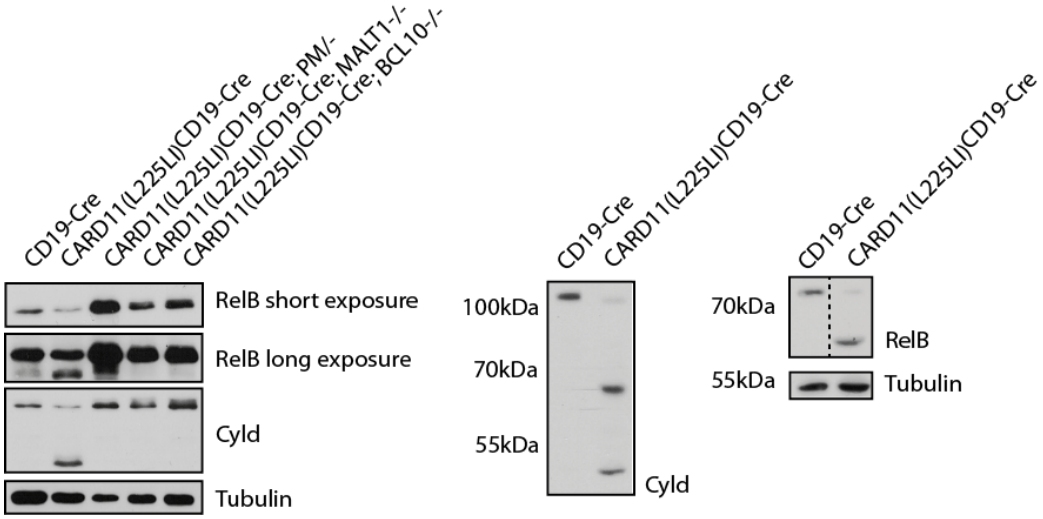

Figure 26: Assessment of constitutive paracaspase activity in different genotypes

CD19-Cre and CARD11(L225LI)$^{CD19\text{-}Cre}$ samples were prepared from MACS-purified B cells (pooled) from spleens from 5-day-old mice. Other genotypes were sacrificed at ages between 6 and 12 weeks and splenic B cells were MACS-purified. Cytosolic extracts were prepared and analyzed for RelB and CYLD. Equal loading was verified by Tubulin. Western blot lysates were obtained from at least 3 independent experiments.

3.3.6. IKK and JNK control viability of primary CARD11(L225LI)-expressing B cells

The CARD11(L225LI)$^{CD19\text{-}Cre}$ mice succumb prematurely to a lethal lymphoproliferation, which depends on functional CBM complex formation. A genetic approach (CARD11(L225LI)$^{CD19\text{-}Cre}$;BCL10-/-, CARD11(L225LI)$^{CD19\text{-}Cre}$;Malt1-/- and CARD11(L225LI)$^{CD19\text{-}Cre}$;PM/-) showed that full oncogenic potential of CARD11(L225LI) is CBM-dependent. To examine cell proliferation, B cells were labeled with a proliferation dye.

CARD11(L225LI)$^{CD19\text{-}Cre}$ cells were treated with different mitogenic stimuli to analyze proliferation upon engagement of diverse receptors. Interestingly, the addition of different stimuli for 48 hours, such as α-CD40, CpG, α-IgM or LPS, did not increase proliferation of CARD11(L225LI)-expressing cells compared to untreated cells, which proliferated vigorously. In contrast to CARD11(L225LI)-expressing cells the addition of

CpG and LPS triggered proliferation of CD19-Cre B cells, which did not divide without the addition of external stimuli (Figure 27a). In contrast to B cells from CD19-Cre mice, the CARD11(L225LI)-expressing B lymphocytes survived for at least 10 days under these conditions and even expanded (Figure 27b).

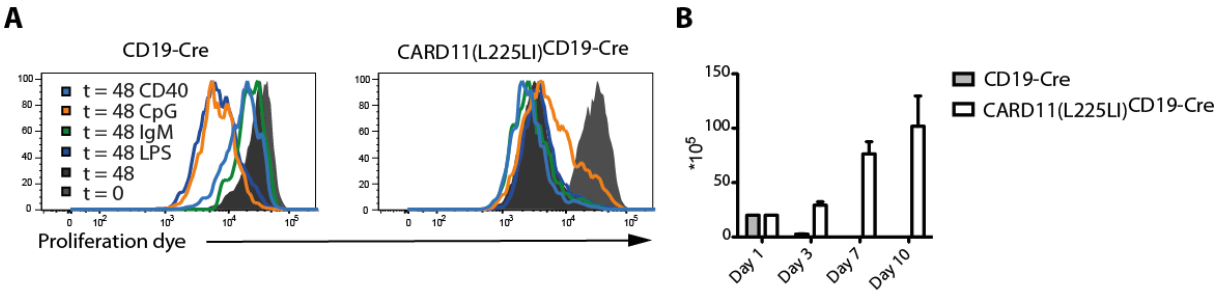

Figure 27: Proliferation of CARD11(L225LI)-expressing B cells
A) Proliferation of CD19-positive live cells was measured upon different stimuli after 48 hours: α-CD40; CpG; α-IgM; LPS; Experiment was conducted twice with total n = 3. B) Survival and proliferation of splenocytes from CD19-Cre and CARD11(L225LI)$^{CD19\text{-}Cre}$ mice was evaluated by Trypan Blue exclusion. Experiment was conducted twice with total n = 7. Data are presented as mean ± SEM.

These results are consistent with the notion that ca-CARD11 is a strong driver of B cell survival and proliferation and in line with the massive expansion of B cells in CARD11(L225LI)$^{CD19\text{-}Cre}$ mice. On a molecular level we also observed a constitutive activation of NF-κB and JNK signaling *in vitro* with high nuclear levels of RelA, cRel and p50 or activated c-Jun and Atf2. To test whether the autonomous downstream signaling of CARD11(L225LI) could be pharmacologically manipulated, we treated the cells with well characterized small molecule inhibitors for IKK or JNK (Lee and Hung, 2008; Gururajan, 2005).

As the IKK inhibitor Bay11-7082 blocks the kinase activity of IKKα and IKKβ and inhibits irreversibly the phosphorylation of IκBα, treatment by this inhibitor should abolish the translocation of the canonical NF-κB subunits (Keller et al., 2000; Rauert-Wunderlich et al., 2013; Lee and Hung, 2008). Indeed, IKK inhibition resulted in a strong reduction of nuclear NF-κB family members RelA, cRel, and p50 (Figure 28a).

All JNK isoforms are inhibited by SP600125, which shows minimal off-target effects for MKK4 and MKK6 (Bennett et al., 2001). The recently discovered JNK-in-8 inhibitor was optimized to reduce off-target effects due to irreversible binding to the conserved

catalytic cysteine in JNK (Zhang et al., 2012). The inhibition of JNK kinase activity with both inhibitors blocked the presence of phosphorylated c-Jun and reduced the levels of phosphorylated Atf2 in the nucleus (Figure 28b, c).

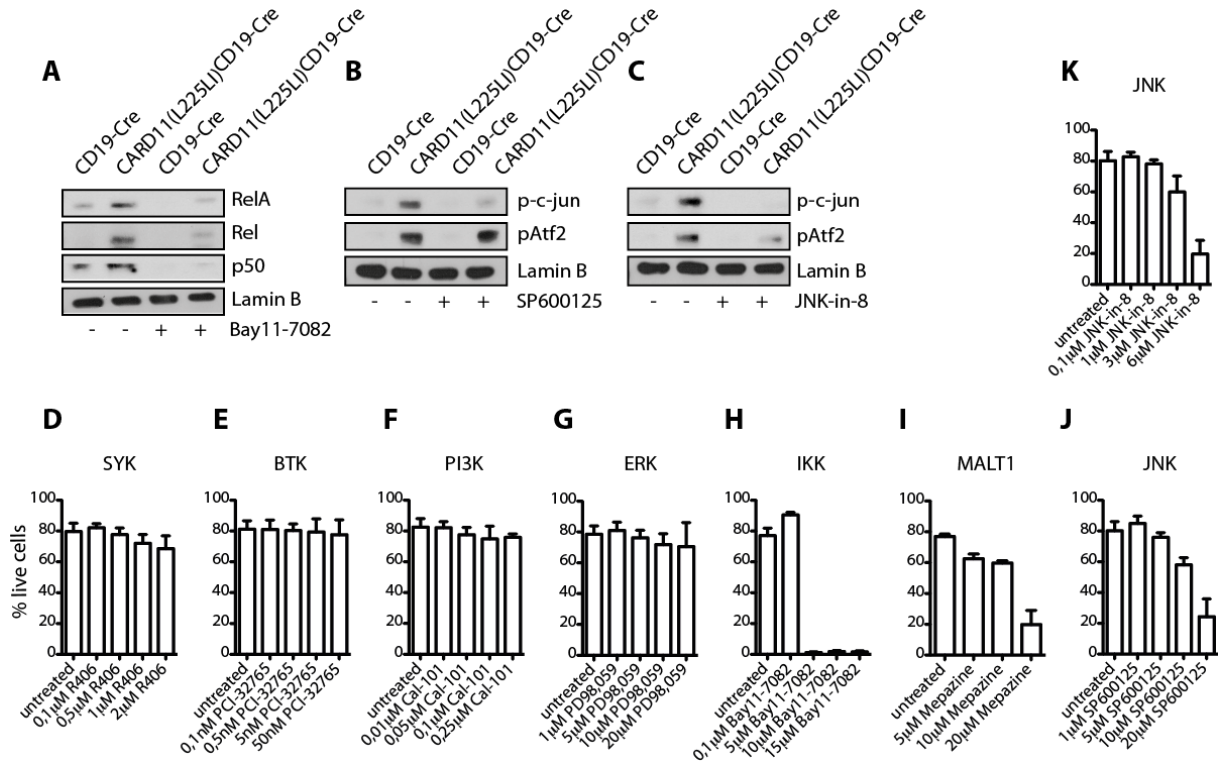

Figure 28: JNK and IKK inhibitors are toxic to CARD11(L225LI)-expressing cells
A) CD19-Cre and CARD11(L225LI)$^{CD19\text{-}Cre}$ splenocytes were left untreated or treated with 15µM Bay11-7082 for four hours, nuclear lysates were examined for the presence of RelA, cRel and p50. B) CD19-Cre and CARD11(L225LI)$^{CD19\text{-}Cre}$ splenocytes were left untreated or treated with 20µM SP600125 for four hours or with C) 10µM JNK-in-8 for four hours; nuclear lysates were examined for the presence of p-c-Jun and pAtf2. Experiments were conducted three times. D-L) Cells were cultured untreated (solvent control DMSO) or in presence of indicated concentrations of following inhibitors: R406 D), Cal-101 E), PCI-32765 F), PD98,059 G), Bay11-7082 H), Mepazine I), SP600125 J) and JNK-in-8 K) for 48 hours, then Annexin V-negative and 7AAD-negative cells were determined by flow cytometry. Experiment was performed at least twice with total n ≥ 4. Data are presented as mean ± SEM.

Next, CARD11(L225LI)$^{CD19\text{-}Cre}$ cells were treated with different inhibitors and the frequency of live cells was measured 48 hours after treatment at indicated concentrations. Neither SYK (R406) (Figure 28d), BTK (Figure 28e), PI3K (Figure 28f) or ERK (Figure 28g) inhibition did significantly affect the viability of CARD11(L225LI)-expressing B cells in culture. These findings are in line with the

established role of CBM complexes downstream of SYK and presumably BTK and PI3K (reviewed in (Staudt, 2010)) and the independence of CBM activity from ERK MAPK signaling. The inhibition of NF-κB signaling killed CARD11(L225LI)-expressing B cells, which is in line with known sensitivity of human ABC-DLBCL cells to IKK inhibition (Figure 28h). As expected from genetic data (CARD11(L225LI)$^{CD19\text{-}Cre}$;PM/-), Mepazine, which is recently in the focus as promising therapeutic for DLBCL (previously used in the treatment of chronic schizophrenic patients (Whittier et al., 1960; Nagel et al., 2012)) also efficiently killed CARD11(L225LI)$^{CD19\text{-}Cre}$ cells (Figure 28i). Intriguingly, the pharmacological inhibition of JNK signaling with SP600125 (JNK inhibitor) (Figure 28j) or with another independent JNK inhibitor (JNK-in-8) also induced cell death in CARD11(L225LI)-expressing cells (Figure 28k) demonstrating that the massive expansion of CARD11(L225LI)-expressing B cells is not only NF-κB dependent but in addition critically requires JNK signaling.

Due to the high toxicity of NF-κB inhibition, IKK inhibitors are so far not used in clinics. Therefore, we were interested in lowering concentrations of Bay11-7082 to a minimum (Figure 29). We combined low doses of SP600125 and Bay11-7082 and found that we could reduce both to a minimal level for significant toxicity to lymphoma cells (Figure 29a). We obtained similar results by combining JNK-in-8 and Bay11-7082 (Figure 29b).

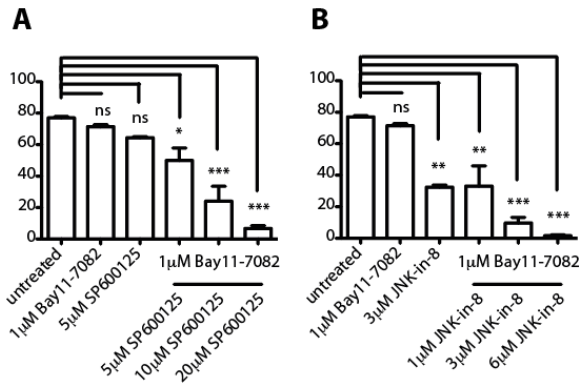

Figure 29: Dose titration for IKK and JNK inhibitor combination
CARD11(L225LI)$^{CD19\text{-}Cre}$ splenocytes were treated for 48 hours with single inhibitors such as Bay11-7082, SP600125 and JNK-in-8 and in different combinations. Annexin V-negative and 7AAD-negative cells were determined by flow cytometry. Experiment was performed at least twice with total n≥3. Data are presented as mean ± SEM.

To test, whether inhibitor treatment led to cell cycle arrest followed by cell death or to cell death within the current cell cycle phase, cells were labeled with a proliferation dye for 48 hours (Figure 30) and within a second approach with Bromodeoxyuridine (BrdU) (Figure 31).

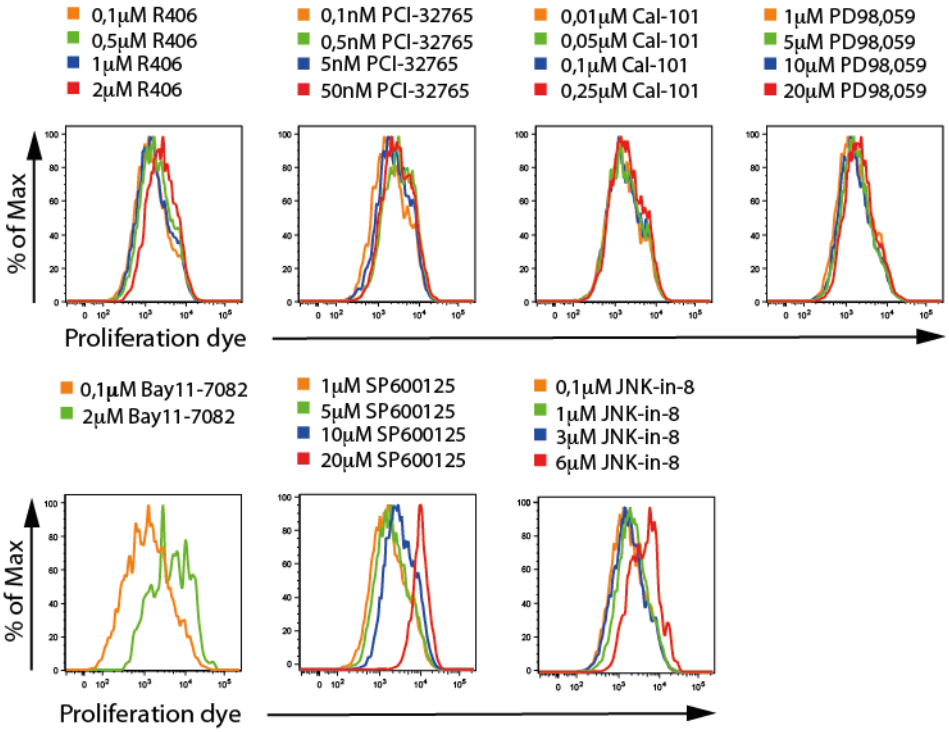

Figure 30: JNK and IKK inhibitors do not severely impair proliferation
CARD11(L225LI)$^{CD19\text{-}Cre}$ splenocytes were labeled with a proliferation dye and cultured untreated (solvent control DMSO) or in presence of indicated concentrations of following inhibitors: R406, PCI-32765, Cal-101, PD98,059, Bay11-7082, SP600125 and JNK-in-8 for 48 hours, then Annexin V-negative and 7AAD-negative cells were determined by flow cytometry. Experiment was performed at least twice with total n ≥ 4.

The dilution of the proliferation dye in CARD11(L225LI)-expressing B cells was measured by flow cytometry and revealed that neither SYK, BTK, PI3K or ERK inhibition did affect cell proliferation of CARD11(L225LI)-expressing B cells in culture, and that even treatment with IKK and JNK inhibitors diminished proliferation at highest concentrations just slightly.

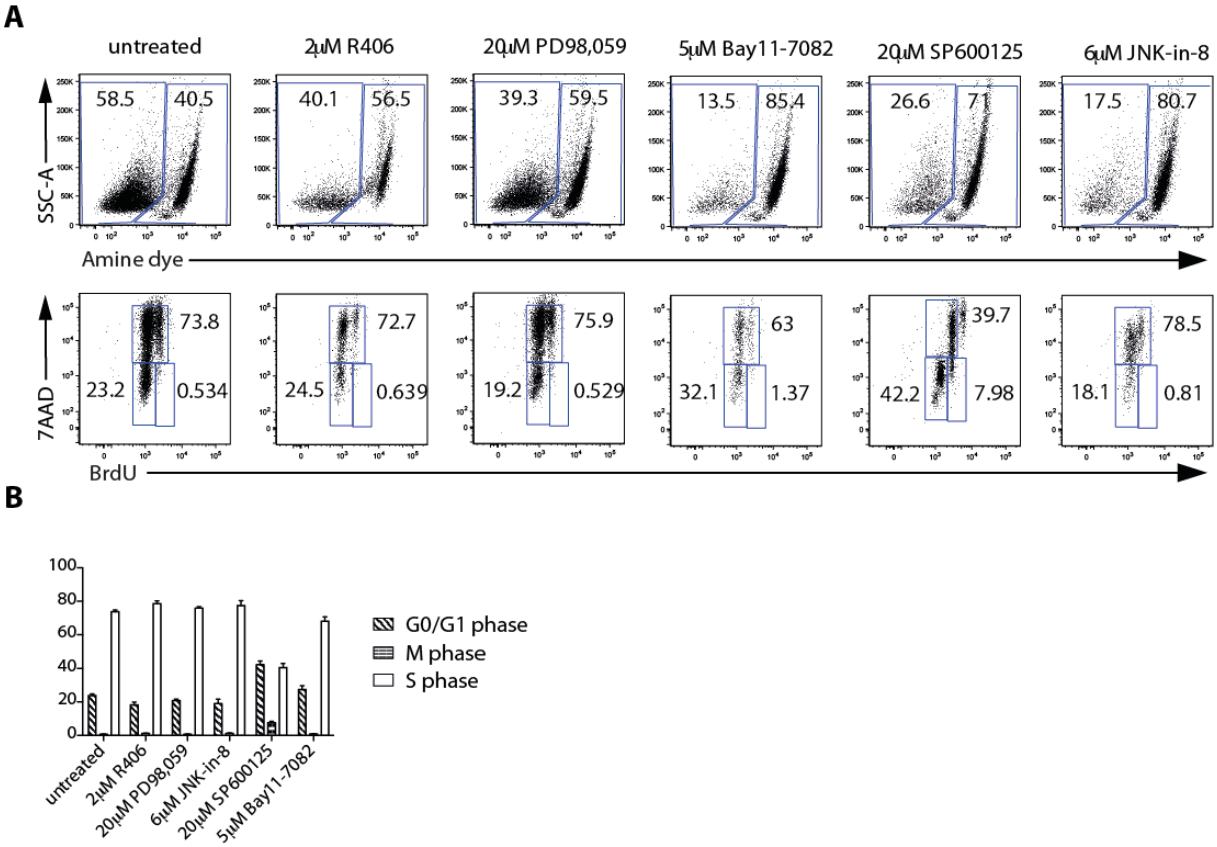

Figure 31: IKK and JNK inhibition do not cause cell cycle arrest

A) CARD11(L225LI)$^{CD19\text{-}Cre}$ splenocytes were labeled with BrdU and left either untreated or were treated with different inhibitors at given concentrations for 48 hours. First gate was set on live cells, which are Amine dye-negative and further gated on 7AAD and BrdU. G0/G1: BrdU low and 7AAD low; Synthesis (S): BrdU high and 7AAD high; Mitose (M): BrdU high and 7AAD low. B) Summary of cell cycle distribution of live cells. Data are presented as mean, the experiment was conducted once with n = 5.

A BrdU assay was performed with selected inhibitors to analyze effects on the cell cycle. Already within the untreated sample, a decreased frequency of live cells was found compared to untreated cells from experiments performed for Figure 28. This might have been due to BrdU toxicity (Figure 31). To analyze the cell cycle phases, live CARD11(L225LI)$^{CD19\text{-}Cre}$ cells were stained intracellularly for BrdU. The combination with 7AAD, which is a DNA intercalating marker, allows the identification of DNA contents within dividing or non-dividing cells. Therefore, cells in the G0/G1 phase were defined as BrdU low and 7AAD low, in the synthesis (S) phase as BrdU high and 7AAD high, which appeared as a double peak and in the mitose (M) phase as BrdU high and 7AAD low. This assay showed that more than 70% of the CARD11(L225LI)$^{CD19\text{-}Cre}$ cells were in the S phase, whereas less than 1% of the cells were in the M phase. The

distribution of the cell cycle phases were not affected by the treatment with R406, PD98,059 and JNK-in-8. However, whereas treatment with the Bay11-7082 inhibitor led to a mild increase of cells within the G0/G1 phase, the SP600125 inhibitor doubled the frequency of cells in this phase. From this experiment, one could conclude that JNK and IKK inhibition in CARD11(L225LI)$^{CD19\text{-}Cre}$ cells rather kills cells within the actual cell cycle phase than leading to cell cycle arrest and subsequent cell death.

CARD11(L225LI) expression in early B cell compartments lead to fatal lymphoproliferative disease. Malignant cells resembled terminally differentiated plasma cells, which proliferated spontaneously in culture. The oncogenic potential of CARD11(L225LI) strictly depends on BCL10 and MALT1 engagement, which is required for further IKK and JNK activation. The pharmacological inhibition of IKK as well as of JNK impaired the survival of the malignant cells *in vitro* and killed the cells within the S phase, which is the predominant cell cycle phase of CARD11(L225LI)-expressing cells.

3.4. Effect of CARD11(L225LI) expression in activated B cells

3.4.1. Absence of germinal center B cells in CARD11(L225LI) $^{Cγ1\text{-}Cre}$ mice

We induced the CARD11(L225LI) mutation via CD19-Cre in a large population of B cells in our mouse model, which resulted in a polyclonal malignancy. In the human, DLBCL most likely originate within a limited B cell population in or after the GC. For this reason, we intercrossed the CARD11(L225LI) mice with the Cγ1-Cre mouse strain (Casola et al., 2006). In these mice, Cre is expressed from the constant gamma 1 heavy chain (IgG1) locus and Cre-mediated transgene expression is restricted to IgG1-positive B cells, therefore to a small population at the steady state level (Xu et al., 2012). The IgG1 class switch was induced by immunization with sheep red blood cells (SRBs). Cγ1-Cre and CARD11(L225LI)$^{stop FL}$ double transgenic mice are called throughout this study CARD11(L225LI)$^{Cγ1\text{-}Cre}$ mice. Un-immunized CARD11(L225LI)$^{Cγ1\text{-}Cre}$ mice did not manifest obvious signs of illness, and were analyzed at the age of 2-3 months (Figure 32).

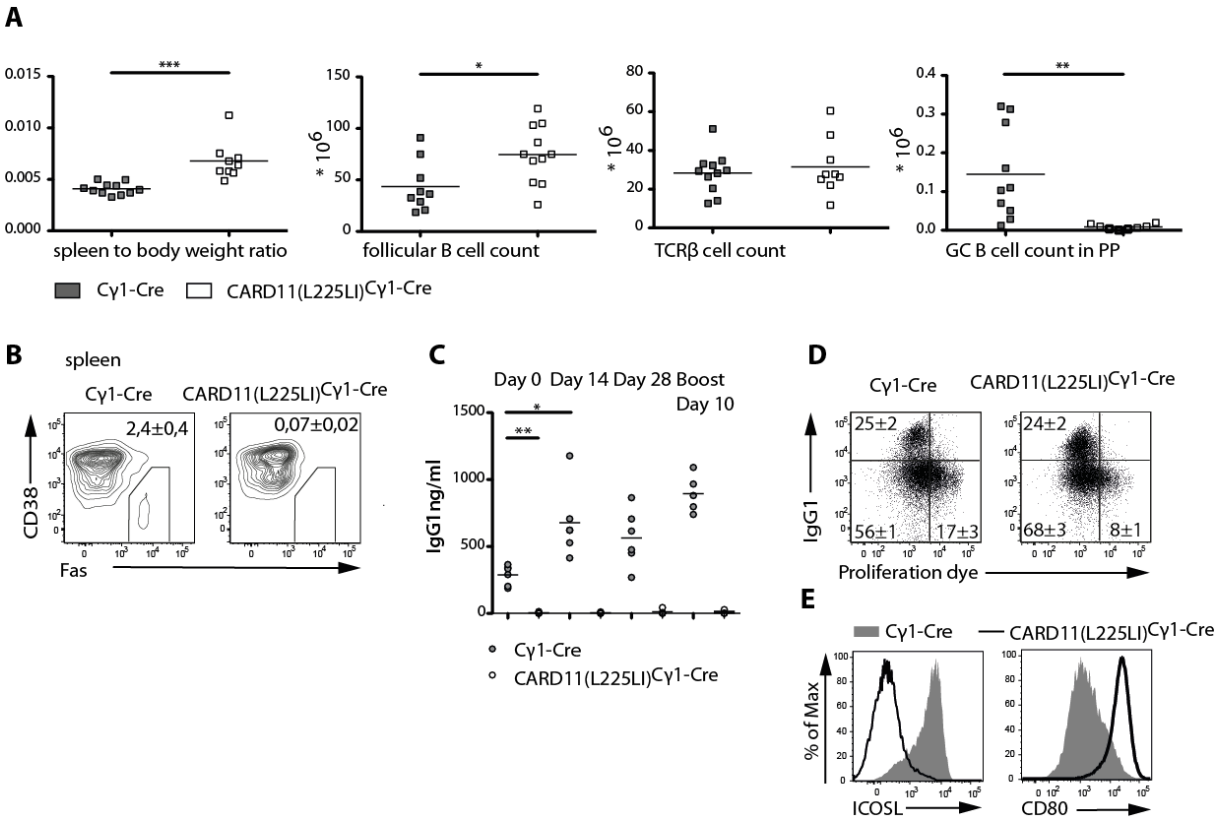

Figure 32: Characterization 2-3 month-old CARD11(L225LI)$^{Cγ1\text{-}Cre}$ animals

A) Spleen to body weight ratio; total cell counts from splenic FO B cells (B220+AA4.1-IgM+CD23+) and splenic T cells (TCRβ+); GCB cell count (CD19+CD38-Fas+) in PPs of 6-12 week-old Cγ1-Cre and CARD11(L225LI)$^{Cγ1\text{-}Cre}$ animals. B) Spleens were analyzed 9 days after immunization with sheep red blood cells by flow cytometry. Splenocytes were gated on CD19-positive lymphocytes. Data are shown as mean ± SEM of n = 4 per genotype. C) IgG1 serum antibodies at day 14 and day 28 after primary SRBC immunization, and 10 days after secondary immunization, n = 5 per genotype, experiment was conducted twice. D) Splenic B cells were MACS-purified, labeled with proliferation dye and cultured in the presence of 4 ng/ml IL-4 and 4 µg/ml α-CD40 for 96 hours; in vitro class switch was assessed by surface expression of IgG1; E) B cells from D) were further analyzed for surface expression of ICOS ligand (ICOSL) and CD80. FACS blots are representative of two independent experiments. Data are represented as mean ± SD of n = 4 per genotype.

2-3 month-old CARD11(L225LI)$^{Cγ1\text{-}Cre}$ mice showed splenomegaly due to an increase in mature B cells (B220+AA4.1-IgM+CD23+), whereas T cell counts were comparable to control animals. The permanent contact of gut-antigens with B cells within the PPs results in an ongoing GCB reaction with class switch recombination also to the IgG1 isotype. Therefore, IgG1-expressing and hence eGFP-expressing cells were expected to be present without immunization within the PPs (Calado et al., 2012). Surprisingly,

gut-residual Peyer´s patches (PP) were almost gone and remaining PPs showed absence of the GCB population (Figure 32a).

For this reason animals were immunized with SRBs to force IgG1 expression in splenic B cells. In the immunized CARD11(L225LI)$^{C\gamma1\text{-}Cre}$ animals, we again did not detect GCBs in the spleen as well as in PPs (Figure 32b). Furthermore, the measurement of serum IgG1 levels revealed that the IgG1 class switch is defective in CARD11(L225LI)$^{C\gamma1\text{-}Cre}$ *in vivo* (Figure 32c).

To assess whether IgG1 expression could be induced *in vitro*, splenic B cells from Cγ1-Cre and CARD11(L225LI)$^{C\gamma1\text{-}Cre}$ animals were cultured in conditions favorable for an IgG1 class switch. This assay revealed that transgenic cells were able to recombine and to express surface IgG1 and eGFP (Figure 32d). Another important observation within this assay was that surface expression of ICOS ligand (ICOSL) and CD80, which are necessary for the interaction between GCB and T_{FH} within the GC, were deregulated in CARD11(L225LI)-expressing B cells. CARD11(L225LI)$^{C\gamma1\text{-}Cre}$ B cells failed to up-regulate ICOSL and expressed CD80 at very high levels (Figure 32e).

When using the Cγ1-Cre strain for CARD11(L225LI) expression, eGFP-positive cells were neither detected before nor after immunization, and GCBs were not present in PPs in 2-3 month-old CARD11(L225LI)$^{C\gamma1\text{-}Cre}$ mice. Yet, we found splenomegaly due to an increase in mature B cells in these animals. Although the class switch *in vitro* was functional, several surface marker were dysregulated on CARD11(L225LI)-expressing B cells *in vitro* and the humoral immune response was defective *in vivo.*

3.4.2. Germinal center-specific expression of CARD11(L225LI) leads to lymphomagenesis

Unexpectedly, CARD11(L225LI)$^{C\gamma1\text{-}Cre}$ had to be sacrificed around the age of 8 month due to visible lymphadenopathy and splenomegaly (Figure 33a, b). Diseased animals showed systemic cytokines such as IL-10 and TNFα (Figure 33c). Interestingly, eGFP expression was found in B cells, but also in CD4-positive T cells (Figure 33d). CD8-positive T cells were eGFP-negative. The occurrence of eGFP-positive CD4-positive T cells was

surprising as the Cγ1-Cre strain was described to be B cell-specific and expression in T cells negligible (about 0.1%) (Casola et al., 2006).

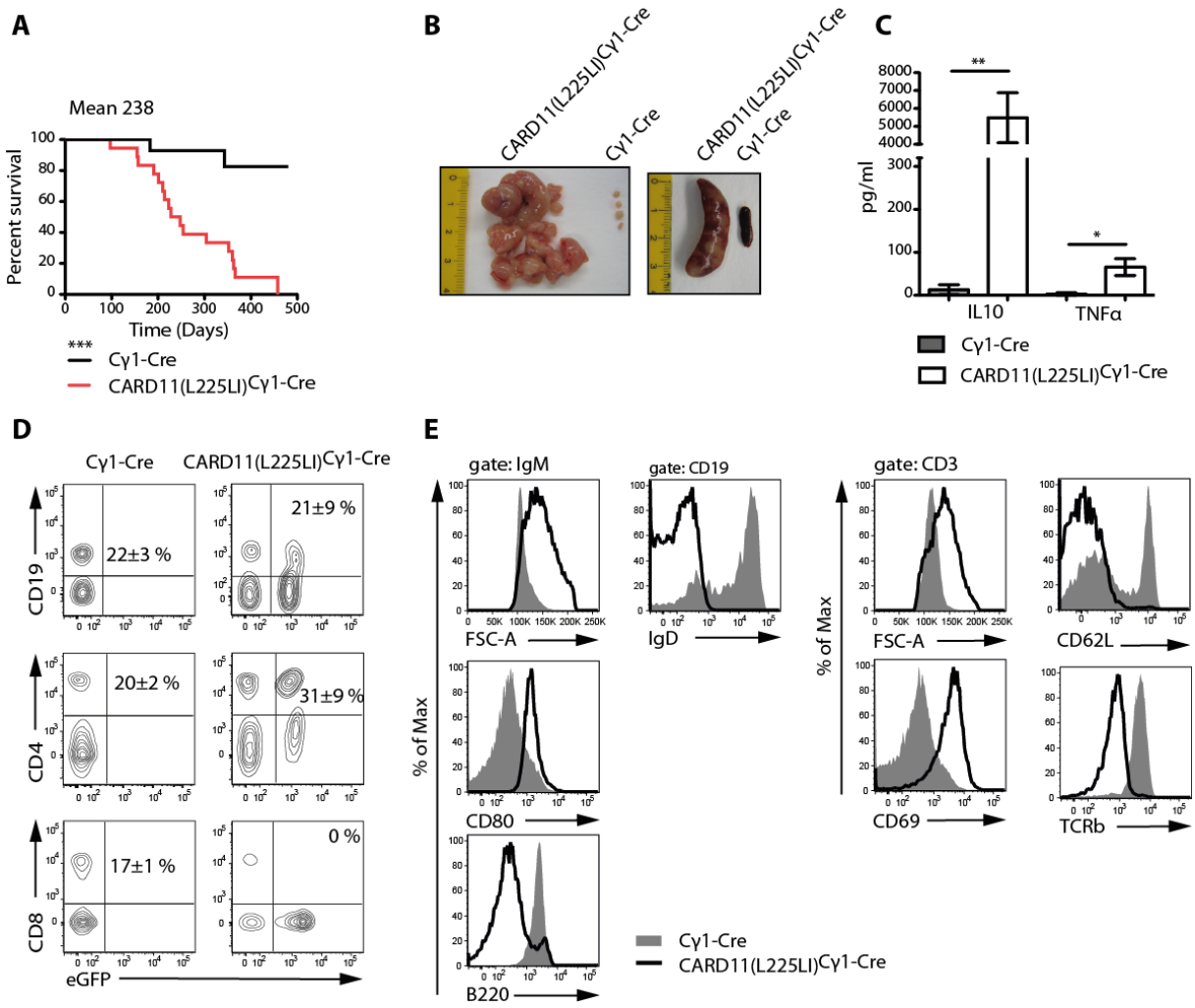

Figure 33: CARD11(L225LI)$^{Cγ1\text{-}Cre}$ animals develop mixed lymphoma

A) Kaplan-Meier curves of Cγ1-Cre and CARD11(L225LI)$^{Cγ1\text{-}Cre}$ animals n ≥ 14. B) Lymph nodes (left) and spleens (right) of Cγ1-Cre and CARD11(L225LI)$^{Cγ1\text{-}Cre}$ animals. C) Serum levels of the cytokines IL-10 and TNFα from 6 mice per genotype. D) Lymph nodes were examined for eGFP expression in CD19-, CD4- and CD8-positive cells. Data are shown as mean ± SD, n ≥ 5 per genotype. E) Flow cytometric analysis of cells from lymph nodes. Plots in left column show representative surface marker expression gated on IgM-positive B cells (FSC-A). Plots in right column are pregated on CD3-positive T cells.

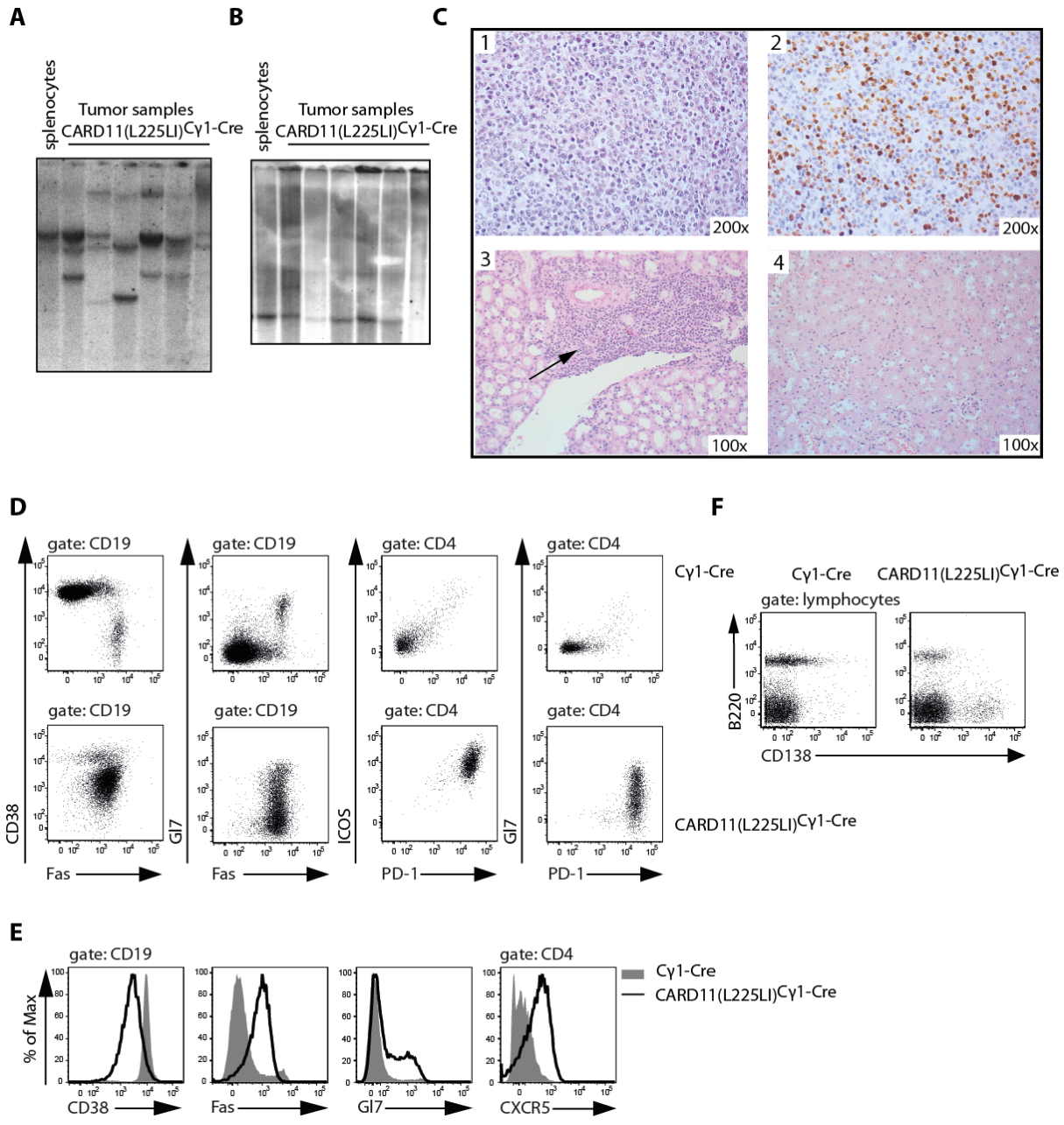

Figure 34: Characterization of CARD11(L225LI)$^{Cγ1\text{-}Cre}$ tumor cells

A-B) Southern blot analysis for tumor clonality using a (A) JH4 probe for B cell receptor rearrangement and a (B) TCRβ2 probe for T cell receptor rearrangement. C) Representative immunohistochemical staining of spleens from terminally-ill CARD11(L225LI)$^{Cγ1\text{-}Cre}$ mice; 1 and 2 depict lymph nodes from CARD11(L225LI)$^{Cγ1\text{-}Cre}$ mice; 3 shows a kidney with tumor infiltration from a CARD11(L225LI)$^{Cγ1\text{-}Cre}$ mouse and 4 displays a control kidney. 1, 3 and 4 are stained with H&E and 2 against the proliferation marker Ki-67 D) Cell surface stainings of CD19-positive B cells from Peyer's patches of Cγ1-Cre control mice (upper row) or from diseased CARD11(L225LI)$^{Cγ1\text{-}Cre}$ animals (lower row). E) Representative overlays of CD38, Fas, Gl7 and CXCR5 histograms for control and transgenic animals. F) Analysis of a control spleen and tumor showing B220 and CD138 staining on total lymphocyte gate.

CARD11(L225LI)-expressing B cells (CD19+IgM+) were enlarged in cell size compared to control B cells and strongly activated (CD80 up-regulation), additionally they down-regulated B220 and IgD surface expression (Figure 33d). CD4-positive T cells (CD3+) were also enlarged and displayed an activated/memory phenotype, as indicated by the up-regulation of CD69 and down-regulation of CD62L and TCRβ.

Southern blot analysis revealed clonal origin of tumor-infiltrating B cells (Figure 34a) and polyclonal identity of T cells (Figure 34b). The histological examination of transgenic lymph nodes confirmed a high-grade lymphoma consisting of proliferating (proliferation index of more than 38%) large B cells with prominent nucleoli and smaller T lymphocytes, which intermingled tumor B cell-blasts (Figure 34c 1, 2). Kidneys were infiltrated by the high-grade lymphoma (Figure 34c 3). Further examination of surface markers showed the presence two main tumor B cell entities, plasma cells (B220- CD138+) as seen before within CARD11(L225LI)$^{CD19\text{-}Cre}$ (Figure 34f) and GCB-similar cells categorized by down-regulation of CD38 and up-regulation of Fas and Gl7. The T cell population was alike to T_{FH} cells co-expressing PD-1 and ICOS as well as CXCR5 (Figure 34e) (Nutt and Tarlinton, 2011).

Induction of transgene expression at the GC in CARD11(L225LI)$^{Cγ1\text{-}Cre}$ mice led to a mixed high-grade lymphoma consisting of polyclonal, T_{FH}-like T cells, and also of clonal B cells resembling GCBs. The altered B cell differentiation in comparison to the B cell population found in CARD11(L225LI)$^{CD19\text{-}Cre}$ mice might be caused by secondary hits blocking terminal differentiation.

3.4.3. CARD11(L225LI)$^{Cγ1\text{-}Cre}$ tumors display AP-1 and NF-κB activation

We were interested whether different signaling between CARD11(L225LI)$^{Cγ1\text{-}Cre}$ tumor cells and CARD11(L225LI)$^{CD19\text{-}Cre}$ plasma cells was the reason for the observed phenotypic differences. Examination of the cytosolic protein fraction showed a heterogeneous pattern in CARD11(L225LI)$^{Cγ1\text{-}Cre}$–derived tumor samples (Figure 35a). Also CARD11(L225LI) protein was expressed at different levels measured by HA tag protein band densities. All tumor samples showed strong expression of the NF-κB target gene Bcl_{xL}, while IκBα phosphorylation was very heterogeneous. JNK activation and

c-Jun stabilization was found in almost all tumor lysates. Nuclear fractions showed enhanced translocation of NF-κB and heterogeneous translocation of AP-1 subunits to the nucleus in CARD11(L225LI)-expressing samples (Figure 35b, c). Low *Bcl-6* and high *Iκbα* gene expression (Figure 35d) was in line with the observation that GCB-DLBCL biopsies with mutant CARD11 have a higher NF-κB gene expression signature and pathway activity than those with WT CARD11 (Lenz et al., 2008).

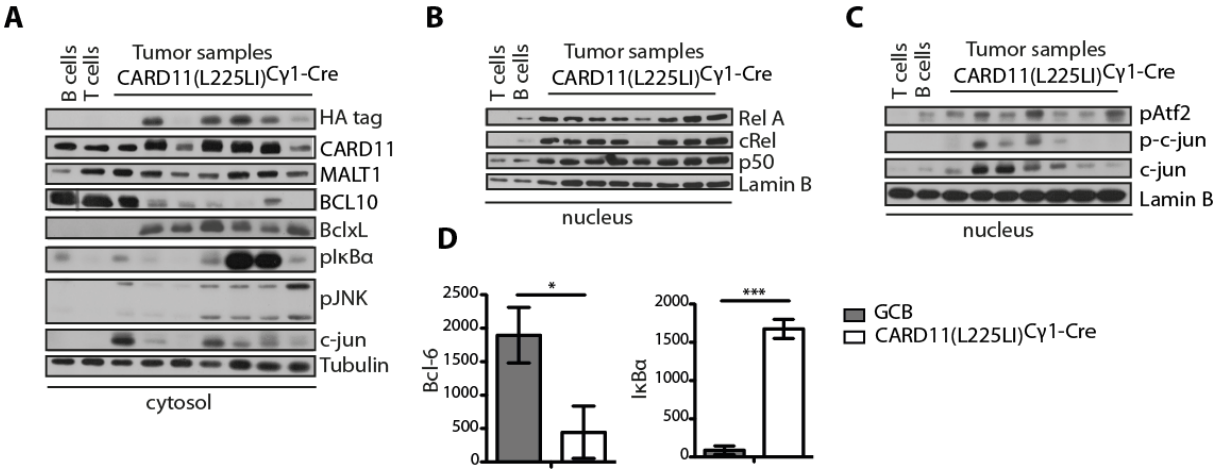

Figure 35: Signaling in CARD11(L225LI)$^{Cγ1\text{-}Cre}$ tumor samples

A) Western blot analysis of cytosolic lysates from MACS-purified splenic T and B cells and 8 different tumor samples. Examination of CBM protein expression (HA tag, CARD11, MALT1, BCL10), NF-κB activation (Bcl_{xL}, pIκBα), JNK pathway activation (pJNK, c-Jun); equal loading was verified by Tubulin. B) Nuclear lysates were prepared from samples from A) Nuclear translocation of NF-κB subunits (RelA, cRel, p50) was examined. C) Nuclear translocation of AP-1 transcription factor subunits (pAtf2, p-c-Jun, c-Jun); equal loading was controlled in nuclear extracts by Lamin B and in cytosolic fractions by Tubulin. D) Relative *Bcl-6* and *Iκbα* transcript levels. Values represent normalized levels to *Hrpt1*. GCBs were MACS-purified from three SRBC-immunized mice. qRT PCR was performed with 8 different tumor samples.

CARD11(L225LI)$^{Cγ1\text{-}Cre}$ tumor samples showed similar signaling events as CARD11(L225LI)$^{CD19\text{-}Cre}$ lymphoma cells, though with heterogeneous presence of activated molecules. This could be due to the long latency of disease onset in CARD11(L225LI)$^{Cγ1\text{-}Cre}$ mice and the possible acquirement of additional mutations.

3.4.4. Induced expression of CARD11(L225LI) in IgG1-positive B cells *in vitro* leads to AP-1 and NF-κB activation

To exclude paracrine activation through microenvironment and second hits, splenic CARD11(L225LI)$^{Cγ1\text{-}Cre}$ B cells (MACS-purified) were recombined *in vitro* by culturing them in presence of α-CD40 and IL-4 for 72 hours. These culturing conditions favor an IgG1 class switch and should lead to CARD11(L225LI) expression in IgG1-expressing cells.

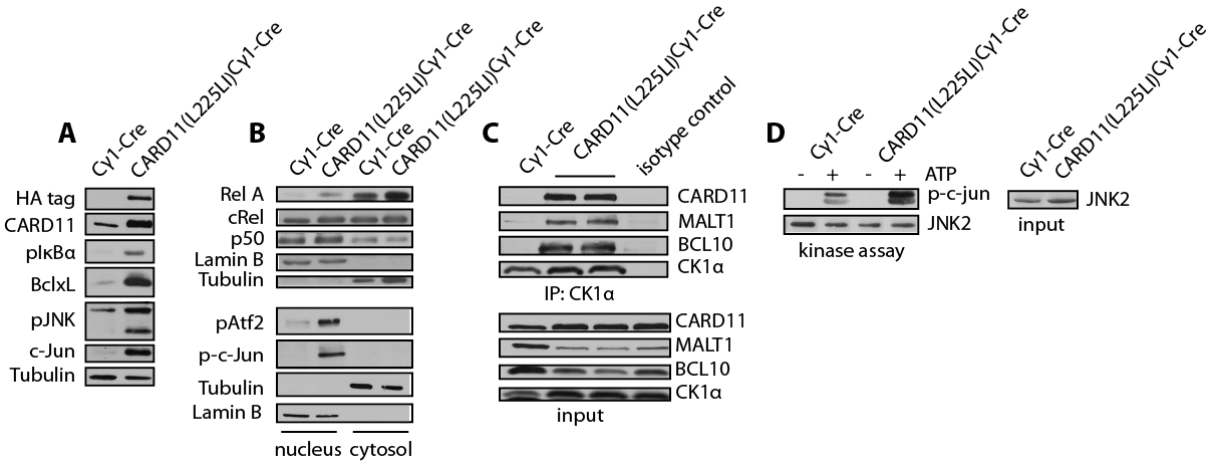

Figure 36: Signaling of *in vitro*-recombined CARD11(L225LI)$^{Cγ1\text{-}Cre}$ B cells
MACS-purified splenic B cells from Cγ1-Cre and CARD11(L225LI)$^{Cγ1\text{-}Cre}$ mice (age 2 – 3 month) were cultured for 72 hours in the presence of 2 ng/ml IL-4 and 2 µg/ml α-CD40. Recombination, which can be measured by eGFP expression, was at least 90%. A) Cytosolic cell lysates were subjected to Western blot analysis. Examination of CBM protein expression expression (HA tag, CARD11, MALT1, BCL10), NF-κB activation (Bcl_{xL}, pIκBα), JNK pathway activation (pJNK, c-Jun); equal loading was verified by Tubulin. B) Nuclear lysates were prepared from samples from A) Nuclear translocation of NF-κB subunits (RelA, cRel, p50) and of AP-1 transcription factor subunits (pAtf2, p-c-Jun, c-Jun) was determined; equal loading was controlled in nuclear extracts by Lamin B and in cytosolic fractions by Tubulin. C) Lysates were immunoprecipitated with anti-CK1α and immunocomplexes were analyzed for the presence for CARD11, BCL10, MALT1 or CK1α by immunoblotting. D) JNK2 kinase assay was performed. Lysates were immunobloted for phosphorylated c-Jun as measure for JNK2 kinase activity. Western blot lysates and immunoprecipitations were obtained from at least 3 independent experiments.

Western blot analysis of cytosolic extracts obtained from *in vitro*-recombined B cells were similar to the signaling of ex vivo analyzed CARD11(L225LI)$^{CD19\text{-}Cre}$ B cells and

CARD11(L225LI)$^{Cγ1\text{-}Cre}$ tumor samples (Figure 36a). Constitutive NF-κB activation assessed by Bcl_{xL}, pIκBα presence as well as JNK pathway activation (cytosolic pJNK, c-Jun) were found. Nuclear lysates of Cγ1-Cre and CARD11(L225LI)$^{Cγ1\text{-}Cre}$ cells showed comparable NF-κB activation most likely due to the culturing conditions with α-CD40 and IL-4. AP-1 activation was stronger in CARD11(L225LI)$^{Cγ1\text{-}Cre}$ B cells as indicated by enhanced translocation of AP-1 subunits to the nuclei of CARD11(L225LI)$^{Cγ1\text{-}Cre}$ B cells (Figure 36b). Co-IP with CK1α confirmed constitutive CBM complex formation (Figure 36c). To measure JNK kinase activity, JNK2 was immunoprecipitated and incubated together with recombinant c-Jun fusion protein. The samples were treated with ATP and subjected to western blot analysis where c-Jun phosphorylation was assessed as read-out for JNK2 kinase activity (Figure 36d).

The analysis of *in vitro*-recombined CARD11(L225LI)$^{Cγ1\text{-}Cre}$ B cells allowed us to examine signaling events under controlled settings: transgene expression for exact 48 hours (expression of eGFP begins under culturing conditions with IL-4 and α-CD40 at 24 hours), no influence by microenvironment and systemic cytokines secreted by other cell types. Analysis of these B cells supported signaling data obtained from CARD11(L225LI)$^{CD19\text{-}Cre}$ and CARD11(L225LI)$^{Cγ1\text{-}Cre}$ tumor samples.

3.4.5. Induced CARD11(L225LI) expression promotes cell survival *in vitro*, which is controlled by IKK and JNK activity

To further study the growth behavior of CARD11(L225LI)-expressing B lymphocytes, *in vitro*-recombined CARD11(L225LI)$^{Cγ1\text{-}Cre}$ B cells were cultured for 24 hours in presence of α-CD40 and IL-4. Then they were transferred to media without these mitogenic stimuli. The *in vitro*- recombined CARD11(L225LI)$^{Cγ1\text{-}Cre}$ B cells started to express eGFP after 24 hours in presence of α-CD40 and IL-4.

In contrast to control Cγ1-Cre B cells, the CARD11(L225LI)-expressing B lymphocytes expanded without stimuli (Figure 37a). Next, different inhibitors were added and Annexin V- and 7AAD-negative cells were measured at different time points by flow cytometry. SYK inhibition (R406) showed minor effects on percentages of live CARD11(L225LI)$^{Cγ1\text{-}Cre}$ B cells (Figure 37b). PI3K (Cal-101), BTK (PCI-32765) and ERK

(PD98,059) inhibition did not affect cell survival (Figure 37c, d, e). Consistent with the results from *ex vivo* inhibitor treated CARD11(L225LI)$^{CD19\text{-}Cre}$ cells, IKK (Bay11-7082) and JNK (SP600125 and JNK-in-8) inhibition efficiently led to cell death of CARD11(L225LI)-expressing B cells (Figure 37f, g, h). These findings further supported the idea that CARD11(L225LI) driven proliferation and cell survival is not only NF-κB dependent but in addition required JNK signaling.

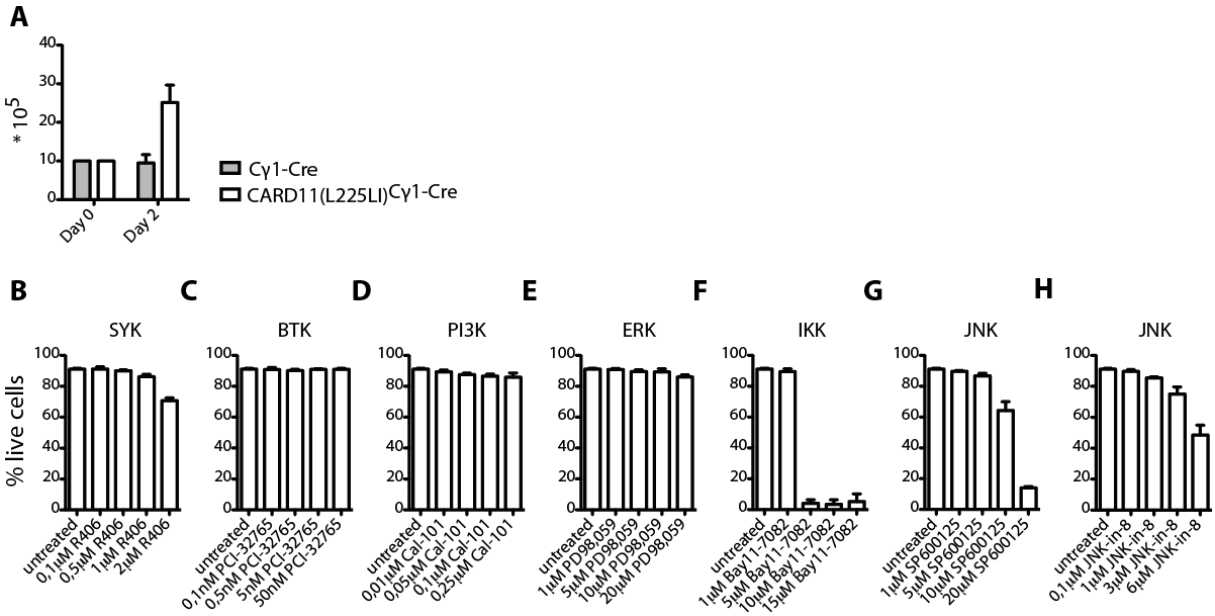

Figure 37: JNK and IKK inhibitors are toxic to CARD11(L225LI)-expressing cells
A-H) MACS-purified splenic B cells were cultured in the presence of 2ng/ml IL-4 and 2μg/ml α-CD40 for 48 hours and then transferred to media lacking IL-4 and α-CD40. (A) Live cells were determined by Trypan Blue exclusion. (B-H) CARD11(L225LI)$^{Cγ1\text{-}Cre}$ B cells were cultured without inhibitors (untreated) or in presence of indicated concentrations of R406 (B), PCI-32765 (C), Cal-101 (D), PD98,059 (E), Bay11-7082 (F), SP600125 (G) and JNK-in-8 (H) for 48 hours, then Annexin V- and 7AAD-double negative cells were determined by flow cytometry. Experiment was performed at least twice with in total n ≥ 3. Data are presented as mean ± SD.

To test whether inhibitor treatment led to cell cycle arrest followed by cell death in *in vitro*-recombined CARD11(L225LI)$^{Cγ1\text{-}Cre}$ B cells, those were also labeled with a proliferation dye (Figure 38). In conclusion with the fact that R406 is mildly toxic to *in vitro*-recombined CARD11(L225LI)$^{Cγ1\text{-}Cre}$ B cells, slight decrease in cell proliferation was observed after 48 hours treatment. Neither BTK, PI3K or ERK inhibition did affect cell proliferation of *in vitro*-recombined CARD11(L225LI)$^{Cγ1\text{-}Cre}$ B cells (Figure 38). In contrast, CARD11(L225LI)-expressing cells were efficiently killed by the inhibition of

JNK kinase activity and IKK inhibition. The decreased viability and proliferation of *in vitro*-recombined CARD11(L225LI)$^{C\gamma1\text{-}Cre}$ B cells treated with R406 could suggest that within this experimental setup SYK influences B cell proliferation CARD11-independent.

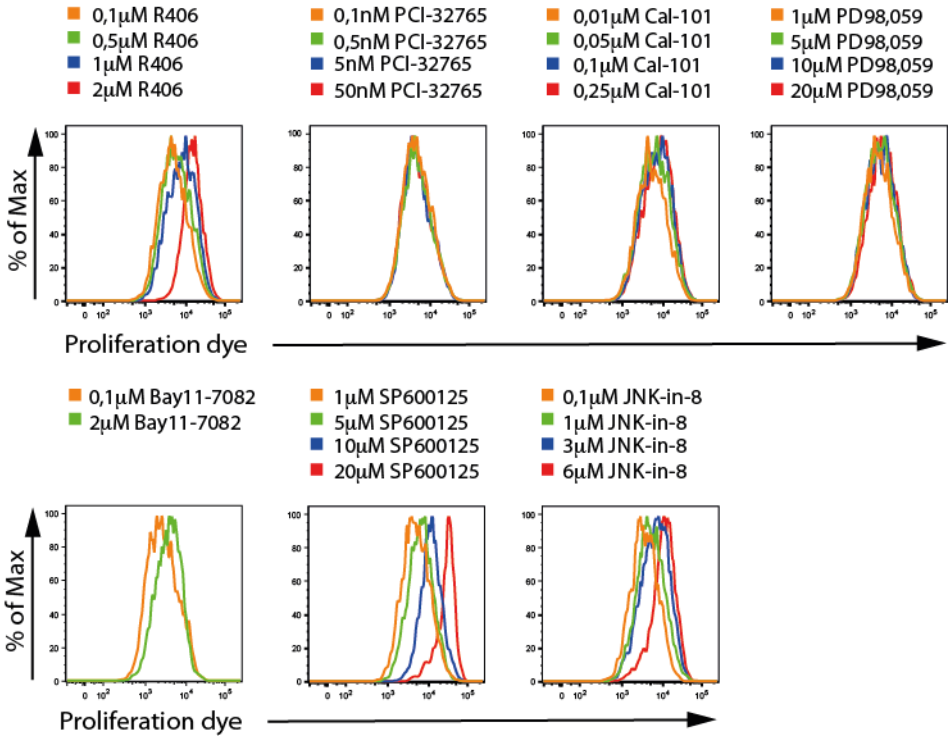

Figure 38: B cell proliferation upon inhibitor treatment

CARD11(L225LI)$^{C\gamma1\text{-}Cre}$ splenocytes were labeled with a proliferation dye and cultured untreated (solvent control DMSO) or in presence of indicated concentrations of following inhibitors: R406, Cal-101, PCI-32765, PD98,059, Bay11-7082, SP600125 and JNK-in-8 for 48 hours, then Annexin V-negative and 7AAD-negative cells were determined by flow cytometry. Experiment was performed at least twice with total n ≥ 3.

3.5. DLBCL

Since both NF-κB and JNK signaling are critical for autonomous growth of *ex vivo*-derived CARD11(L225LI)-expressing B cell and because CBM activities are essential for ABC-DLBCL survival even in tumors that have upstream mutations, the role of JNK signaling in human ABC-DLBCL was investigated next.

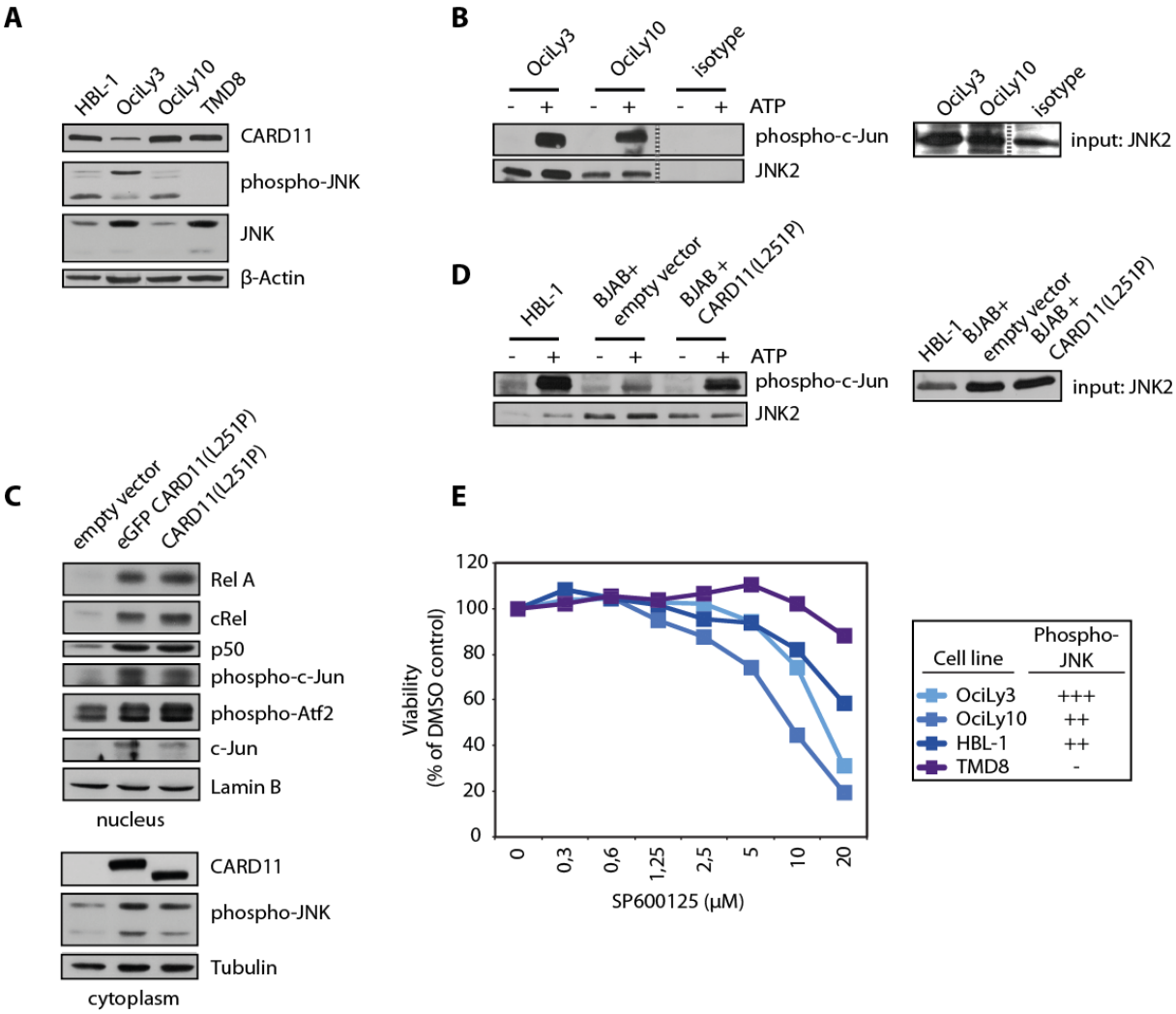

Figure 39: JNK inhibition selectively affects survival of ABC-DLBCL cells

A) Total cell lysates from different ABC-DLBCL (OciLy3, OciLy10, HBL-1 and TMD8) lymphoma cell lines were examined for CARD11, pJNK, JNK, and β-Actin. B) JNK2 kinase assay was performed with the ABC cell lines OciLy3, OciLy10. C) The GCB cell line BJAB was transfected with empty vector (pTop), eGFP-tagged CARD11 harboring the OciLy3 CARD11 mutation (CARD11(L251P)) and CARD11(L251P) without tag. Nuclear lysates were examined for cRel, p50, RelA, phosphorylated Atf2 and c-Jun; cytosolic extracts were blotted for pJNK and CARD11 expression. Equal loading was controlled in nuclear extracts by Lamin B and in cytosolic fractions by Tubulin. D) JNK2 kinase assay was performed with the ABC cell line HBL-1 and BJABs expressing empty vector or CARD11(L251P). All lysates, in vitro kinase assays were prepared and examined in 2 independent experiments. E) Different ABC-DLBCL cell lines (OciLy3, OciLy10, HBL-1 and TMD8) were treated for 48 hours with increasing concentrations of the JNK inhibitor SP600125, cell viability was measured by CellTiter-Glo Luminescent assay. Representative experiment is shown from 6 independent experiments.

To this end, a set of phenotypically well characterized ABC-DLBCL cell lines (OciLy3, OciLy10, HBL-1 and TMD8) was used (Lenz et al., 2008; Ferch et al., 2009; Kloo et al.,

2011). Interestingly, in 3 out of 4 ABC-DLBCL lines constitutive JNK phosphorylation was observed (Figure 39a). Further *in vitro* JNK kinase assays using lysates from cell lines with constitutive JNK phosphorylation and c-Jun as a substrate confirmed constitutive JNK activity in human ABC-DLBCL cells (Figure 39b). To directly test whether CARD11 mutants would simultaneously activate NF-κB and JNK signaling in human lymphoma cells, the GCB-DLBCL cell line BJAB that does not exhibit NF-κB or JNK activation was transduced with constructs expressing the CARD11 mutation observed in the OciLy3 cell line (L251P) alone or fused to GFP.

Indeed, enforced CARD11(L251P) expression in BJAB cells resulted in the activation of NF-κB as measured by nuclear presence of RelA, cRel and p50 and in addition to JNK activation as determined by western blotting with activation state specific antibodies against phosphorylated JNK (Figure 39c). Subsequent JNK kinase assays confirmed these findings (Figure 39d). Finally, we investigated whether a pharmacological treatment with the JNK inhibitor SP600125 would affect the survival of human ABC-DLBCL cells. Intriguingly, a SP600125 mediated dose-dependent cell killing was observed in the ABC-DLBCL cell lines OciLy3, OciLy10 and HBL-1, which were the tumor cell lines with constitutive JNK activation. Moreover, the TMD8 line, which did not exhibit constitutive JNK activation, was also resistant to SP600125 treatment (Figure 39e).

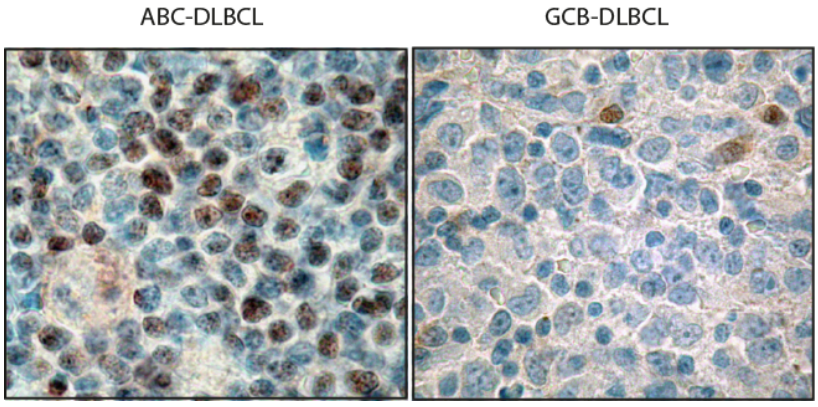

Case	Phospho-JNK
ABC-DLBCL	26/47 ≈ 55%
GCB-DLBCL	0/20 ≈ 0%

Figure 40: JNK activation is found in primary DLBCL biopsies
Primary patient-derived ABC-DLBCL and GCB-DLBCL biopsies were analyzed with phospho-JNK specific antibodies. Representative data are shown. 400x magnification.

To address whether JNK activation plays a role DLBCL patients, 20 GCB-DLBCL and 47 ABC-DLBCL cases were analyzed for the presence of activated JNK (Figure 40). Indeed,

we could show that none of the GCB-DLBCL samples and more than 55% of the ABC-DLBCL biopsies were stained positive for phosphorylated JNK.

Collectively, primary cells from both CARD11(L225LI)$^{Cγ1\text{-}Cre}$ and CARD11(L225LI)$^{CD19\text{-}Cre}$ animals as well as human lymphoma cell lines, which express mutated CARD11 or which are dependent on CBM signaling, showed besides constitutive NF-κB signaling constitutively activated JNK signaling and most strikingly were dependent on JNK signaling for survival. Intriguingly, we were able to show JNK activation in DLBCL patients-derived histologies and thereby provide evidence that targeting the JNK pathway might be a useful therapeutic approach for the treatment of DLBCL.

4. DISCUSSION

4.1. Implications of CARD11 dysregulation

CARD11 is a scaffolding molecule that is essential for antigen receptor-mediated activation of the NF-κB and JNK signaling pathways in hematopoietic cells. For this, CARD11 is composed of several domains with different functions, which are necessary to facilitate the assembly of multiprotein complexes at the plasma membrane in response to external signals and to further transduce these signals. Biochemical studies showed that most CARD11 domains are required for NF-κB activation *in vitro* (Mccully and Pomerantz, 2008). CARD11 deficiency *in vivo* results in defective lymphocyte activation and proliferation and drastically impairs adaptive immunity in mice (Hara et al., 2003). Congruently, a loss-of-function mutation in the GUK domain of CARD11 was found to cause severe combined immunodeficiency characterized by agammaglobulinemia and profoundly deficient T cell function despite normal T and B lymphocytes counts (Greil et al., 2013).

Interestingly, biochemical studies and sequencing of primary patient-derived material revealed the existence of CARD11 gain-of-function mutations. *In vitro*-generated mutations affecting different domains such as the linker region (Sommer et al., 2005) and the N-terminal latch domain (Chan et al., 2012) yielded in strong NF-κB activation due to impaired auto-inhibition of CARD11. A family with a hereditary polyclonal B cell lymphocytosis had germline mutations within the coiled-coil domain resulting in constitutive NF-κB activation (Snow et al., 2012). Similarly, somatic mutations in the coiled-coil domain of CARD11 are associated with a poor prognosis for the very aggressive disease DLBCL due to strong NF-κB activation (Lenz et al., 2008).

The severe effects of loss-of-function as well as of gain-of-function mutations in CARD11 suggest a central role for CARD11 in adaptive immunity and pathogenesis. Therefore, we were interested in the consequence of expressing a gain-of-function mutant version of CARD11 *in vivo*. For this, we targeted the DLBCL-derived coiled-coil mutation CARD11(L225LI) for conditional expression in murine B cells *in vivo*.

4.2. CARD11(L225LI) expression in early B cell development results in plasma cell hyperplasia and cytokine burst

CARD11 mutations are frequently present in ABC-DLBCL. ABC-DLBCL resemble *in vitro*-activated B cells and show constitutive NF-κB activation. At a lower rate, CARD11 mutations occur in GCB-DLBCL, these patients show a high NF-κB target gene expression unlike to GCB-DLBCL generally (Staudt, 2010).

Indeed, the expression of CARD11(L225LI) led to strong B cell activation and their massive expansion in CARD11(L225LI)$^{CD19\text{-}Cre}$ mice. Unexpectedly, CARD11(L225LI)-expressing B cells mainly differentiated into plasma cells and expressed high levels of *Prdm1*, *Irf-4* and *Xbp-1*. Although it is assumed that human ABC-DLBCL acquire mutations blocking terminal differentiation such as loss-of-function mutations in Blimp-1 to prevent cell cycle arrest due to Blimp-1-mediated repression of c-myc (Pasqualucci et al., 2006; Lin et al., 1997), we found that CARD11(L225LI)-expressing B cells vigorously proliferated and expressed c-myc (data not shown). Conditional ablation of Blimp-1 and cooperate CARD11(L225LI) expression could be a feasible approach to mimic human ABC-DLBCL by preventing terminal differentiation. A similar strategy was used by Calado et al., in which ca-IKKβ and Blimp-1 disruption were investigated in GCBs simultaneously (Calado et al., 2010).

CARD11(L225LI)-expressing B cells infiltrated bone marrow and liver as detected by histologic examination (data not shown). Further *in vivo* investigations revealed that CARD11(L225LI)$^{CD19\text{-}Cre}$ mice developed an aggressive lymphoma with 100% penetrance to which animals succumbed 6 days after birth. To date, there is no other murine B cell lymphoma model with this very short latency and complete penetrance based on the expression of one mutated gene (reviewed in (Donnou et al., 2012)). The Eμ-BRD2 mice develop spontaneous DLBCL at 28 weeks of age (Greenwald, 2003). Even the very aggressive Eμ-myc transgene promotes lymphoid tumors with lethal outcome not before 5-9 weeks after birth (Adams et al., 1985).

Sera from moribund CARD11(L225LI)$^{CD19\text{-}Cre}$ mice showed massive levels of inflammatory cytokines, which could add to premature lethality. Flow cytometric analysis revealed that CARD11(L225LI)-expressing B cells produced IL-6 and TNFα. IL-6

is a pleiotropic cytokine with implications in B cell homeostasis, differentiation and inflammation. IL-6 is necessary for plasma cell differentiation (Cassese et al., 2003) and targeted overexpression of IL-6 leads to plasmacytoma development in mice (Kovalchuk et al., 2002). Presumably, CARD11(L225LI)-expressing B cells produce IL-6 for their maintenance comparable to ABC-DLBCL cells, which also autonomously produce IL-6 to sustain their proliferation (Lam et al., 2008; Ferch et al., 2009). Therefore, IL-6 might contribute to the plasmacytic differentiation of the malignant B cells in CARD11(L225LI)$^{CD19\text{-}Cre}$ mice. Additionally, TNFα and IL-1α were found in high concentrations in sera from CARD11(L225LI)$^{CD19\text{-}Cre}$ mice. Activated mononuclear phagocytes, rather than B cells, are the typical producers for these cytokines. Both TNFα and IL-1α are potent proinflammatory cytokines that trigger local inflammation at low concentrations, and induce at higher concentrations fever and acute-phase plasma proteins. However, only TNFα in high systemic concentrations ends in death by septic shock (Abbas et al., 2011). In murine B cells, TNFα in low levels supports class switch recombination, whereas high levels oppose AID action and class switch recombination (Frasca et al., 2012). Besides its intriguing role in inflammation TNFα is also associated with tumorigenesis as it acts as growth factor for tumors and mediates proliferation (Balkwill, 2009). In addition, we found high levels of IL-10, which typically plays a crucial role in the suppressive function of regulatory T cells (Taylor et al., 2006). For DLBCL it has been shown that IL-10 secretion oppresses the “healthy“ tumor microenvironment (Gupta et al., 2012). Therefore, it seems likely that CARD11(L225LI)$^{CD19\text{-}Cre}$ mice die due to the massive lymphoproliferation combined to the cytokine burst.

4.2.1. The role of antigen in CARD11(L225LI)-driven lymphoma

The differentiation of B cells into antibody-secreting plasma cells mostly involves antigen encounter. Therefore, the question arises whether CARD11(L225LI)-expressing B cells differentiate into plasma cells in a self- or foreign antigen-dependent manner or independently of antigen contact.

Experiments using a syngeneic transplantation model showed that different coiled-coil mutations in CARD11 could overcome self-antigen induced cell death by massive T

cell-independent proliferation and Blimp-1-mediated plasma cell differentiation, which includes the production of self-reactive antibodies (Jeelall et al., 2012).
The CD19-Cre-driven expression of CARD11(L225LI) also promoted Blimp-1-mediated plasma cell differentiation. Interestingly, CARD11(L225LI)$^{CD19\text{-}Cre}$ mice succumbed six days after birth to aggressive lymphoma, whereas mice within the transplantation model survived at least 12 days after transplantation. This indicates, that the aggressive phenotype of CARD11(L225LI) expression *in vivo* depends on T cell help either due to direct cellular contact or by the release of cytokines. However, further research will be needed to determine the role of antigen recognition in lymphomagenesis.

4.2.2. Oncogenic potential of CARD11(L225LI) relies on functional CBM complex formation

BCL10 or MALT1, respectively, were ablated *in vivo* to assess their roles in CARD11(L225LI)-triggered lymphomagenesis. Strikingly, BCL10- and MALT1-deficient CARD11(L225LI)$^{CD19\text{-}Cre}$ mice were rescued from premature lethality suggesting that the constitutive assembly of CBM complexes triggered by CARD11(L225LI) was responsible for perinatal death and intriguingly excludes important CBM independent functions of CARD11(L225LI) in pathogenesis.

BCL10-deficient B cells show impaired cell division and survival due to defective NF-κB activation after BCR engagement *in vitro* (Greenwald, 2003; Ferch et al., 2007). Interestingly, CARD11(L225LI) expression could not prevent apoptosis of BCL10-deficient B cells after BCR stimulation *in vitro* (data not shown). Flow cytometric analysis of BCL10-deficient CARD11(L225LI)$^{CD19\text{-}Cre}$ mice showed slight reduction of splenic B cells when compared to BCL10-deficient mice. Further analysis of splenic B cells from BCL10-deficient CARD11(L225LI)$^{CD19\text{-}Cre}$ mice revealed that B cells were neither activated nor enlarged when compared to B cells CARD11(L225LI)$^{CD19\text{-}Cre}$ mice expressing BCL10.

In contrast to BCL10 ablation in B cells, MALT1 deficiency does not impair B cell proliferation, however is essential for cRel translocation to the nucleus (Ferch et al., 2007). Even though viable MALT1-deficient B cell show reduced survival in culture

when compared to WT B cells upon BCR stimulation, MALT1-deficient B cells survive better than BCL10-deficient B cells *in vitro* (Ferch et al., 2007). CARD11(L225LI)-expressing MALT1-deficient splenic B cells were of normal cell size and not activated. Interestingly, we found elevated B cell numbers in PPs, spleen and peritoneal cavity of CARD11(L225LI)$^{CD19\text{-}Cre}$;MALT1-/- mice suggesting differential requirement of BCL10 and MALT1 for B cell homeostasis.

4.2.3. CARD11(L225LI) expression leads to cooperate activation of NF-κB and AP-1

The CBM complex is one of the most important signaling complexes in lymphocytes as it mediates antigen receptor triggered NF-κB and JNK signaling pathway activation and hence is essential for lymphocyte function (Thome et al., 2010; Hara et al., 2003; Blonska et al., 2007). Consistently, CARD11(L225LI) simultaneously triggered autonomous NF-κB and JNK signaling leading to nuclear NF-κB and AP-1 translocation and activity.

CBM complex formation was indispensable for NF-κB and AP-1 activation because BCL10- and MALT1-deficient CARD11(L225LI)-expressing B cells were not able to activate the IKK complex and JNK. Most strikingly, we found that CARD11(L225LI)-expressing MALT1 paracaspase-deficient animals were also rescued from premature lethality. However, the splenic B cell compartment was enlarged and the B cells appeared strongly activated and were increased in cell size. When we analyzed the signaling in CARD11(L225LI)-expressing MALT1 paracaspase-deficient B cells, we found no IKK activity but constitutive activation of JNK. These results were surprising as paracaspase-deficient lymphocytes are able to activate the IKK complex upon antigen receptor engagement (unpublished data). Importantly, this suggests that the role of MALT1 paracaspase function differs between WT B cells and CARD11(L225LI)-expressing B cells. Additionally, we could demonstrate by expressing CARD11(L225LI) on a MALT1 paracaspase-deficient background that paracaspase activity is dispensable but at the same time MALT1 as scaffolding molecule is indispensable for constitutive JNK and B cell activation. These data also imply that constitutive JNK activation is not sufficient to trigger lymphomagenesis indicating that simultaneous IKK and JNK activation is tumorigenic.

NF-κB activation in lymphoma plays a crucial role in tumor maintenance, promotion and fosters an inflammatory milieu sustaining malignant cells. Accordingly, we found in CARD11(L225LI)-expressing malignant cells enhanced expression of the anti-apoptotic molecule *Bcl_{xL}*, cytokines such as *IL-6* and *Irf4*, which leads to activation and plasma cell differentiation (Ferch et al., 2009; Klein et al., 2006).

Although AP-1 plays a role in B cell development, the role of JNK and AP-1 activation in tumorigenesis is neglected, so far. Generally, AP-1 subunits play different roles in B cell development and function: c-fos, has been implicated in plasma cell differentiation (Ohkubo et al., 2005), whereas junD deficient B cells hyperproliferate upon stimulation (Meixner et al., 2004).
Even though, the transforming potential of c-Jun *in vitro* has been known for long time (reviewed in (Jochum et al., 2001)), its role in tumor development is still unclear. Previous studies demonstrated that Atf2/c-Jun dimers lead to cell proliferation *in vitro* (Huguier et al., 1998; van Dam et al., 1998). The presence of activated AP-1 forms in various B cell lymphoma indicates a possible involvement of JNK/AP-1 in tumorigenic or tumor-sustaining processes. In HL and anaplastic large cell lymphoma, overexpression of c-Jun is found to induce proliferation and to suppress apoptosis (Mathas et al., 2002). Another study found that JNK is essential for the survival BCR-ABL transformed B lymphoblasts (Hess et al., 2002). Marginal Zone lymphoma showed upregulation of AP-1 transcription factor subunits (Trøen et al., 2010) and also Mantle cell lymphoma display constitutive JNK activity (Wang et al., 2009).

Interestingly, c-Jun/AP-1 activation also leads to the transition from G1 to S phase and maintains B cell proliferation (Schreiber et al., 1999). Hence, we assume that c-Jun mediates S phase transition in CARD11(L225LI)-expressing B cells and maintains proliferation.

4.2.4. CARD11(L225LI)-expressing B cells show nuclear translocation of β-catenin

CARD11 acts as scaffolding molecule and assembles protein complexes to enable signal transduction. Therefore, it might not be surprising that a mutation, which blocks auto-inhibition (Lamason et al., 2010), is also able to assemble molecules, which are not recruited or bound by the WT protein.

One of these molecules is CK1α; a serine/threonine kinase, which regulates β-catenin and Wnt activity. CK1α is recruited to the CBM complex in DLBCL where it phosphorylates CARD11 and enhances NF-κB signaling (Bidère et al., 2009). In CARD11(L225LI)-expressing cells, CK1α was also recruited to the CBM. Interestingly, further biochemical analysis revealed that CARD11(L225LI)-expressing cells showed nuclear translocation of the Wnt transcription factors β-catenin and Lef1. Congruently, the NF-κB and AP-1 target gene Wnt10b (Katoh and Katoh, 2007) was strongly overexpressed within CARD11(L225LI)$^{CD19\text{-}Cre}$ B cells compared to B cells derived from CD19-Cre animals (data not shown).

However, we believe that nuclear translocation of β-catenin might be a secondary effect of NF-κB and AP-1 activation. As a consequence of NF-κB and AP-1 activation Wnt10b is secreted and could bind to the extracellular Wnt receptor Frizzled, which would lead to β-catenin stabilization due to inhibition of the Wnt destruction complex. Stabilized β-catenin would then be able to translocate to the nucleus and bind to Wnt promoter regions (Clevers and Nusse, 2012). To date, little is known about Wnt signaling in B cell lymphoma. Yet, one recent study showed enhanced nuclear translocation of β-catenin in DLBCL by immunohistochemistry (Ge et al., 2012). Constitutive Wnt activation in lymphoma sustains growth and proliferation by upregulation of c-myc. Consistent with NF-κB and Wnt activation we found increased expression of *c-myc* and enhanced nuclear translocation of c-myc in CARD11(L225LI)-expressing cells (data not shown).

4.3. Germinal center-specific CARD11(L225LI) expression leads to lymphomagenesis

We generated the conditional CARD11(L225LI) mouse to model human DLBCL *in vivo*. For this purpose, CARD11(L225LI)$^{stop FL}$ mice were bred to the germinal center-specific Cγ1-Cre mouse strain to determine the consequence of CARD11(L225LI) expression within the GCB compartment. This approach was chosen because CARD11(L225LI) expression in early B cell stages resulted in an aggressive lymphoproliferative disease with terminal differentiation of the malignant B cell population, which is unlike the phenotype of human DLBCL. To be as close as possible to the human cell-of-origin, GC-specific expression of CARD11(L225LI) was utilized because ABC- as well as GCB-DLBCL most likely originate from a GCB or a post-GCB.

Generally, PPs are B cell follicles within lymphoid tissues of the GALT, which are not quiescent and show ongoing GC reactions due to antigens derived from food and commensal microbiota presented via resident APCs (Cebra et al., 1998). Consequently, GCBs within PPs eventually class switch to the IgG1 isotype and express the CARD11(L225LI) transgene in the CARD11(L225LI)$^{Cγ1\text{-}Cre}$ mice. Strikingly, GCBs were not detectable by flow cytometry in PPs of 2-3 months old CARD11(L225LI)$^{Cγ1\text{-}Cre}$ mice indicating the loss of this population. In parallel, CARD11(L225LI)$^{Cγ1\text{-}Cre}$ mice show an expansion of the mature splenic B cell pool, which did not express the CARD11(L225LI) transgene, leading to the assumption that the GALT-associated CARD11(L225LI) expression together with loss of CARD11(L225LI)-positive GCBs promoted changes in the B cell pool. Even after immunization no B cells entered the GC reaction in the spleen and potentially resulting IgG1 antibodies were absent in CARD11(L225LI)$^{Cγ1\text{-}Cre}$ mice.

Hence, the IgG1 class switch was performed *in vitro* to show that CARD11(L225LI) expression is functional in B cells-derived from CARD11(L225LI)$^{Cγ1\text{-}Cre}$ mice. Here we found that CARD11(L225LI)-expressing cells were not able to up-regulate ICOSL, which is important for the GC reaction. ICOSL-deficient mice lack GCBs and serum immunoglobulins after immunization (Wong, 2003). Recent studies show that ICOS-deficient T cells or ICOSL-deficient B cells fail to form GCs because bystander FO B cells at the T-B border cannot recruit T cells to the GC (Xu et al., 2013). Whether the absence of most GCBs in 2-3 month-old CARD11(L225LI)$^{Cγ1\text{-}Cre}$ mice is due to B

cell-intrinsic mechanisms or because of deregulated interactions between GCBs and T_{FH} cells is still unclear. It is possible that CARD11(L225LI)-mediated corporate activation of NF-κB and AP-1 led to hyperactivation-mediated cell death. Interestingly, mice expressing ca-IKKβ under the control of Cγ1-Cre showed normal survival, GC development and transgene expression (Calado et al., 2010).

Around the age of 8 months, CARD11(L225LI)$^{Cγ1\text{-}Cre}$ mice succumbed to a high-grade lymphoma according to pathologic assessment. The disease onset in CARD11(L225LI)$^{Cγ1\text{-}Cre}$ mice was short in comparison to other GCB-DLBCL mouse models: the standard GCB-DLBCL mouse model, which was generated by targeted Bcl-6 overexpression has an average latency period of 15 months (Cattoretti et al., 2005). Another recently published model for ABC-DLBCL, in which Blimp-1 disruption is combined to constitutive NF-κB activation, even showed a median survival of 15 months (Calado et al., 2010).

4.3.1. Limitations of CARD11(L225LI)$^{Cγ1\text{-}Cre}$ mice

The lymphoma to which CARD11(L225LI)$^{Cγ1\text{-}Cre}$ mice succumbed consisted of activated CARD11(L225LI)-expressing T cells (CD4-positive) and B cells (CD19-positive). Southern blot analysis revealed clonal origin of tumor B cells. CARD11(L225LI)-expressing T cells were more frequent within the tumor samples compared to B cells, and thus of polyclonal origin. The recombination of Cγ1-Cre in T cells was unexpected because the Cre recombinase is linked in this mouse strain to transcription of IgG1 constant region gene segment, which is solely expressed by B cells and unspecific recombination in T cells was not reported previously (Casola et al., 2006). In contrast, undesired recombination within CD4-positive T cells when using the GC-specific AID-Cre mouse strain is known (Crouch et al., 2007). The presence of CARD11(L225LI)-expressing CD4-positive T cells indicates a similar mechanism for the Cγ1-Cre strain.

To address whether CARD11(L225LI)-expressing T cells and T cells generally are essential for malignant B cell development, maintenance and activation in CARD11(L225LI)$^{Cγ1\text{-}Cre}$ mice, one could breed CARD11(L225LI)$^{Cγ1\text{-}Cre}$ mice on Foxn1^{nu}

background. The latter mice, also known as nude mice, have a mutation in the Foxn1 gene that leads to defective development of the thymic epithelium and anlage, and therefore lack of a thymus and hence T cells (Pantelouris, 1968). Such a study would prevent CARD11(L225LI) expression in T cells. Alternatively, by using α-CD4 depleting antibodies *in vivo*, the effect of CD4 T cell ablation on lymphomagenesis could be studied. This approach has the limitation that depleting antibodies are expensive and must be regularly administered in order to maintain T cell depletion (Arora et al., 2006).

4.3.2. Lymphoma cells resemble GCBs and T_{FH}s and display cooperate NF-κB and AP-1 activation

Interestingly, CD4-positive tumor cells from CARD11(L225LI)$^{Cγ1\text{-}Cre}$ mice closely resembled T_{FH} cells. They expressed typical surface marker such as ICOS, PD-1 and CXCR5 (Nutt and Tarlinton, 2011). High levels of IL-10 were found within the serum samples of tumor mice. Notably, T_{FH} cells produce IL-10, which promotes B cell survival and antibody production (Schaerli et al., 2000; Kim et al., 2001; King et al., 2008). The CD19-positive compartment of CARD11(L225LI)$^{Cγ1\text{-}Cre}$-derived tumors resembled strongly activated GCBs in that they expressed lower levels of CD38, and higher levels of Fas, Gl7 and the activation marker CD80. In contrast to WT CARD11, the presence of CARD11 mutations in GCB-DLBCL decreases the expression of GC-associated genes (*Bcl-6* mRNA expression) and increases the expression of NF-κB genes (*Iκbα* gene expression) (Lenz et al., 2008). Accordingly, we found that CARD11(L225LI) expression led to increased expression of NF-κB genes and reduced the expression of *Bcl-6* in tumor biopsies.

Compared to the CARD11(L225LI)$^{CD19\text{-}Cre}$ animals, where all B cells differentiated into plasma cells, CARD11(L225LI)$^{Cγ1\text{-}Cre}$ lymphoma showed just partial plasma cell differentiation. This indicates that B cells from CARD11(L225LI)$^{Cγ1\text{-}Cre}$-derived tumors could have acquired additional mutations blocking terminal differentiation within the latency of 8 month. By targeting CARD11(L225LI) expression to the GC, we are able to present a model reproducing the transformation of a GCB and thus, resembling human GCB-DLBCL. Even though CARD11(L225LI)-expressing CD4-positive T cells are present

in this lymphoma, we used tumor biopsies to analyze the impact of CARD11(L225L) expression on signaling within these lymphoma.

Tumor biopsies of terminally-ill CARD11(L225LI)$^{Cγ1\text{-}Cre}$ mice as well as *in vitro*-recombined B cells from healthy CARD11(L225LI)$^{Cγ1\text{-}Cre}$ mice showed corporate activation of NF-κB and AP-1, which was also found in B cells from CARD11(L225LI)$^{CD19\text{-}Cre}$ mice.

4.4. Clinical perspectives

DLBCL is a rapidly growing and aggressive type of NHL. The overall survival rate for all DLBCL subgroups averages 50% upon chemotherapy and anti-CD20 monoclonal antibody (rituximab) treatment. Thus new therapeutic strategies are urgently needed for the treatment of this disease. To identify new therapeutic targets, patient-derived biopsies were sequenced for cancer-gene mutations. Based on these data the particular tumor-driving signaling pathways were determined and enabled a patient-adjusted therapy (Lenz and Staudt, 2010).

The sequencing approach resulted in the detection of frequently occurring mutations (see section 1.3.3.). To identify potential therapeutic strategies for lymphoma entities with mutated CARD11, primary lymphoma cells from CARD11(L225LI)$^{CD19\text{-}Cre}$ mice and also *in vitro*-recombined B cells from CARD11(L225LI)$^{Cγ1\text{-}Cre}$ mice were treated with different inhibitors *in vitro*.

Receptor-proximal BTK inhibition is a promising approach for treatment of DLBCL. Recently clinical trial phase 3 studies have been initiated to test the efficacy of combined treatment with the BTK inhibitor PCI-32765 and chemotherapy. *In vitro* studies showed the sensitivity of ABC-DLBCL cell lines (OciLy10, TMD8) harboring BCR-proximal CD79A/B mutations towards BTK inhibition, whereas proliferation and survival of the CARD11-mutant OciLy3 ABC-DLBCL cell line was not affected by inhibition of BTK (Staudt et al., 2011). Accordingly, we found that treatment with the BTK inhibitor PCI-32765 did not inhibit proliferation nor lead to cell death in CARD11(L225LI)-expressing cells indicating that BTK acts upstream of

CARD11(L225LI) and is not a therapeutic target in DLBCL with mutant CARD11 (summarized in Figure 41).

Another feature of ABC-DLBCL with chronic active BCR signaling (TMD8, HBL-1) is constitutive PI3K activity, which is essential for lymphoma cell survival (Kloo et al., 2011). CARD11(L225LI)-expressing primary murine lymphoma cells did not undergo cell death after PI3K inhibition with Cal-101 suggesting independence of the PI3K signaling pathway and other molecular mechanisms.

Recent preclinical studies have shown that DLBCL express high levels of SYK and that functional SYK signaling is indispensable for lymphoma cell proliferation and survival. Interestingly, the ABC-DLBCL cell line OciLy3 with mutant CARD11 is resistant to SYK inhibitor treatment (Cheng et al., 2011). Primary CARD11(L225LI)-expressing cells were also not sensitive to SYK inhibition by R406 treatment, suggesting that SYK plays a role upstream of mutated CARD11.

We found that JNK is constitutive active in CARD11(L225LI)-expressing cells and were able to show JNK activity is indispensable for lymphoma cell survival *in vitro*. For JNK blockage, we treated the lymphocytes with SP600125; a derivate is currently in clinical trials for idiopathic pulmonary fibrosis (NCT01203943) for which constitutive JNK activation has been shown (Plantevin Krenitsky et al., 2012; Shi-Wen et al., 2006; Wagner and Nebreda, 2009). Intriguingly, the pharmacological inhibition of JNK signaling with SP600125 as well with the new JNK inhibitor JNK-in-8 (Zhang et al., 2012) triggered cell death of CARD11(L225LI)-expressing cells. CARD11(L255LI)-expressing cells were also treated with PD98,059 to exclude the activity of another MAPK ERK. Indeed, CARD11(L255LI)-expressing cells were resistant to ERK inhibition.

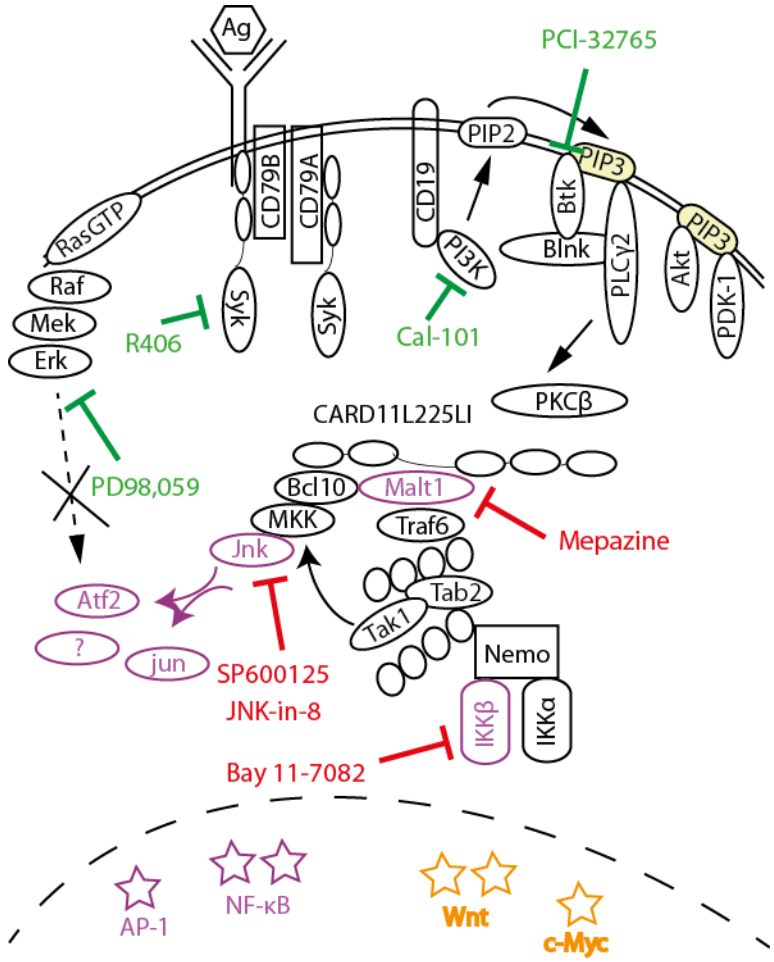

Figure 41: Therapeutic approaches
This simplified schematic drawing summarizes inhibitors used within this thesis and their effect on survival of primary CARD11(L225LI)-expressing B cells. Inhibitors (R406, Cal-101, PCI-32765, PD98,059) in green did not impair cell survival. Red inhibitors (SP600125, JNK-in-8, Bay11-7082) were toxic to primary lymphoma cells. The mutated CARD11 molecule is highlighted in red. Signaling molecules and transcription, which were directly activated by CARD11(L225LI) are depicted in violet and those, which were most likely activated secondarily are shown in yellow.

Blockage of NF-κB signaling with the IKK inhibitor Bay 11-7082 triggered death of CARD11(L225LI)-expressing cells. This is in line to the well-known sensitivity of human ABC-DLBCL cells towards IKK inhibition (Davis et al., 2001b; Staudt, 2010). Cell death upon JNK and IKK inhibition demonstrated that the pathological growth of CARD11(L225LI)-expressing B cells is not only dependent on dysregulated NF-κB signaling but also critically requires JNK kinase activity.

To investigate whether JNK signaling is essential for the survival of human ABC-DLBCL samples, diverse ABC-DLBCL lymphoma cell lines were tested. Indeed, JNK was constitutively active in 3 out of 4 ABC-DLBCL cell lines (HBL-1, OciLy10, OciLy3). We repeatedly observed in various assays that the ABC cell line TMD8 does not show constitutive JNK activation, and was therefore used as a negative control in our assays. It was also possible to activate JNK in the GCB-DLBCL cell line BJAB by the introduction of mutated CARD11 originating from the ABC-DLBCL cell line OciLy3. We were able to confirm the presence of active JNK exclusively in patient biopsies from the ABC-DLBCL subtype and as JNK inhibition was selectively toxic to ABC-DLBCL cell lines with active JNK suggesting JNK blockage for the treatment of ABC-DLBCL and in particular for DLBCL patients with CARD11 mutations.

4.5. Conclusion

The CBM complex is essential for normal BCR induced AP-1 and NF-κB signaling and for survival of ABC-DLBCL tumor cells. Knock-downs of CARD11, BCL10 and MALT1 were selectively toxic to all tested ABC-DLBCL cell lines (Ngo et al., 2006). This and our data suggest that most ABC-DLBCL-derived mutations in CD79A/B (Davis et al., 2010), MyD88 (Ngo et al., 2010), CARD11 (Lenz et al., 2008) rely on a functional CBM complex, which simultaneously activates NF-κB and JNK signaling. Clinical studies showed therapeutic success by using SYK, BTK and PI3K inhibitors for the treatment of NHL. However, these approaches are ineffective in lymphoma entities with mutated CARD11 and cannot be translated to these (Staudt et al., 2011).

This work provides the framework for targeting JNK in DLBCL entities, which are unresponsive to standard treatment and SYK, BTK or PI3K inhibition. A possible therapeutic advantage of JNK inhibition is that it might reduce side effects as it targets the receptor signaling pathway downstream and therefore does not interfere with other pathways such as Ca^{2+} and PI3K signaling. Additionally, the combination of NF-κB and JNK inhibition was tested to potentially limit the toxicities associated with full NF-κB blockade and found that each inhibitor could be drastically reduced while preserving efficient killing of primary CARD11(L225LI)-expressing cells.

Because the current treatment options for DLBCL are limited and selective NF-κB inhibitors have failed clinical trials, our results suggest that inhibition via JNK blockage with such inhibitors as SP600125 derivatives or low dose combinations of IKK and JNK inhibitors could become a therapeutic option for a subset of DLBCL patients.

5. SUMMARY

Activated B cell-like (ABC) diffuse large B cell lymphoma (DLBCL) is an aggressive prevalent Non-Hodgkin-Lymphoma (NHL) characterized by constitutive active NF-κB signaling. Lymphoma cell survival depends on the activation of the NF-κB pathway via CARD11, BCL10 and MALT1 (CBM). Yet, due to high toxicities, selective inhibitors targeting IKKs downstream of the CBM complex do not reach the clinic. Thus, other drug targets are urgently needed.

To investigate the consequences of pathogenic CARD11 activities *in vivo*, we generated conditional knock-in mice that allow an inducible expression of the human lymphoma-derived gain of function mutant CARD11(L225LI). Surprisingly, targeted expression of CARD11(L225LI) in the early B cell lineage resulted in an aggressive malignant lymphoproliferation leading to lethality as early as 6 days after birth and in mature class-switched B cells at the age of 8 month. CARD11(L225LI) assembles constitutively with BCL10 and MALT1 and genetic deficiencies in either of them completely rescued the CARD11(L225LI) triggered lethality indicating that the constitutive assembly of these complexes is absolutely essential for pathogenesis. Molecularly, CARD11(L225LI) activated NF-κB and c-Jun N-terminal kinase (JNK) signaling pathways and synergy between these signaling cascades was essential for the survival and proliferation of CARD11(L225LI)-expressing primary murine B cells. Likewise, we observed a constitutive activation of JNK signaling in human ABC-DLBCL cells and demonstrated that pharmacological JNK inhibition was toxic for cells with constitutive JNK activation. Together, our results demonstrate that constitutive activation of CARD11-BCL10-MALT1 signaling via lymphoma-derived mutations trigger rapid lethal lymphoproliferation due to combined aberrant NF-κB and JNK signaling and reveal JNK signaling as a potential therapeutic target for the disease.

6. MATERIAL

6.1. Plasmids

ROSA26 targeting vector

The original pROSA26 vector was modified (Friedrich and Soriano, 1991). A short (1 kb) and a long (4 kb) homology arm allow homologous recombination within the murine *ROSA26* locus. A *loxP* sites-flanked STOP cassette and a neomycin-geneticin resistance gene for embryonic stem cell selection precede the gene of interest, which is followed by a frt sites-flanked IRES-eGFP coding sequence, which allows the concomitant expression of eGFP.

pMIG

The retroviral plasmid contains a MSCV-based promoter after which the gene of interest is inserted. The gene is connected to IRES-GFP allowing bicistronic expression.

pRetroSUPER

Modified MSCV-based retroviral expression vector with puromycine resistance cassette (Lenz et al., 2008).

6.2. Cell lines

- PhoenixE (packaging cell line)
- Bal-17 (mature murine B cell lymphoma line)
- HBL-1, BJAB, OciLy3, OciLy10 and TMD-8 (human lymphoma cell lines)

6.3. Mouse strains

All animals were housed under specific pathogen free conditions in ventilated cages (Thoren MaxiMiser caging systems or TechniPlast IVC). Studies were conducted in compliance to federal and institutional guidelines. The government of Upper Bavaria approved animal protocols.

CARD11(L225LI)$^{stop FL}$

The *Card11(L225LI)* cDNA was generated by in-frame addition of a HA tag sequence upstream of the human *WT Card11* cDNA. The L225LI mutation 10 (Lenz et al., 2008), which is an isoleucin-insertion at amino acid position 225, was introduced by mutagenesis PCR (Stratagene). The resulting cDNA was cloned into the ubiquitously expressed ROSA26 vector (Sasaki et al., 2006), which was linearized and electroporated into 129Ola ES cells. Clones were verified by Southern blot analysis with the ROSA26 probe and specific PCR. PolyGene AG, Switzerland, performed embryonic stem cell culture, electroporation and blastocyst injections.

CD19-Cre

The Cre recombinase gene is placed into the *CD19* locus, thereby expressing Cre instead of the *Cd19* gene from the CD19 promoter (Rickert et al., 1997).

Cγ1-Cre

The Cre recombinase gene is inserted into the constant gamma1 chain locus, thereby expressing Cre instead of the *Cγ1* gene from the endogenous promoter (Casola et al., 2006).

BCL10 knock-out

The endogenous BCL10 locus was targeted by the insertion of a neomycin resistance gene cassette in antisense orientation between exons 2 and 3, which disrupts the *Bcl10* gene (Ruland et al., 2001).

MALT1 knock-out

The murine MALT1 locus was targeted by the insertion of a neomycin resistance gene cassette in antisense orientation between exons 8 and 9, which disrupts the *Malt1* gene (Ruland et al., 2003).

Paracaspase mutant (PM) knock-in

The MALT1 paracaspase mutant mouse was generated by point mutation of cysteine 464 to an alanine, inactivating the paracaspase activity (unpublished, Gewies, A and Gorka, O. et al.).

6.4. Oligonucleotides

Genotyping		
CARD11(L225LI)$^{stop FL}$	long geno fwd	act cgg gtg agc atg tct tta atc
	short geno rev	gtg atc tgc aac tcc agt ctt tct a
	IRES geno rev	ata cgc ttg agg aga gcc att tg
	Carma geno fwd	aaggacaagatcggcgaggag
CD19-Cre	CD19 tg a	gcg gtc tgg cag taa aaa cta tc
	CD19 tg b	gtg aaa cag cat tgc tgt cac tt
	WT CD19 c	cct ctc cct gtc tcc ttc ct
	WT CD19 d	tgg tct gag aca ttg aca atc a
Cγ1-Cre	Cγ1 fwd	tgt tgg gac aaa cga gca atc
	Cγ1	gtc atg gca atg cca agg tcg cta g
	Cγ1 rev	ggt ggc tgg acc aat gta aat a
BCL10-/-	BCL10 wt	ttg gct ctc tgc tct cct cac t
	BCL10 com	cgc tct gag gac tgt ggg act g
	Neo	ggg tgg gat tag ata aat gcc tgc tc
MALT1-/-	MALT1 wt	act ttc atc ttg cca gca ctc ttt ctt a
	MALT1 com	ctg ctg ctg aca tgc tac aat atg ctg
	Neo	ggg tgg gat tag ata aat gcc tgc tc
PM	PM fwd	ctggtggcacacacttttag
	PM rev	ccaacatacatacgaatggac

qRT PCR	**sense**	**antisense**
Irf4	ggaaactcctcaccaaagca	ggcccaacaagctagaaaga
Prdm1	tagacttcaccgatgagggg	accaaggaacctgcttttca
Xbp1	agcttttacgggagaaaactcac	ccaagcgtgttcttaactcct
c-Jun	gggacacagctttcacccta	gaaaagtagcccccaacctc
Bcl-6	ccggcacgctagtgatgtt	tgtcttatgggctctaaactgct
Ικbα	cctgcagcagactccactc	gacacgtgtggccattgtag
Hrpt1	gctgacctgctggattacat	ttggggctgtactgcttaac

6.5. Probes

Electrophoretic mobility shift assay probes

AP-1 consensus oligonucleotide 5´CGC TTG ATG ACT CAG CCG GAA 3´and NF-κB probe 5´ AGT TGA GGG GAC TTT CCC AGG C 3´ (Licor).

Southern blot

The ROSA26 probe was amplified with the forward (fwd) primer 5´gatcaaaacactaatgaactt3´ and reverse (rev) 5´ ttaattaaaacgaatatttggaat3´. The JH4 probe was amplified with the fwd primer 5´tgaaggatctgccagaactgaa3´ and rev 5´tgcaatgctcagaaaactccat 3´, the TCRβ2 probe was generated with following primers fwd 5´gaggaaggtgacgaaagagga 3´ and rev 5´atttgggtggaagcgagag 3´.

6.6. Western blot antibodies

Western blots were probed for CARD11 (1D12) #4435, pAKT (D9E) #4060, p50 #3035, BCL10 (C78F1) #4237, Bcl_{xL} #2762, pIκBα #9241, p-c-Jun #8794, pJNK #9251, JNK #9252, JNK2 #4672, pAtf2 #5112, AKT #9272 all antibodies obtained from cell signaling technology; β-Actin #5060 Sigma, Anti-HA High Affinity (3F10) Roche, RelA #sc-372, Tubulin (B-7) # sc-5286, Lamin B (M-20) # sc-6217, cRel #sc-71, CK1α #sc6477, c-Jun #sc-1694, c-myc #sc-789 all Santa Cruz, MALT1 (Genentech).

6.7. FACS antibodies

B220 (RA3-6B2); TCR-β (H57-597); CD4 (Gk1.5); CD5 (53–7.3); CD8 (53–6.7); CD62L (MEL-14); CD86 (GL1); IgM (II/41); CD23 (B3B4); CD80 (16-1QA1); CD19 (1D3); IL-6 (MP5-20F3); TNFα (MP6-XT22); CD25 (PC61.5); c-kit (2B8); IgD (11-26c); CD275 (HK5.3); CD69 (H1.2 F3); Gl7 (Gl-7); CD279 (PD-1); CD278 (7E.17G9); C1qRp (AA4.1); CD38 (90) all eBioscience; CD138 (281-2); Fas (Jo2); IgG1 (A85-1); CXCR5 (3) BD.

7. METHODS

7.1. Cell culture techniques for cell lines

7.1.1. PhoenixE

PhoenixE packaging cells were maintained in 1x DMEM with 10% (v/v) FCS, 1% (v/v) L-glutamine, 0.1% (v/v) 2-mercaptoethanol, 1% (v/v) penicillin-streptomycin (all Gibco) 2×10^6 cells per 10cm plate, and splitted at a ratio of 1:5 every second day by trypsinization (1% (v/v) Trypsin/EDTA). PhoenixE express *gag, pol*, and *env* genes, which allow retroviral production. 24h prior to transfection 3×10^6 PhoenixE cells were seeded per 10cm plate in 1x DMEM, with 10% (v/v) FCS, 1% (v/v) penicillin-streptomycin to achieve a 70% cell confluence on the day of transfection. PhoenixE cells were pretreated for 30 minutes in DMEM supplemented with 40µM chloroquine. Chloroquine enhances the transfection efficiency by its lysosomal neutralizing activity. During this incubation step 12µg of the respective retroviral expression vector were mixed with 125mM $CaCl_2$ in 2x HBSS buffer pH 7.05 (140mM NaCl, 0.75mM Na_2HPO_4, 25mM HEPES), and incubated at RT for 13min. Formed DNA/$CaCl_2$ precipitates were then added dropwise to chloroquine-pretreated PhoenixE cells followed by a change of medium after 6h of incubation. Virus-containing supernatant was collected 48h and 72h post transfection, 0.45µm filtered and stored at $4^{\circ}C$.

7.1.2. Bal-17

Bal-17 cells were grown in 1x RPMI, supplemented with 10% (v/v) FCS, 1% (v/v) L-glutamine, 0.1% (v/v) 2-mercaptoethanol, 1% (v/v) penicillin-streptomycin (all purchased from Gibco) at a density of 0.1×10^6 cells/ml and splitted at a density of 0.5×10^6 cells/ml. For spininfection 0.5×10^6 Bal-17 were seeded within 4ml viral supernatant, 40µg polybrene and 100µl 1M Hepes in a six well plate. Polybrene was added to enhance the viral adsorption. Spininfection was performed for 90 minutes at 30 degrees and 2400rpm. Cells were rested for 90 minutes, new viral supernatant was added and spininfection repeated. Then the cells were transferred to 1x RPMI,

supplemented with 10% (v/v), FCS, 1% (v/v) L-glutamine, 0.1% (v/v) mercapto-ethanol, 1% (v/v) penicillin-streptomycin and cultured at 37 degrees over night. The procedure was repeated the next day.

All cells were cultivated under standard cell culture conditions at 5% CO_2, 37 degrees, and a relative humidity of 95%. Cells were counted with Trypan Blue by light microscopy (0.4% (w/v) Trypan Blue Stain, Gibco).

7.1.3. Human lymphoma cell lines

Human DLBCL cell lines HBL-1 and BJAB were cultured in RPMI 1640 with 10% FCS, and OciLy3, OciLy10 and TMD-8 were cultured in IMDM supplemented with 20% human plasma.

For efficient retroviral transductions, cell lines were engineered to express the murine ecotropic receptor as previously described (Ngo et al., 2006). Additionally, these cell lines were engineered to express the bacterial tetracycline repressor allowing doxycycline-inducible *Card11* cDNA expression (Ngo et al., 2006). The *Card11* OciLy3 mutant cDNAs were expressed from a modified pRetroSUPER-based vector as described before (Lenz et al., 2008). After infection of BJAB cells carrying the empty vector, the eGFP-fused or unfused CARD11 OciLy3 mutant (CARD11(L251P)) construct were selected using 3µg/ml puromycin (Sigma) until >90% cells were positive for the transduced construct. The ratio of selected cells was estimated using FACS analyses for eGFP-positive cells after a 2-day doxycycline induction (Sigma) of selected cells harboring the eGFP-fused CARD11 OciLy3 mutant. The cell viability was determined using FACS analyses after Propidium Iodide staining. To induce the CARD11 OciLy3 mutant expression, 20µg/ml doxycycline were added to the culture medium for 48h. Annette Wolf conducted DLCBCL cell line culture and cell viability assays.

7.1.4. Cell viability assay DLBCL

Cells were seeded in 96-well round bottom plates at a concentration of $5x10^4$ cells/ml and were treated with serial dilutions of the JNK inhibitor or DMSO as solvent control in concentrations between 20µM and 0,625µM. After incubation for 48h, the cell viability

was detected using the CellTiter-Glo Luminescent Cell Viability Assay (Promega) according to the manufacturer's protocol. The cell treatment and cell viability detection was performed in duplicates.

7.2. Primary murine cells

7.2.1. B cell purification

Splenic B cells were MACS-purified by CD43-depletion (mouse B Cell Isolation Kit, Miltenyi Biotec GmbH) according to manufacturer´s instructions. Primary CD19-Cre and CARD11(L225LI)$^{CD19\text{-}Cre}$ B cells were harvested and rested in RPMI 1% BSA for one hour before cell lysis.

7.2.2. B cell stimulation

Retroviral transduced GFP-expressing Bal-17 cells were sorted by flow cytometry and expanded for EMSA. Cells were either rested or stimulated with 10µg/ml Fab2 α-IgM (Jackson ImmunoResearch Laboratories, Inc.) for 90 minutes.

MACS-purified splenic B cells were stained with proliferation dye and cultured in 1x RPMI, supplemented with 10% (v/v), FCS, 1% (v/v) L-glutamine, 0.1% (v/v) mercapto-ethanol, 1% (v/v) penicillin-streptomycin and stimulated for 48 hours with different agents: α-CD40 2,5µg/ml (eBioscience); CpG: 0.1µg/ml (Invivogen); α-IgM: 10µg/ml (Jackson ImmunoResearch Laboratories, Inc.); LPS 20µg/ml (Invivogen)

7.2.3. *In vitro*-class switch recombination

Splenic B cells were purified by MACS-based CD43-positive cell depletion. B cells were stained with proliferation dye and incubated for 96 hours in 1x RPMI, supplemented with 10% (v/v), FCS, 1% (v/v) L-glutamine, 0.1% (v/v) mercapto-ethanol, 1% (v/v) penicillin-streptomycin and additionally 4ng/ml IL-4 (R&D) and 4,5µg/ml α-CD40 (eBioscience).

7.2.4. Inhibitor treatment primary lymphoma cells

Splenocytes were grown in RPMI 10% FCS containing 1% L-Glutamine and 0.1% β-mercaptoethanol. Bay11-7082, SP600125, PD98,059 were obtained from Sigma Aldrich; JNK-in-8 was got from Merck; Cal-101 and PCI-32765 were bought from SelleckChem; R406 was ordered from ICS International Clinical Service GmbH**.** Mepazine was a gift from Daniel Krappmann. The inhibitors were solved in DMSO and used in indicated concentrations. Cells were harvested at different time points and stained with Annexin V and 7-AAD (eBioscience) and acquired by flow cytometry.

7.3. Mouse methods

7.3.1. Immunizations

Six- to 12-week old animals were immunized intraperitoneal (i.p.) with $1x10^9$ SRBC in PBS (Biozol). For GCB purification protocol from Cato et al. was applied (Cato et al., 2011).

7.3.2. Serum cytokines and immunoglobulin levels

Mouse blood was collected by submandibular vein puncture. Blood was clotted on ice and serum was obtained by centrifugation. Serum cytokines were measured with the Th1/Th2 FlowCytomix kit (Bender Med Systems) according to protocol. Immunoglobulin levels were measured in diluted sera by the mouse immunoglobulin panel according to standard protocol (Mouse immunoglobulin Panel, Southern Biotech). Plates were coated over night with unlabeled α-mouse Ig (heavy and light chain) in coating buffer (ELISA /ELISPOT Coating buffer powder (eBioscience)). Plates were blocked with 1% BSA (w/v) in 1x PBS. Standards and diluted sera were pipetted in dilution series. For detection alkaline phosphatase-labeled goat α-mouse Ig screening antibodies were applied and phosphatase tablets added as substrate. Measurement was performed on a Magellan plate reader.

7.3.3. Histology

Mouse organs were fixed in 4% formaldehyde and paraffin embedded. Dr. Markus

Kremer analyzed murine histologies. Sections were stained with H&E. Ki-67 (SP6; Thermo Fisher Scientific) staining was performed on an automated immunostainer (Leica Bond III) according to the company's protocols.

Prof. Dr. Alexandar Tzankov provided analyzed 67 well characterized DLBCL cases for which the cell-of-origin subtype according to the Tally algorithm was known (Meyer et al., 2011). Cases were considered evaluable if at least one positive stained nucleus (internal positive control) was present. Immunoperoxidase stain was performed on an automated immunostainer (Benchmark; Ventana/Roche). Primary antibody dilution pJNK #4668 (Cell Signaling Technology) was used 1:50. Antigen retrieval achieved by cell conditioning (CC1; Ventana/Roche) treatment for 92 minutes.

7.4. Molecular biology

7.4.1. Western blot

Lysates

Cells were lysed in a low-salt buffer using Buffer A (0.2% Nonidet P40, 10mM Hepes pH 7.9, 10mM KCl, 0.1mM EDTA, 0.1mM EGTA, 1mM DTT, 1mM PMSF and protease inhibitors) to obtain cytoplasmic extracts. Protein extracts of pelleted nuclei as well as total cell extracts were generated using RIPA buffer (0.5 M Tris-HCl pH 7.4, 1.5 M NaCl, 2.5% deoxycholic acid, 10% Nonidet P40, 10mM EDTA, 10mM NaF, 1mM $NaVO_4$ and protease inhibitors) for western blot analysis. Nuclear lysates for EMSA were obtained by lysis in Buffer C 20mM HEPES pH 7.9, 0.4 M, 0.1mM EDTA, 0.1mM EGTA, 10mM NaF, 1mM $NaVO_4$ and protease inhibitors. The protein concentrations were quantified using Bradford reagent (DC protein assay, Bio-Rad) according to manufacturer's instructions. Lysates were denaturated in SDS sample buffer (62.5mM Tris/HCl (pH6.8), 2% SDS (w/v), 10% glycerol (v/v), 5% 2-mercaptoethanol (v/v), 0.02% bromphenol blue (w/v)) at 95°C for 5min before western blot analysis.

Co-immunoprecipitations

Co-immunoprecipitations were performed as described earlier in (Bidère et al., 2009). Briefly, $2x10^7$ cells were lysed 30 minutes on ice in 50 mM Tris pH 7.4, 150 mM NaCl, 1% Triton X-100, 1% NP-40 and 2 mM EDTA) supplemented with 10mM NaF, 1mM $NaVO_4$

and protease inhibitors. Samples were pre-cleared with protein G-sepharose (Amersham) for 1 h. Upon pre-clearing primary antibodies were incubated over night. Precipitation was performed with Sepharose G beads (Amersham) for 1 hour. Upon washing and sample denaturation, lysates were subjected to western blot analysis.

Nonradioacative JNK2 kinase assay

$2x10^7$ cells were lysed 10 minutes on ice in 50mM Hepes pH7.4, 250mM NaCl, 1% NP-40 and 1mM EDTA. Protease Inhibitor Cocktail (Calbiochem), 1mM Na_3VO_4 and 1mM NaF were added freshly. Then cells were put on a shaker in cold room for another 5 minutes. 10% were saved as input from lysates. Lysates were pre-cleared with Sepharose A (GE healthcare) and incubated over night with JNK2 antibody #4672 (Cell Signaling Technology). Immunocomplexes were treated with Sepharose A, and then beads were divided on two eppendorf tubes. Beads were washed once with kinase buffer. Kinase buffer: 25mM Tris-HCl, 5mM β-glycerophosphate, 2mM DTT, 0.1mM Na_3VO_4, 10mM $MgCl_2$ was supplied with 1 μg recombinant c-Jun #6093 per sample. One tube was incubated without ATP and the other with 1mM ATP #9804 in kinase buffer for 30 minutes at 30 degrees (Cell Signaling Technology). Reaction was stopped by the addition of 5x sample buffer (protocol was adapted from (Blonska et al., 2007)).

SDS Page

Protein mixtures were separated by discontinuous SDS PAGE. In discontinuous PAGE, the acrylamide gel is composed of a stacking gel where negatively charged proteins are detained at the separation line (5% (v/v) acrylamide, 0.625mM Tris pH 6.8, 0.1% (w/v) SDS, 0.1% (w/v) APS, 0.006% (w/v) TEMED), and a resolving gel where proteins are separated according to molecular weight (10% (v/v) acrylamide, 3.75mM Tris pH 8.8, 0.1% (w/v) SDS, 0.1% (w/v) APS, 0.004% (w/v) TEMED).

The gel was run in 25mM Tris (pH 8), 2M glycine, 1% SDS (w/v) at 150V. Afterwards, resolved proteins were transferred electrophoretically from the SDS PAGE onto a PVDF (Amersham Hybond, GE Healthcare) membrane via a wet blotting approach in transfer buffer (50mM Tris (pH 8.5), 40mM glycine, 0.03% SDS (w/v), 20% methanol (v/v) added prior to use) at 0.4A for 2 hours. Membranes were blocked for 20 minutes in 5% BSA (w/v) in TBST (0.025% Tween-20 (v/v), 20mM Tris (pH7.4), 137mM NaCl) and then probed with antigen specific primary antibodies (dilution range 1:1000–1:2000) over night. Antibody dilutions were prepared in 5% BSA (w/v) in TBST. For

chemiluminesence-based detection, HRP-conjugated secondary antibodies (dilution 1:2000) were added for 2 hours at RT, then Lumigen TMA-6, Solution A+B (GE Healthcare) or Detection Reagent 1+2/Peroxid Solution (Thermo Scientific, Pierce) were applied.

Electrophoretic mobility shift assay (EMSA)

For EMSA 5µg nuclear lysates (Buffer C) were incubated in 20 µl binding buffer (5mM HEPES (pH 7.8), 50mM KCl, 0.5mM dithiothreitol, 1 µg Poly (dI-dC) and 10% glycerol) complemented with IRDye700-labeled, double-stranded oligonucleotide probes for NF-κB or AP-1 for 30 minutes at RT in the dark. Labeling was stopped by the addition of sample buffer were electrophoretically separated on a 5% polyacrylamide gel. EMSAs were analyzed using Odyssey Infrared Imaging System (Licor Biosciences). AP-1 consensus oligonucleotide 5´CGC TTG ATG ACT CAG CCG GAA 3´and NF-κB probe 5´ AGT TGA GGG GAC TTT CCC AGG C 3´ (Licor).

7.4.2. RNA and Real time PCR

Total RNA was obtained from MACS-purified splenic B cells by Trizol purification combined to RNeasy columns (Quiagen), transcribed into cDNA by Superscript II reverse transcriptase (Invitrogen) and used as template for qRT PCR with Sybr Green Core Kit (Eurogenentec). The analysis was performed on a LightCycler LC480 (Roche). Samples were measured in duplicates and normalized to housekeeping gene *Hrpt1*.

7.4.3. Genomic DNA and Southern blot

Genomic DNA was obtained from tumor samples and from MACS-purified splenic B or T cells by Phenol/Chloroform purification. 20µg of gDNA were digested with EcoRI HF (NEB) and loaded. Southern blot was performed as described earlier (Pechloff et al., 2010).

7.4.4. Flow cytometry

Single cell suspensions were obtained according to standard methods, treated with red blood cell lysis buffer and transferred into PBS containing 3% FCS. After incubation with

Fc-block (CD16/32), cells were stained for 30 minutes at 4 degree and washed afterwards. For intracellular stainings cells were fixed with 2% formaldehyde and permeabilized with ice-cold 70% methanol for at least 20 minutes on ice, stained and acquired on a FACSCanto II (BD) and analyzed using FlowJo software (Tree Star, Inc.).

For proliferation assays cells were incubated with the Cell Proliferation Dye eFluor 670 (eBioscience) according to manufacurer´s protocol and cultured for indicated time periods in RPMI medium containing 10% FCS, 1% Penicillin/Streptomycin and 0.1% β-Mercaptoethanol. The fluorescent proliferation dye unspecifically binds to cellular proteins. Cell division leads to equal distribution of the dye to daughter cells, which is measured by reduction of the fluorescence intensity of the dye. Before acquisition by flow cytometry cells were stained with the live/dead fixable dead cell stain kit (Invitrogen) according to manufacturer´s instructions.

CD19-Cre CARD11(L225LI) cells were incubated with a final concentration of 10µM BrdU in cell culture medium, for staining and acquisition the manual was followed (BD Pharmingen BrdU Flow Kits). BrdU is incorporated into newly synthesized DNA as analogue of thymidine; it is diluted after each cell division, so that is a useful measure for cell cycle and division.

7.5. Statistics

Statistical significance was analyzed using the unpaired two-tailed Student's t test or one-way ANOVA with Tukey post test. ***, statistically significant ($P < 0.0001$); **, $P < 0.01$; *, $P < 0.05$; ns, not statistically significant ($P \geq 0.05$).

8. ABBREVIATIONS

ABC activated B cell-like

AID activation-induced-deaminase

AP-1 activator protein 1

Atf2 activating transcription factor 2

ATR ataxia-telangiectasia-related

Bcl B cell lymphoma

BCR B cell receptor

Blimp-1 B lymphocyte-induced maturation protein 1

BLNK B cell linker protein

BrdU Bromodeoxyuridine

BTK Bruton's tyrosine kinase

c-myc myelocytomatosis viral oncogene homolog

Ca^{2+} calcium

Calr Calreticulin

CaM Calmodulin

CARD11 CARD domain-containing MAGUK protein 11

CBM CARD11-BCL10-MALT1

Chek1 checkpoint kinase 1

cIAP cellular inhibitor of apoptosis

CK1α casein kinase 1 α

CLP common lymphoid progenitor

Co-IP Co-immunoprecipitation

CRAC calcium release activated channel

CXCR C-X-C chemokine receptor

CYLD cylindromatosis

D diversity

DAG diacylglycerol

DC dendritic cell

DD death domain

DLBCL diffuse large B cell lymphoma

eGFP enhanced green fluorescent protein

ELK-1 ETS domain-containing protein 1

ER endoplasmatic reticulum

ERK extracellular signal-regulated kinase

Fwd forward

FDC follicular dendritic cells

FO follicular

Fos Finkel-Biskis-Jinkins murine osteogenic sarcoma

FOXO forkhead box protein O

G guanine

GC germinal center

GCB Germinal center B cell

H heavy

HL Hodgkin´s lymphoma

HRS Hodgkin and Reed Sternberg

ICOS Inducible costimulator

ICOSL Inducible costimulator ligand

IFNγ interferon-γ

IKK inhibitor of NF-κB kinase

IL interleukin

IP immunoprecipitation

i.p. intra-peritoneal

IRAK IL-1 receptor-associated kinase

IRES internal-ribosomal-entry site

IRF4 Interferon regulatory factor 4

ITAM immuno-receptor tyrosine-based activation motifs

IκB inhibitor of NF-κB

J joining

Jak janus kinase

JIP Jnk-interacting-protein

JNK c-Jun N-terminal kinase

L light

LoxP-flanked FL

M mitose

Maf musculoaponeurotic fibrosarcoma oncogene homolog

MAGUK membrane-associated guanylate kinase

MALT mucosa-associated lymphoid tissue

MALT1 mucosa-associated lymphoid tissue translocation gene 1

MAPKK MAP kinase kinases

MAPKKK MAP kinase kinase kinases

Mef2c monocyte enhancer factor 2C

MEK Mitogen-activated extracellular signal-regulated kinase

MHC major histocompatibility complex

MKK mitogen-activated protein kinase kinases

mTorc1 mammalian target of rapamycin 1

MyD88 myeloid differentiation primary-response gene 88

MZ marginal zone

NEMO NF-κB essential modulator

NF-AT nuclear factor of activated T cells

NF-κB nuclear factor- κB

NHL Non-Hodgkin´s lymphoma

NK natural killer

OTU ovarian tumor

pA polyA

PAMP pathogen-associated molecular pattern

PD-1 programmed cell death-1

PDK-1 phosphoinositide-dependent protein kinase 1

PDZ postsynaptic density 95, disc large and zonula occludens 1

PH pleckstrin homology

PI3K phosphoinositide-3-kinase

PIP2 phosphatidylinositol 4,5-bisphosphate

PIP3 phosphatidylinositol 3,4,5-triphosphate

PKC protein kinase C

PLCγ2 phospholipase Cγ2

PMBL primary-mediastinal B cell lymphoma

PNA peanut agglutinin

PRDM1 PR domain zinc finger protein 1

PRR pattern-recognition-receptors

RAG recombination-activating genes

RasGRP RAS guanyl releasing protein

Rev reverse

RHD Rel-homology-domain

RIP receptor-interacting protein 1

S synthesis

SA splice acceptor

SAPK stress-activated MAP kinase

SCF β TrCP Skpl, Cull, the F-box protein β-transducin repeat containing protein

SH src homology

STAT signal transducer and activator of transcription

STIM stromal interaction molecule

Suppl. supplementary

SYK spleen tyrosine kinase

TAB2 TAK1-binding protein 2

TAD transactivation domain

TAK1 TGFβ-activated kinase 1

TCR T cell receptor

TdT terminal-deoxynucleotidyl-transferase

T_{FH} follicular helper T cells

TGF transforming growth factor

TI T-independent

TLR toll like receptors

TRADD TNFα receptor associated via death domain

TRAF 6 TNFα receptor-associated factor 6

U uracil

UPR unfolded-protein response

V variable

Xbp1 X-box binding protein 1

ZF zinc fingers

9. REFERENCES

Abbas, A.K., A.H.H. Lichtman, and S. Pillai. 2011. Cellular and Molecular Immunology. Saunders. 1 pp.

Adams, J.M., A.W. Harris, C.A. Pinkert, L.M. Corcoran, W.S. Alexander, S. Cory, R.D. Palmiter, and R.L. Brinster. 1985. The c-myc oncogene driven by immunoglobulin enhancers induces lymphoid malignancy in transgenic mice. *Nature*. 318:533–538.

Aiba, Y., M. Oh-Hora, S. Kiyonaka, Y. Kimura, A. Hijikata, Y. Mori, and T. Kurosaki. 2004. Activation of RasGRP3 by phosphorylation of Thr-133 is required for B cell receptor-mediated Ras activation. *Proc Natl Acad Sci USA*. 101:16612–16617.

Alizadeh, A., M. Eisen, R. Davis, C. Ma, I. Lossos, A. Rosenwald, J. Boldrick, H. Sabet, T. Tran, and X. Yu. 2000. Distinct types of diffuse large B-cell lymphoma identified by gene expression profiling. *Nature*. 403:503–511.

Alugupalli, K.R., J.M. Leong, R.T. Woodland, M. Muramatsu, T. Honjo, and R.M. Gerstein. 2004. B1b lymphocytes confer T cell-independent long-lasting immunity. *Immunity*. 21:379–390. doi:10.1016/j.immuni.2004.06.019.

Anderson, K.E., J. Coadwell, L.R. Stephens, and P.T. Hawkins. 1998. Translocation of PDK-1 to the plasma membrane is important in allowing PDK-1 to activate protein kinase B. *Curr. Biol.* 8:684–691.

Angel, P., K. Hattori, T. Smeal, and M. Karin. 1988. The jun proto-oncogene is positively autoregulated by its product, Jun/AP-1. *Cell*. 55:875–885.

Angelin-Duclos, C., G. Cattoretti, K.I. Lin, and K. Calame. 2000. Commitment of B lymphocytes to a plasma cell fate is associated with Blimp-1 expression in vivo. *J Immunol*. 165:5462–5471.

Arora, S., R.A. McDonald, G.B. Toews, and G.B. Huffnagle. 2006. Effect of a CD4-Depleting Antibody on the Development of Cryptococcus neoformans-Induced Allergic Bronchopulmonary Mycosis in Mice. *Infection and Immunity*. 74:4339–4348. doi:10.1128/IAI.01989-05.

Bakiri, L., D. Lallemand, E. Bossy-Wetzel, and M. Yaniv. 2000. Cell cycle-dependent variations in c-Jun and JunB phosphorylation: a role in the control of cyclin D1 expression. *The EMBO Journal*. 19:2056–2068. doi:10.1093/emboj/19.9.2056.

Balkwill, F. 2009. Tumour necrosis factor and cancer. *Nat Rev Cancer*. 9:361–371. doi:10.1038/nrc2628.

Batista, F.D., and N.E. Harwood. 2009. The who, how and where of antigen presentation to B cells. *Nat Rev Immunol*. 9:15–27. doi:10.1038/nri2454.

Baumgarth, N. 2011. The double life of a B-1 cell: self-reactivity selects for protective effector functions. *Nat Rev Immunol*. 11:34–46. doi:10.1038/nri2901.

Bennett, B.L., D.T. Sasaki, B.W. Murray, E.C. O'Leary, S.T. Sakata, W. Xu, J.C. Leisten, A. Motiwala, S. Pierce, Y. Satoh, S.S. Bhagwat, A.M. Manning, and D.W. Anderson. 2001. SP600125, an anthrapyrazolone inhibitor of Jun N-terminal kinase. *Proc Natl Acad Sci USA*. 98:13681–13686. doi:10.1073/pnas.251194298.

Bertin, J. 2001. CARD11 and CARD14 Are Novel Caspase Recruitment Domain (CARD)/Membrane-associated Guanylate Kinase (MAGUK) Family Members that Interact with BCL10 and Activate NF-kappa B. *Journal of Biological Chemistry*. 276:11877–11882. doi:10.1074/jbc.M010512200.

Bhoumik, A., S. Takahashi, W. Breitweiser, Y. Shiloh, N. Jones, and Z. Ronai. 2005. ATM-dependent phosphorylation of ATF2 is required for the DNA damage response. *Mol Cell*. 18:577–587. doi:10.1016/j.molcel.2005.04.015.

Bidère, N., V.N. Ngo, J. Lee, C. Collins, L. Zheng, F. Wan, R.E. Davis, G. Lenz, D.E. Anderson, D. Arnoult, A. Vazquez, K. Sakai, J. Zhang, Z. Meng, T.D. Veenstra, L.M. Staudt, and M.J. Lenardo. 2009. Casein kinase 1α governs antigen-receptor-induced NF-κB activation and human lymphoma cell survival. *Nature*. 457:92–96. doi:10.1038/nature07613.

Blank, V. 2008. Small Maf Proteins in Mammalian Gene Control: Mere Dimerization Partners or Dynamic Transcriptional Regulators? *Journal of Molecular Biology*. 376:913–925. doi:10.1016/j.jmb.2007.11.074.

Blonska, M., B.P. Pappu, R. Matsumoto, H. Li, B. Su, D. Wang, and X. Lin. 2007. The CARMA1-Bcl10 Signaling Complex Selectively Regulates JNK2 Kinase in the T Cell Receptor-Signaling Pathway. *Immunity*. 26:55–66. doi:10.1016/j.immuni.2006.11.008.

Brown, K.D., E. Claudio, and U. Siebenlist. 2008. The roles of the classical and alternative nuclear factor-kappaB pathways: potential implications for autoimmunity and rheumatoid arthritis. *Arthritis Res Ther*. 10:212. doi:10.1186/ar2457.

Brunet, A., A. Bonni, M.J. Zigmond, M.Z. Lin, P. Juo, L.S. Hu, M.J. Anderson, K.C. Arden, J. Blenis, and M.E. Greenberg. 1999. Akt promotes cell survival by phosphorylating and inhibiting a Forkhead transcription factor. *Cell*. 96:857–868.

Burgering, B.M.T., and G.J.P.L. Kops. 2002. Cell cycle and death control: long live Forkheads. *Trends in Biochemical Sciences*. 27:352–360.

Calado, D.P., B. Zhang, L. Srinivasan, Y. Sasaki, J. Seagal, C. Unitt, S. Rodig, J. Kutok, A. Tarakhovsky, M. Schmidt-Supprian, and K. Rajewsky. 2010. Constitutive Canonical NF-kB Activation Cooperates with Disruption of BLIMP1 in the Pathogenesis of Activated B Cell-like Diffuse Large Cell Lymphoma. *Cancer Cell*. 18:580–589. doi:10.1016/j.ccr.2010.11.024.

Calado, D.P., Y. Sasaki, S.A. Godinho, A. Pellerin, K. Köchert, B.P. Sleckman, I.M. de Alborán, M. Janz, S. Rodig, and K. Rajewsky. 2012. The cell-cycle regulator c-Myc is essential for the formation and maintenance of germinal centers. *Nat Immunol*. 13:1092–1100. doi:10.1038/ni.2418.

Caroll, M.C., and A.P. Prodeus. 1998. Linkages of innate and adaptive immunity. *Current Opinion in Immunology*. 10:36–40.

Casola, S., G. Cattoretti, N. Uyttersprot, S.B. Koralov, J. Seagal, J. Segal, Z. Hao, A. Waisman, A. Egert, D. Ghitza, and K. Rajewsky. 2006. Tracking germinal center B cells expressing germ-line immunoglobulin gamma1 transcripts by conditional gene targeting. *Proc Natl Acad Sci USA*. 103:7396–7401. doi:10.1073/pnas.0602353103.

Cassese, G., S. Arce, A.E. Hauser, K. Lehnert, B. Moewes, M. Mostarac, G. Muehlinghaus, M. Szyska, A. Radbruch, and R.A. Manz. 2003. Plasma cell survival is mediated by synergistic effects of cytokines and adhesion-dependent signals. *J Immunol*. 171:1684–1690.

Cato, M.H., I.W. Yau, and R.C. Rickert. 2011. Magnetic-based purification of untouched mouse germinal center B cells for ex vivo manipulation and biochemical analysis. *Nat Protoc*. 6:953–960. doi:10.1038/nprot.2011.344.

Cattoretti, G., L. Pasqualucci, G. Ballon, W. Tam, S.V. Nandula, Q. Shen, T. Mo, V.V. Murty, and R. Dalla-Favera. 2005. Deregulated BCL6 expression recapitulates the pathogenesis of human diffuse large B cell lymphomas in mice. *Cancer Cell*. 7:445–455. doi:10.1016/j.ccr.2005.03.037.

Cebra, J.J., S.B. Periwal, G. Lee, F. Lee, and K.E. Shroff. 1998. Development and maintenance of the gut-associated lymphoid tissue (GALT): the roles of enteric bacteria and viruses. *Dev. Immunol.* 6:13–18.

Cerutti, A. 2008. The regulation of IgA class switching. *Nat Rev Immunol*. 8:421–434. doi:10.1038/nri2322.

Chahwan, R., W. Edelmann, M.D. Scharff, and S. Roa. 2012. AIDing antibody diversity by error-prone mismatch repair. *Semin Immunol*. 24:293–300. doi:10.1016/j.smim.2012.05.005.

Chan, W., T.B. Schaffer, and J.L. Pomerantz. 2012. A quantitative signaling screen identifies CARD11 mutations in the CARD and LATCH Domains that induce Bcl10 ubiquitination and human lymphoma cell survival. *Molecular and Cellular Biology*. doi:10.1128/MCB.00850-12.

Chaudhuri, J., and F.W. Alt. 2004. Class-switch recombination: interplay of transcription, DNA deamination and DNA repair. *Nature Publishing Group*. 4:541–552. doi:10.1038/nri1395.

Che, T., Y. You, D. Wang, M.J. Tanner, V.M. Dixit, and X. Lin. 2004. MALT1/paracaspase is a signaling component downstream of CARMA1 and mediates T cell receptor-induced NF-kappaB activation. *J Biol Chem*. 279:15870–15876. doi:10.1074/jbc.M310599200.

Chen, K., and A. Cerutti. 2010. New insights into the enigma of immunoglobulin D. *Immunological Reviews*. 237:160–179. doi:10.1111/j.1600-065X.2010.00929.x.

Cheng, S., G. Coffey, X.H. Zhang, R. Shaknovich, Z. Song, P. Lu, A. Pandey, A.M. Melnick, U. Sinha, and Y.L. Wang. 2011. SYK inhibition and response prediction in diffuse large B-cell lymphoma. *Blood*. 118:6342–6352. doi:10.1182/blood-2011-02-333773.

Chiappella, A., and U. Vitolo. 2012. Lenalidomide in diffuse large B-cell lymphomas.

Advances in Hematology. 2012:498342. doi:10.1155/2012/498342.

Clevers, H., and R. Nusse. 2012. Wnt/β-catenin signaling and disease. *Cell*. 149:1192–1205. doi:10.1016/j.cell.2012.05.012.

Coiffier, B., C. Thieblemont, E. Van Den Neste, G. Lepeu, I. Plantier, S. Castaigne, S. Lefort, G. Marit, M. Macro, C. Sebban, K. Belhadj, D. Bordessoule, C. Ferme, and H. Tilly. 2010. Long-term outcome of patients in the LNH-98.5 trial, the first randomized study comparing rituximab-CHOP to standard CHOP chemotherapy in DLBCL patients: a study by the Groupe d"Etudes des Lymphomes de l"Adulte. *Blood*. 116:2040–2045. doi:10.1182/blood-2010-03-276246.

Compagno, M., W.K. Lim, A. Grunn, S.V. Nandula, M. Brahmachary, Q. Shen, F. Bertoni, M. Ponzoni, M. Scandurra, A. Califano, G. Bhagat, A. Chadburn, R. Dalla-Favera, and L. Pasqualucci. 2009. Mutations of multiple genes cause deregulation of NF-kappaB in diffuse large B-cell lymphoma. *Nature*. 459:717–721. doi:10.1038/nature07968.

Coornaert, B., M. Baens, K. Heyninck, T. Bekaert, M. Haegman, J. Staal, L. Sun, Z.J. Chen, P. Marynen, and R. Beyaert. 2008. T cell antigen receptor stimulation induces MALT1 paracaspase-mediated cleavage of the NF-kappaB inhibitor A20. *Nat Immunol*. 9:263–271. doi:10.1038/ni1561.

Crouch, E.E., Z. Li, M. Takizawa, S. Fichtner-Feigl, P. Gourzi, C. Montaño, L. Feigenbaum, P. Wilson, S. Janz, F.N. Papavasiliou, and R. Casellas. 2007. Regulation of AID expression in the immune response. *J Exp Med*. 204:1145–1156. doi:10.1084/jem.20061952.

Dal Porto, J.M., S.B. Gauld, K.T. Merrell, D. Mills, A.E. Pugh-Bernard, and J. Cambier. 2004. B cell antigen receptor signaling 101. *Molecular Immunology*. 41:599–613. doi:10.1016/j.molimm.2004.04.008.

Davis, R., K. Brown, U. Siebenlist, and L. Staudt. 2001a. Constitutive nuclear factor κB activity is required for survival of activated B cell–like diffuse large B cell lymphoma cells. *J Exp Med*. 194:1861.

Davis, R.E., K.D. Brown, U. Siebenlist, and L.M. Staudt. 2001b. Constitutive nuclear factor kappaB activity is required for survival of activated B cell-like diffuse large B cell lymphoma cells. *J Exp Med*. 194:1861–1874.

Davis, R.E., V.N. Ngo, G. Lenz, P. Tolar, R.M. Young, P.B. Romesser, H. Kohlhammer, L. Lamy, H. Zhao, Y. Yang, W. Xu, A.L. Shaffer, G. Wright, W. Xiao, J. Powell, J.-K. Jiang, C.J. Thomas, A. Rosenwald, G. Ott, H.K. Muller-Hermelink, R.D. Gascoyne, J.M. Connors, N.A. Johnson, L.M. Rimsza, E. Campo, E.S. Jaffe, W.H. Wilson, J. Delabie, E.B. Smeland, R.I. Fisher, R.M. Braziel, R.R. Tubbs, J.R. Cook, D.D. Weisenburger, W.C. Chan, S.K. Pierce, and L.M. Staudt. 2010. Chronic active B-cell-receptor signalling in diffuse large B-cell lymphoma. *Nature*. 463:88–92. doi:10.1038/nature08638.

Davis, R.J. 2000. Signal transduction by the JNK group of MAP kinases. *Cell*. 103:239–252.

Donnou, S., C. Galand, V. Touitou, C. Sautès-Fridman, Z. Fabry, and S. Fisson. 2012. Murine Models of B-Cell Lymphomas: Promising Tools for Designing Cancer Therapies. *Advances in Hematology*. 2012:1–13. doi:10.1016/j.biopha.2010.01.004.

Engels, N., B. Wollscheid, and J. Wienands. 2001. Association of SLP-65/BLNK with the B cell antigen receptor through a non-ITAM tyrosine of Ig-alpha. *Eur. J. Immunol.* 31:2126–2134.

Ferch, U., B. Kloo, A. Gewies, V. Pfander, M. Duwel, C. Peschel, D. Krappmann, and J. Ruland. 2009. Inhibition of MALT1 protease activity is selectively toxic for activated B cell-like diffuse large B cell lymphoma cells. *Journal of Experimental Medicine*. 206:2313–2320. doi:10.1084/jem.20091167.

Ferch, U., C.M. zum Büschenfelde, A. Gewies, E. Wegener, S. Rauser, C. Peschel, D. Krappmann, and J. Ruland. 2007. MALT1 directs B cell receptor-induced canonical nuclear factor-kappaB signaling selectively to the c-Rel subunit. *Nat Immunol*. 8:984–991. doi:10.1038/ni1493.

Ferguson, A.R. 2004. Marginal zone B cells transport and deposit IgM-containing immune complexes onto follicular dendritic cells. *Int. Immunol.* 16:1411–1422. doi:10.1093/intimm/dxh142.

Fontan, L., C. Yang, V. Kabaleeswaran, L. Volpon, M.J. Osborne, E. Beltran, M. Garcia, L. Cerchietti, R. Shaknovich, S.N. Yang, F. Fang, R.D. Gascoyne, J.A. Martinez-Climent, J.F. Glickman, K. Borden, H. Wu, and A. Melnick. 2012. MALT1 small molecule inhibitors specifically suppress ABC-DLBCL in vitro and in vivo. *Cancer Cell*. 22:812–824. doi:10.1016/j.ccr.2012.11.003.

Frasca, D., M. Romero, A. Diaz, S. Alter-Wolf, M. Ratliff, A.M. Landin, R.L. Riley, and B.B. Blomberg. 2012. A molecular mechanism for TNF-α-mediated downregulation of B cell responses. *The Journal of Immunology*. 188:279–286. doi:10.4049/jimmunol.1003964.

Friedrich, G., and P. Soriano. 1991. Promoter traps in embryonic stem cells: a genetic screen to identify and mutate developmental genes in mice. *Genes Dev*. 5:1513–1523. doi:10.1038/5007.

Fruman, D.A. 2012. Akt and mTOR in B cell activation and differentiation. 1–12. doi:10.3389/fimmu.2012.00228/abstract.

Fu, C., C.W. Turck, T. Kurosaki, and A.C. Chan. 1998. BLNK: a central linker protein in B cell activation. *Immunity*. 9:93–103.

Fujimoto, M., Y. Fujimoto, J.C. Poe, P.J. Jansen, C.A. Lowell, A.L. DeFranco, and T.F. Tedder. 2000. CD19 regulates Src family protein tyrosine kinase activation in B lymphocytes through processive amplification. *Immunity*. 13:47–57.

Gaide, O., F. Martinon, O. Micheau, D. Bonnet, M. Thome, and J. Tschopp. 2001. Carma1, a CARD-containing binding partner of Bcl10, induces Bcl10 phosphorylation and NF-κB activation. *FEBS Letters*. 496:121–127. doi:10.1016/S0014-5793(01)02414-0.

Galli, S.J., N. Borregaard, and T.A. Wynn. 2011. Phenotypic and functional plasticity of cells of innate immunity: macrophages, mast cells and neutrophils. *Nat Immunol*. 12:1035–1044. doi:10.1038/ni.2109.

Gary-Gouy, H. 2002. Human CD5 promotes B-cell survival through stimulation of

autocrine IL-10 production. *Blood*. 100:4537–4543. doi:10.1182/blood-2002-05-1525.

Gauld, S.B., and J.C. Cambier. 2004. Src-family kinases in B-cell development and signaling. *Oncogene*. 23:8001–8006. doi:10.1038/sj.onc.1208075.

Ghosh, S., and M.S. Hayden. 2008. New regulators of NF-κB in inflammation. *Nat Rev Immunol*. 8:837–848. doi:10.1038/nri2423.

Ghosh, S., M.J. May, and E.B. Kopp. 1998. NF-kappa B and Rel proteins: evolutionarily conserved mediators of immune responses. *Annu Rev Immunol*. 16:225–260. doi:10.1146/annurev.immunol.16.1.225.

Gisselbrecht, C., B. Glass, N. Mounier, D. Singh Gill, D.C. Linch, M. Trneny, A. Bosly, N. Ketterer, O. Shpilberg, H. Hagberg, D. Ma, J. Briere, C.H. Moskowitz, and N. Schmitz. 2010. Salvage regimens with autologous transplantation for relapsed large B-cell lymphoma in the rituximab era. *Journal of Clinical Oncology*. 28:4184–4190. doi:10.1200/JCO.2010.28.1618.

Godin, I.E., J.A. Garcia-Porrero, A. Coutinho, F. Dieterlen-Lièvre, and M.A. Marcos. 1993. Para-aortic splanchnopleura from early mouse embryos contains B1a cell progenitors. *Nature*. 364:67–70. doi:10.1038/364067a0.

Goetz, C.A., and A.S. Baldwin. 2008. NF-κB pathways in the immune system: control of the germinal center reaction. *Immunol Res*. 41:233–247. doi:10.1007/s12026-008-8033-1.

Grädler, U., D. Schwarz, V. Dresing, D. Musil, J. Bomke, M. Frech, H. Greiner, S. Jäkel, T. Rysiok, D. Müller-Pompalla, and A. Wegener. 2013. Structural and Biophysical Characterization of the Syk Activation Switch. *Journal of Molecular Biology*. 425:309–333. doi:10.1016/j.jmb.2012.11.007.

Greenwald, R.J. 2003. E -BRD2 transgenic mice develop B-cell lymphoma and leukemia. *Blood*. 103:1475–1484. doi:10.1182/blood-2003-06-2116.

Greil, J., T. Rausch, T. Giese, O.R. Bandapalli, V. Daniel, I. Bekeredjian-Ding, A.M. Stütz, C. Drees, S. Roth, J. Ruland, J.O. Korbel, and A.E. Kulozik. 2013. Whole-exome sequencing links caspase recruitment domain 11 (CARD11) inactivation to severe combined immunodeficiency. *J. Allergy Clin. Immunol.* 131:1376–83.e3. doi:10.1016/j.jaci.2013.02.012.

Grönwall, C., J. Vas, and G.J. Silverman. 2012. Protective Roles of Natural IgM Antibodies. *Front Immunol*. 3:66. doi:10.3389/fimmu.2012.00066.

Gupta, M., J.J. Han, M. Stenson, M. Maurer, L. Wellik, G. Hu, S. Ziesmer, A. Dogan, and T.E. Witzig. 2012. Elevated serum IL-10 levels in diffuse large B-cell lymphoma: a mechanism of aberrant Janus kinase 2 activation. *Blood*. doi:10.1182/blood-2011-10-388538.

Gupta, S., D. Campbell, B. Derijard, and R.J. Davis. 1995. Transcription factor ATF2 regulation by the JNK signal transduction pathway. *Science*. 267:389–393.

Gupta, S., T. Barrett, A.J. Whitmarsh, J. Cavanagh, H.K. Sluss, B. Derijard, and R.J. Davis. 1996. Selective interaction of JNK protein kinase isoforms with transcription factors. *The EMBO Journal*. 15:2760–2770.

Gururajan, M. 2005. c-Jun N-terminal kinase (JNK) is required for survival and proliferation of B-lymphoma cells. *Blood*. 106:1382–1391. doi:10.1182/blood-2004-10-3819.

Haas, K.M., J.C. Poe, D.A. Steeber, and T.F. Tedder. 2005. B-1a and B-1b Cells Exhibit Distinct Developmental Requirements and Have Unique Functional Roles in Innate and Adaptive Immunity to S. pneumoniae. *Immunity*. 23:7–18. doi:10.1016/j.immuni.2005.04.011.

Hailfinger, S., G. Lenz, V. Ngo, A. Posvitz-Fejfar, F. Rebeaud, M. Guzzardi, E.-M.M. Penas, J. Dierlamm, W.C. Chan, L.M. Staudt, and M. Thome. 2009. Essential role of MALT1 protease activity in activated B cell-like diffuse large B-cell lymphoma. *Proceedings of the National Academy of Sciences*. 106:19946–19951. doi:10.1073/pnas.0907511106.

Hanahan, D., and R.A. Weinberg. 2011. Hallmarks of Cancer: The Next Generation. *Cell*. 144:646–674. doi:10.1016/j.cell.2011.02.013.

Hara, H., T. Wada, C. Bakal, I. Kozieradzki, S. Suzuki, N. Suzuki, M. Nghiem, E.K. Griffiths, C. Krawczyk, B. Bauer, F. D'Acquisto, S. Ghosh, W.C. Yeh, G. Baier, R. Rottapel, and J.M. Penninger. 2003. The MAGUK family protein CARD11 is essential for lymphocyte activation. *Immunity*. 18:763–775.

Hayakawa, K., R.R. Hardy, D.R. Parks, and L.A. Herzenberg. 1983. The “Ly-1 B” cell subpopulation in normal immunodefective, and autoimmune mice. *J Exp Med*. 157:202–218.

Hayden, M.S., and S. Ghosh. 2012. NF- B, the first quarter-century: remarkable progress and outstanding questions. *Genes Dev*. 26:203–234. doi:10.1101/gad.183434.111.

Henkel, T., T. Machleidt, I. Alkalay, M. Krönke, Y. Ben-Neriah, and P.A. Baeuerle. 1993. Rapid proteolysis of I kappa B-alpha is necessary for activation of transcription factor NF-kappa B. *Nature*. 365:182–185. doi:10.1038/365182a0.

Herzenberg, L.A. 2000. B-1 cells: the lineage question revisited. *Immunological Reviews*. 175:9–22.

Herzog, S., M. Reth, and H. Jumaa. 2009. Regulation of B-cell proliferation and differentiation by pre-B-cell receptor signalling. *Nat Rev Immunol*. 9:195–205. doi:10.1038/nri2491.

Hess, J., P. Angel, and M. Schorpp-Kistner. 2004. AP-1 subunits: quarrel and harmony among siblings.

Hess, P., G. Pihan, C.L. Sawyers, R.A. Flavell, and R.J. Davis. 2002. Survival signaling mediated by c-Jun NH2-terminal kinase in transformed B lymphoblasts. *Nature Genetics*. 32:201–205. doi:10.1038/ng946.

Hibi, M., A. Lin, T. Smeal, A. Minden, and M. Karin. 1993. Identification of an oncoprotein- and UV-responsive protein kinase that binds and potentiates the c-Jun activation domain. *Genes Dev*. 7:2135–2148. doi:10.1101/gad.7.11.2135.

Hogan, P.G., L. Chen, J. Nardone, and A. Rao. 2003. Transcriptional regulation by calcium, calcineurin, and NFAT. *Genes Dev*. 17:2205–2232. doi:10.1101/gad.1102703.

Hombach, J., L. Leclercq, A. Radbruch, K. Rajewsky, and M. Reth. 1988. A novel 34-kd protein co-isolated with the IgM molecule in surface IgM-expressing cells. *The EMBO Journal*. 7:3451–3456.

Huguier, S., J. Baguet, S. Perez, H. van Dam, and M. Castellazzi. 1998. Transcription factor ATF2 cooperates with v-Jun to promote growth factor-independent proliferation in vitro and tumor formation in vivo. *Molecular and Cellular Biology*. 18:7020–7029.

Hymowitz, S.G., and I.E. Wertz. 2010. A20: from ubiquitin editing to tumour suppression. *Nat Rev Cancer*. 10:332–341. doi:10.1038/nrc2775.

Ip, Y.T., and R.J. Davis. 1998. Signal transduction by the c-Jun N-terminal kinase (JNK)--from inflammation to development. *Curr. Opin. Cell Biol.* 10:205–219.

Iqbal, J., W.G. Sanger, D.E. Horsman, A. Rosenwald, D.L. Pickering, B. Dave, S. Dave, L. Xiao, K. Cao, Q. Zhu, S. Sherman, C.P. Hans, D.D. Weisenburger, T.C. Greiner, R.D. Gascoyne, G. Ott, H.K. Muller-Hermelink, J. Delabie, R.M. Braziel, E.S. Jaffe, E. Campo, J.C. Lynch, J.M. Connors, J.M. Vose, J.O. Armitage, T.M. Grogan, L.M. Staudt, and W.C. Chan. 2004. BCL2 Translocation Defines a Unique Tumor Subset within the Germinal Center B-Cell-Like Diffuse Large B-Cell Lymphoma. *The American Journal of Pathology*. 165:159–166. doi:10.1016/S0002-9440(10)63284-1.

Janeway, C. 2001. Immunobiology five. Garland Science. 1 pp.

Janeway, C.A. 1989. Approaching the asymptote? Evolution and revolution in immunology. *Cold Spring Harb. Symp. Quant. Biol.* 54 Pt 1:1–13.

Jeelall, Y.S., and K. Horikawa. 2011. Oncogenic MYD88 mutation drives Toll pathway to lymphoma. *Immunol Cell Biol*. 89:659–660. doi:10.1038/icb.2011.31.

Jeelall, Y.S., J.Q. Wang, H.-D. Law, H. Domaschenz, H.K.H. Fung, A. Kallies, S.L. Nutt, C.C. Goodnow, and K. Horikawa. 2012. Human lymphoma mutations reveal CARD11 as the switch between self-antigen-induced B cell death or proliferation and autoantibody production. *Journal of Experimental Medicine*. 209:1907–1917. doi:10.1084/jem.20112744.

Jochum, W., E. Passegué, and E.F. Wagner. 2001. AP-1 in mouse development and tumorigenesis. *Oncogene*. 20:2401–2412. doi:10.1038/sj.onc.1204389.

Joos, S., M.I. Otano-Joos, S. Ziegler, S. Bruderlein, S. du Manoir, M. Bentz, P. Möller, and P. Lichter. 1996. Primary mediastinal (thymic) B-cell lymphoma is characterized by gains of chromosomal material including 9p and amplification of the REL gene. *Blood*. 87:1571–1578.

Kaminski, D.A., and J. Stavnezer. 2006. Enhanced IgA class switching in marginal zone

and B1 B cells relative to follicular/B2 B cells. *J Immunol*. 177:6025–6029.

Kanayama, A., R.B. Seth, L. Sun, C.-K. Ea, M. Hong, A. Shaito, Y.-H. Chiu, L. Deng, and Z.J. Chen. 2004. TAB2 and TAB3 activate the NF-kappaB pathway through binding to polyubiquitin chains. *Mol Cell*. 15:535–548. doi:10.1016/j.molcel.2004.08.008.

Karin, M., and A. Lin. 2002. NF-kappaB at the crossroads of life and death. *Nat Immunol*. 3:221–227. doi:10.1038/ni0302-221.

Kato, M., M. Sanada, I. Kato, Y. Sato, J. Takita, K. Takeuchi, A. Niwa, Y. Chen, K. Nakazaki, J. Nomoto, Y. Asakura, S. Muto, A. Tamura, M. Iio, Y. Akatsuka, Y. Hayashi, H. Mori, T. Igarashi, M. Kurokawa, S. Chiba, S. Mori, Y. Ishikawa, K. Okamoto, K. Tobinai, H. Nakagama, T. Nakahata, T. Yoshino, Y. Kobayashi, and S. Ogawa. 2009. Frequent inactivation of A20 in B-cell lymphomas. *Nature*. 459:712–716. doi:10.1038/nature07969.

Katoh, M., and M. Katoh. 2007. AP1-and NF-kappaB-binding sites conserved among mammalian WNT10B orthologs elucidate the TNFalpha-WNT10B signaling loop implicated in carcinogenesis and adipogenesis. *Int. J. Mol. Med.* 19:699.

Keller, S.A., E.J. Schattner, and E. Cesarman. 2000. Inhibition of NF-kappaB induces apoptosis of KSHV-infected primary effusion lymphoma cells. *Blood*. 96:2537–2542.

Kim, C.H., L.S. Rott, I. Clark-Lewis, D.J. Campbell, L. Wu, and E.C. Butcher. 2001. Subspecialization of CXCR5+ T cells: B helper activity is focused in a germinal center-localized subset of CXCR5+ T cells. *J Exp Med*. 193:1373–1381.

King, C., S.G. Tangye, and C.R. Mackay. 2008. T follicular helper (TFH) cells in normal and dysregulated immune responses. *Annu Rev Immunol*. 26:741–766. doi:10.1146/annurev.immunol.26.021607.090344.

Kirchhofer, D., and D. Vucic. 2012. Protease activity of MALT1: a mystery unravelled. *Biochem. J.* 444:e3–e5. doi:10.1042/BJ20120414.

Kitamura, D., J. Roes, R. Kühn, and K. Rajewsky. 1991. A B cell-deficient mouse by targeted disruption of the membrane exon of the immunoglobulin mu chain gene. *Nature*. 350:423–426. doi:10.1038/350423a0.

Klein, U., and R. Dalla-Favera. 2008. Germinal centres: role in B-cell physiology and malignancy. *Nat Rev Immunol*. 8:22–33. doi:10.1038/nri2217.

Klein, U., S. Casola, G. Cattoretti, Q. Shen, M. Lia, T. Mo, T. Ludwig, K. Rajewsky, and R. Dalla-Favera. 2006. Transcription factor IRF4 controls plasma cell differentiation and class-switch recombination. *Nat Immunol*. 7:773–782. doi:10.1038/ni1357.

Klein, U., Y. Tu, G.A. Stolovitzky, J.L. Keller, J. Haddad, V. Miljkovic, G. Cattoretti, A. Califano, and R. Dalla-Favera. 2003. Transcriptional analysis of the B cell germinal center reaction. *Proc Natl Acad Sci USA*. 100:2639–2644. doi:10.1073/pnas.0437996100.

Kloo, B., D. Nagel, M. Pfeifer, M. Grau, M. Duwel, M. Vincendeau, B. Dorken, P. Lenz, G. Lenz, and D. Krappmann. 2011. Critical role of PI3K signaling for NF- B-dependent

survival in a subset of activated B-cell-like diffuse large B-cell lymphoma cells. *Proceedings of the National Academy of Sciences*. 108:272–277. doi:10.1073/pnas.1008969108.

Kondo, E., and T. Yoshino. 2007. Expression of apoptosis regulators in germinal centers and germinal center-derived B-cell lymphomas: Insight into B-cell lymphomagenesis. *Pathology International*. 57:391–397. doi:10.1111/j.1440-1827.2007.02115.x.

Kovalchuk, A.L., J.S. Kim, S.S. Park, A.E. Coleman, J.M. Ward, H.C. Morse, T. Kishimoto, M. Potter, and S. Janz. 2002. IL-6 transgenic mouse model for extraosseous plasmacytoma. *Proc Natl Acad Sci USA*. 99:1509–1514. doi:10.1073/pnas.022643999.

Koyasu, S. 2003. The role of PI3K in immune cells - Nature Immunology. *Nat Immunol*.

Kumar, H., T. Kawai, and S. Akira. 2011. Pathogen Recognition by the Innate Immune System. *Int Rev Immunol*. 30:16–34. doi:10.3109/08830185.2010.529976.

Kurosaki, T. 1999. Genetic analysis of B cell antigen receptor signaling. *Annu Rev Immunol*. 17:555–592. doi:10.1146/annurev.immunol.17.1.555.

Kurosaki, T. 2011. Regulation of BCR signaling. *Molecular Immunology*. 48:1287–1291. doi:10.1016/j.molimm.2010.12.007.

Kurosaki, T., and M. Kurosaki. 1997. Transphosphorylation of Bruton's tyrosine kinase on tyrosine 551 is critical for B cell antigen receptor function. *J Biol Chem*. 272:15595–15598.

Küppers, R., A. Engert, and M.-L. Hansmann. 2012. Hodgkin lymphoma. *Journal of Clinical Investigation*. 122:3439–3447. doi:10.1172/JCI61245.

Lalor, P.A., L.A. Herzenberg, S. Adams, and A.M. Stall. 1989. Feedback regulation of murine Ly-1 B cell development. *Eur. J. Immunol.* 19:507–513. doi:10.1002/eji.1830190315.

Lam, L.T., G. Wright, R.E. Davis, G. Lenz, P. Farinha, L. Dang, J.W. Chan, A. Rosenwald, R.D. Gascoyne, and L.M. Staudt. 2008. Cooperative signaling through the signal transducer and activator of transcription 3 and nuclear factor- B pathways in subtypes of diffuse large B-cell lymphoma. *Blood*. 111:3701–3713. doi:10.1182/blood-2007-09-111948.

Lamason, R.L., R.R. Mccully, S.M. Lew, and J.L. Pomerantz. 2010. Oncogenic CARD11 Mutations Induce Hyperactive Signaling by Disrupting Autoinhibition by the PKC-Responsive Inhibitory Domain. *Biochemistry*. 49:8240–8250. doi:10.1021/bi101052d.

Langel, F.D., N.A. Jain, J.S. Rossman, L.M. Kingeter, A.K. Kashyap, and B.C. Schaefer. 2008. Multiple protein domains mediate interaction between Bcl10 and MALT1. *J Biol Chem*. 283:32419–32431. doi:10.1074/jbc.M800670200.

Lee, D.-F., and M.-C. Hung. 2008. Advances in targeting IKK and IKK-related kinases for

cancer therapy. *Clin. Cancer Res.* 14:5656–5662. doi:10.1158/1078-0432.CCR-08-0123.

Lenz, G., and L.M. Staudt. 2010. Aggressive lymphomas. *N Engl J Med*. 362:1417–1429. doi:10.1056/NEJMra0807082.

Lenz, G., R.E. Davis, V.N. Ngo, L. Lam, T.C. George, G.W. Wright, S.S. Dave, H. Zhao, W. Xu, A. Rosenwald, G. Ott, H.K. Muller-Hermelink, R.D. Gascoyne, J.M. Connors, L.M. Rimsza, E. Campo, E.S. Jaffe, J. Delabie, E.B. Smeland, R.I. Fisher, W.C. Chan, and L.M. Staudt. 2008. Oncogenic CARD11 mutations in human diffuse large B cell lymphoma. *Science*. 319:1676–1679. doi:10.1126/science.1153629.

Li, Q., and I.M. Verma. 2002. NF-κB regulation in the immune system. *Nat Rev Immunol*. 2:725–734. doi:10.1038/nri910.

Li, Y.S., K. Hayakawa, and R.R. Hardy. 1993. The regulated expression of B lineage associated genes during B cell differentiation in bone marrow and fetal liver. *J Exp Med*. 178:951–960.

Lim, K.-H., Y. Yang, and L.M. Staudt. 2012. Pathogenetic importance and therapeutic implications of NF-κB in lymphoid malignancies. *Immunological Reviews*. 246:359–378. doi:10.1111/j.1600-065X.2012.01105.x.

Lin, K.I., C. Angelin-Duclos, T.C. Kuo, and K. Calame. 2002. Blimp-1-Dependent Repression of Pax-5 Is Required for Differentiation of B Cells to Immunoglobulin M-Secreting Plasma Cells. *Molecular and Cellular Biology*. 22:4771–4780. doi:10.1128/MCB.22.13.4771-4780.2002.

Lin, Y., K. Wong, and K. Calame. 1997. Repression of c-myc transcription by Blimp-1, an inducer of terminal B cell differentiation. *Science*. 276:596–599.

Lucas, P.C., M. Yonezumi, N. Inohara, L.M. McAllister-Lucas, M.E. Abazeed, F.F. Chen, S. Yamaoka, M. Seto, and G. Nunez. 2001. Bcl10 and MALT1, independent targets of chromosomal translocation in malt lymphoma, cooperate in a novel NF-kappa B signaling pathway. *J Biol Chem*. 276:19012–19019. doi:10.1074/jbc.M009984200.

MacLennan, I., K.M. Toellner, A.F. Cunningham, K. Serre, D.M.Y. Sze, E. Zuniga, M.C. Cook, and C.G. Vinuesa. 2003. Extrafollicular antibody responses. *Immunological Reviews*. 194:8–18.

Macpherson, A.J., K.D. McCoy, F.-E. Johansen, and P. Brandtzaeg. 2008. The immune geography of IgA induction and function. *Mucosal Immunol*. 1:11–22. doi:10.1038/mi.2007.6.

Marafioti, T., M. Pozzobon, M.-L. Hansmann, P. Gaulard, T.F. Barth, C. Copie-Bergman, H. Roberton, R. Ventura, J.I. Martín-Subero, R.D. Gascoyne, S.A. Pileri, R. Siebert, E.D. Hsi, Y. Natkunam, P. Möller, and D.Y. Mason. 2005. Expression pattern of intracellular leukocyte-associated proteins in primary mediastinal B cell lymphoma. *Leukemia*. 19:856–861. doi:10.1038/sj.leu.2403702.

Martelli, M., A.J.M. Ferreri, and P. Johnson. 2008. Primary mediastinal large B-cell lymphoma. *Critical Reviews in Oncology/Hematology*. 68:256–263.

doi:10.1016/j.critrevonc.2008.07.020.

Matasar, M., and Word. 2012. Advances in the diagnosis and management of lymphoma. *BLCTT*. 29. doi:10.2147/BLCTT.S15554.

Mathas, S., M. Hinz, I. Anagnostopoulos, D. Krappmann, A. Lietz, F. Jundt, K. Bommert, F. Mechta-Grigoriou, H. Stein, B. Dörken, and C. Scheidereit. 2002. Aberrantly expressed c-Jun and JunB are a hallmark of Hodgkin lymphoma cells, stimulate proliferation and synergize with NF-kappa B. *The EMBO Journal*. 21:4104–4113.

McAllister-Lucas, L.M., M. Baens, and P.C. Lucas. 2011. MALT1 Protease: A New Therapeutic Target in B Lymphoma and Beyond? *Clinical Cancer Research*. 17:6623–6631. doi:10.1158/1078-0432.CCR-11-0467.

Mccully, R.R., and J.L. Pomerantz. 2008. The protein kinase C-responsive inhibitory domain of CARD11 functions in NF-kappaB activation to regulate the association of multiple signaling cofactors that differentially depend on Bcl10 and MALT1 for association. *Molecular and Cellular Biology*. 28:5668–5686. doi:10.1128/MCB.00418-08.

McGee, A.W., S.R. Dakoji, O. Olsen, D.S. Bredt, W.A. Lim, and K.E. Prehoda. 2001. Structure of the SH3-guanylate kinase module from PSD-95 suggests a mechanism for regulated assembly of MAGUK scaffolding proteins. *Mol Cell*. 8:1291–1301.

Meixner, A., F. Karreth, L. Kenner, and E.F. Wagner. 2004. JunD regulates lymphocyte proliferation and T helper cell cytokine expression. *The EMBO Journal*. 23:1325–1335. doi:10.1038/sj.emboj.7600133.

Meyer, P.N., K. Fu, T.C. Greiner, L.M. Smith, J. Delabie, R.D. Gascoyne, G. Ott, A. Rosenwald, R.M. Braziel, E. Campo, J.M. Vose, G. Lenz, L.M. Staudt, W.C. Chan, and D.D. Weisenburger. 2011. Immunohistochemical methods for predicting cell of origin and survival in patients with diffuse large B-cell lymphoma treated with rituximab. *Journal of Clinical Oncology*. 29:200–207. doi:10.1200/JCO.2010.30.0368.

Moreno-Garcia, M.E., K. Sommer, H. Shinohara, A.D. Bandaranayake, T. Kurosaki, and D.J. Rawlings. 2010. MAGUK-Controlled Ubiquitination of CARMA1 Modulates Lymphocyte NF- B Activity. *Molecular and Cellular Biology*. 30:922–934. doi:10.1128/MCB.01129-09.

Motoyama, M. 2004. Positive and Negative Regulation of Nuclear Factor- B-mediated Transcription by I B- , an Inducible Nuclear Protein. *Journal of Biological Chemistry*. 280:7444–7451. doi:10.1074/jbc.M412738200.

Musti, A.M., M. Treier, and D. Bohmann. 1997. Reduced ubiquitin-dependent degradation of c-Jun after phosphorylation by MAP kinases. *Science*. 275:400–402.

Nagel, D., S. Spranger, M. Vincendeau, M. Grau, S. Raffegerst, B. Kloo, D. Hlahla, M. Neuenschwander, J.P. von Kries, K. Hadian, B. Dörken, P. Lenz, G. Lenz, D.J. Schendel, and D. Krappmann. 2012. Pharmacologic Inhibition of MALT1 Protease by Phenothiazines as a Therapeutic Approach for the Treatment of Aggressive ABC-DLBCL. *Cancer Cell*. 22:825–837. doi:10.1016/j.ccr.2012.11.002.

Neefjes, J., M.L.M. Jongsma, P. Paul, and O. Bakke. 2011. Towards a systems understanding of MHC class I and MHC class II antigen presentation. *Nat Rev Immunol*. 11:823–836. doi:10.1038/nri3084.

Newton, A.C. 1997. Regulation of protein kinase C. *Curr. Opin. Cell Biol.* 9:161–167. doi:10.1016/S0955-0674(97)80058-0.

Ngo, V., R. Davis, L. Lamy, X. Yu, H. Zhao, G. Lenz, L. Lam, S. Dave, L. Yang, and J. Powell. 2006. A loss-of-function RNA interference screen for molecular targets in cancer. *Nature*. 441:106–110.

Ngo, V.N., R.M. Young, R. Schmitz, S. Jhavar, W. Xiao, K.-H. Lim, H. Kohlhammer, W. Xu, Y. Yang, H. Zhao, A.L. Shaffer, P. Romesser, G. Wright, J. Powell, A. Rosenwald, H.K. Muller-Hermelink, G. Ott, R.D. Gascoyne, J.M. Connors, L.M. Rimsza, E. Campo, E.S. Jaffe, J. Delabie, E.B. Smeland, R.I. Fisher, R.M. Braziel, R.R. Tubbs, J.R. Cook, D.D. Weisenburger, W.C. Chan, and L.M. Staudt. 2010. Oncogenically active MYD88 mutations in human lymphoma. *Nature*. 470:115–119. doi:10.1038/nature09671.

Nishikori, M. 2005. Classical and alternative NF-κB activation pathways and their roles in lymphoid malignancies. *Journal of Clinical and Experimental Hematopathology*. 45:15–24.

Noels, H., G. van Loo, S. Hagens, V. Broeckx, R. Beyaert, P. Marynen, and M. Baens. 2007. A Novel TRAF6 binding site in MALT1 defines distinct mechanisms of NF-kappaB activation by API2middle dotMALT1 fusions. *J Biol Chem*. 282:10180–10189. doi:10.1074/jbc.M611038200.

Noguchi, K., C. Kitanaka, H. Yamana, A. Kokubu, T. Mochizuki, and Y. Kuchino. 1999. Regulation of c-Myc through phosphorylation at Ser-62 and Ser-71 by c-Jun N-terminal kinase. *J Biol Chem*. 274:32580–32587.

Nutt, S.L., and D.M. Tarlinton. 2011. Germinal center B and follicular helper T cells: siblings, cousins or just good friends? *Nat Immunol*. 131:472–477. doi:10.1038/ni.2019.

O'garra, A., R. Chang, and N. Go. 1992. Ly-1 B (B-1) cells are the main source of B cell-derived interleukin 10. *European journal of …*.

Oeckinghaus, A., E. Wegener, V. Welteke, U. Ferch, S.Ç. Arslan, J. Ruland, C. Scheidereit, and D. Krappmann. 2007. Malt1 ubiquitination triggers NF-κB signaling upon T-cell activation. *The EMBO Journal*. 26:4634–4645. doi:10.1038/sj.emboj.7601897.

Ohkubo, Y., M. Arima, E. Arguni, S. Okada, K. Yamashita, S. Asari, S. Obata, A. Sakamoto, M. Hatano, J. O-Wang, M. Ebara, H. Saisho, and T. Tokuhisa. 2005. A role for c-fos/activator protein 1 in B lymphocyte terminal differentiation. *J Immunol*. 174:7703–7710.

Oracki, S.A., J.A. Walker, M.L. Hibbs, L.M. Corcoran, and D.M. Tarlinton. 2010. Plasma cell development and survival. *Immunological Reviews*. 237:140–159. doi:10.1111/j.1600-065X.2010.00940.x.

Ottersbach, K., A. Smith, A. Wood, and B. GÃ ttgens. 2010. Ontogeny of haematopoiesis:

recent advances and open questions. *British Journal of Haematology*. 148:343–355. doi:10.1111/j.1365-2141.2009.07953.x.

Pacifico, F., and A. Leonardi. 2006. NF-kappaB in solid tumors. *Biochem Pharmacol*. 72:1142–1152. doi:10.1016/j.bcp.2006.07.032.

Packham, G. 2008. The role of NF-kappaB in lymphoid malignancies. *British Journal of Haematology*. 143:3–15. doi:10.1111/j.1365-2141.2008.07284.x.

Pantelouris, E.M. 1968. Absence of thymus in a mouse mutant. *Nature*. 217:370–371.

Pao, L.I., S.J. Famiglietti, and J.C. Cambier. 1998. Asymmetrical phosphorylation and function of immunoreceptor tyrosine-based activation motif tyrosines in B cell antigen receptor signal transduction. *J Immunol*. 160:3305–3314.

Pasqualucci, L., M. Compagno, J. Houldsworth, S. Monti, A. Grunn, S.V. Nandula, J.C. Aster, V.V. Murty, M.A. Shipp, and R. Dalla-Favera. 2006. Inactivation of the PRDM1/BLIMP1 gene in diffuse large B cell lymphoma. *J Exp Med*. 203:311–317. doi:10.1084/jem.20052204.

Pechloff, K., J. Holch, U. Ferch, M. Schweneker, K. Brunner, M. Kremer, T. Sparwasser, L. Quintanilla-Martinez, U. Zimber-Strobl, B. Streubel, A. Gewies, C. Peschel, and J. Ruland. 2010. The fusion kinase ITK-SYK mimics a T cell receptor signal and drives oncogenesis in conditional mouse models of peripheral T cell lymphoma. *Journal of Experimental Medicine*. 207:1031–1044. doi:10.1084/jem.20092042.

Peled, J.U., F.L. Kuang, M.D. Iglesias-Ussel, S. Roa, S.L. Kalis, M.F. Goodman, and M.D. Scharff. 2008. The Biochemistry of Somatic Hypermutation. *Annu Rev Immunol*. 26:481–511. doi:10.1146/annurev.immunol.26.021607.090236.

Perkins, N.D. 2012. The diverse and complex roles of NF-κB subunits in cancer. *Nat Rev Cancer*. doi:10.1038/nrc3204.

Phan, R.T., and R. Dalla-Favera. 2004. The BCL6 proto-oncogene suppresses p53 expression in germinal-centre B cells. *Nature*. 432:635–639. doi:10.1038/nature03147.

Pillai, S., and A. Cariappa. 2009. The follicular versus marginal zone B lymphocyte cell fate decision. *Nat Rev Immunol*. 9:767–777. doi:10.1038/nri2656.

Plantevin Krenitsky, V., L. Nadolny, M. Delgado, L. Ayala, S.S. Clareen, R. Hilgraf, R. Albers, S. Hegde, N. D'Sidocky, J. Sapienza, J. Wright, M. McCarrick, S. Bahmanyar, P. Chamberlain, S.L. Delker, J. Muir, D. Giegel, L. Xu, M. Celeridad, J. Lachowitzer, B. Bennett, M. Moghaddam, O. Khatsenko, J. Katz, R. Fan, A. Bai, Y. Tang, M.A. Shirley, B. Benish, T. Bodine, K. Blease, H. Raymon, B.E. Cathers, and Y. Satoh. 2012. Discovery of CC-930, an orally active anti-fibrotic JNK inhibitor. *Bioorg. Med. Chem. Lett.* 22:1433–1438. doi:10.1016/j.bmcl.2011.12.027.

Pulverer, B.J., J.M. Kyriakis, J. Avruch, E. Nikolakaki, and J.R. Woodgett. 1991. Phosphorylation of c-jun mediated by MAP kinases. *Nature*. 353:670–674. doi:10.1038/353670a0.

Ranuncolo, S.M., J.M. Polo, and A. Melnick. 2008. BCL6 represses CHEK1 and suppresses DNA damage pathways in normal and malignant B-cells. *Blood Cells, Molecules, and Diseases*. 41:95–99. doi:10.1016/j.bcmd.2008.02.003.

Ranuncolo, S.M., J.M. Polo, J. Dierov, M. Singer, T. Kuo, J. Greally, R. Green, M. Carroll, and A. Melnick. 2007. Bcl-6 mediates the germinal center B cell phenotype and lymphomagenesis through transcriptional repression of the DNA-damage sensor ATR. *Nat Immunol*. 8:705–714. doi:10.1038/ni1478.

Rauert-Wunderlich, H., D. Siegmund, E. Maier, T. Giner, R.C. Bargou, H. Wajant, and T. Stühmer. 2013. The IKK inhibitor Bay 11-7082 induces cell death independent from inhibition of activation of NFκB transcription factors. *PLoS ONE*. 8:e59292. doi:10.1371/journal.pone.0059292.

Rawlings, D.J., A.M. Scharenberg, H. Park, M.I. Wahl, S. Lin, R.M. Kato, A.C. Fluckiger, O.N. Witte, and J.P. Kinet. 1996. Activation of BTK by a phosphorylation mechanism initiated by SRC family kinases. *Science*. 271:822–825.

Rebeaud, F., S. Hailfinger, A. Posevitz-Fejfar, M. Tapernoux, R. Moser, D. Rueda, O. Gaide, M. Guzzardi, E.M. Iancu, N. Rufer, N. Fasel, and M. Thome. 2008. The proteolytic activity of the paracaspase MALT1 is key in T cell activation. *Nat Immunol*. 9:272–281. doi:10.1038/ni1568.

Rickert, R.C., J. Jellusova, and A.V. Miletic. 2011. Signaling by the tumor necrosis factor receptor superfamily in B-cell biology and disease. *Immunological Reviews*. 244:115–133. doi:10.1111/j.1600-065X.2011.01067.x.

Rickert, R.C., J. Roes, and K. Rajewsky. 1997. B lymphocyte-specific, Cre-mediated mutagenesis in mice. *Nucleic Acids Research*. 25:1317–1318.

Rolink AG, M.S.B.G.C.R. 2006. Early lymphocyte development in bone marrow and thymus. 1–6.

Roos, J. 2005. STIM1, an essential and conserved component of store-operated Ca2+ channel function. *The Journal of Cell Biology*. 169:435–445. doi:10.1083/jcb.200502019.

Roose, J.P., M. Mollenauer, V.A. Gupta, J. Stone, and A. Weiss. 2005. A diacylglycerol-protein kinase C-RasGRP1 pathway directs Ras activation upon antigen receptor stimulation of T cells. *Molecular and Cellular Biology*. 25:4426–4441. doi:10.1128/MCB.25.11.4426–4441.2005.

Rosenwald, A., G. Wright, K. Leroy, X. Yu, P. Gaulard, R.D. Gascoyne, W.C. Chan, T. Zhao, C. Haioun, T.C. Greiner, D.D. Weisenburger, J.C. Lynch, J. Vose, J.O. Armitage, E.B. Smeland, S. Kvaloy, H. Holte, J. Delabie, E. Campo, E. Montserrat, A. López-Guillermo, G. Ott, H.K. Muller-Hermelink, J.M. Connors, R. Braziel, T.M. Grogan, R.I. Fisher, T.P. Miller, M. LeBlanc, M. Chiorazzi, H. Zhao, L. Yang, J. Powell, W.H. Wilson, E.S. Jaffe, R. Simon, R.D. Klausner, and L.M. Staudt. 2003. Molecular diagnosis of primary mediastinal B cell lymphoma identifies a clinically favorable subgroup of diffuse large B cell lymphoma related to Hodgkin lymphoma. *J Exp Med*. 198:851–862. doi:10.1084/jem.20031074.

Rosenwald, A., G. Wright, W.C. Chan, J.M. Connors, E. Campo, R.I. Fisher, R.D. Gascoyne, H.K. Muller-Hermelink, E.B. Smeland, J.M. Giltnane, E.M. Hurt, H. Zhao, L. Averett, L. Yang, W.H. Wilson, E.S. Jaffe, R. Simon, R.D. Klausner, J. Powell, P.L. Duffey, D.L. Longo, T.C. Greiner, D.D. Weisenburger, W.G. Sanger, B.J. Dave, J.C. Lynch, J. Vose, J.O. Armitage, E. Montserrat, A. López-Guillermo, T.M. Grogan, T.P. Miller, M. LeBlanc, G. Ott, S. Kvaloy, J. Delabie, H. Holte, P. Krajci, T. Stokke, L.M. Staudt, Lymphoma/Leukemia Molecular Profiling Project. 2002. The use of molecular profiling to predict survival after chemotherapy for diffuse large-B-cell lymphoma. *N Engl J Med*. 346:1937–1947. doi:10.1056/NEJMoa012914.

Rothstein, T.L. 2002. Cutting Edge Commentary: Two B-1 or Not To Be One. *The Journal of Immunology*.

Rowley, R.B., A.L. Burkhardt, H.G. Chao, G.R. Matsueda, and J.B. Bolen. 1995. Syk protein-tyrosine kinase is regulated by tyrosine-phosphorylated Ig alpha/Ig beta immunoreceptor tyrosine activation motif binding and autophosphorylation. *J Biol Chem*. 270:11590–11594.

Ruland, J., G.S. Duncan, A. Elia, I. del Barco Barrantes, L. Nguyen, S. Plyte, D.G. Millar, D. Bouchard, A. Wakeham, P.S. Ohashi, and T.W. Mak. 2001. Bcl10 is a positive regulator of antigen receptor-induced activation of NF-kappaB and neural tube closure. *Cell*. 104:33–42.

Ruland, J., G.S. Duncan, A. Wakeham, and T.W. Mak. 2003. Differential requirement for Malt1 in T and B cell antigen receptor signaling. *Immunity*. 19:749–758.

Saito, M., J. Gao, K. Basso, Y. Kitagawa, P.M. Smith, G. Bhagat, A. Pernis, L. Pasqualucci, and R. Dalla-Favera. 2007. A Signaling Pathway Mediating Downregulation of BCL6 in Germinal Center B Cells Is Blocked by BCL6 Gene Alterations in B Cell Lymphoma. *Cancer Cell*. 12:280–292. doi:10.1016/j.ccr.2007.08.011.

Saito, M., U. Novak, E. Piovan, K. Basso, P. Sumazin, C. Schneider, M. Crespo, Q. Shen, G. Bhagat, A. Califano, A. Chadburn, L. Pasqualucci, and R. Dalla-Favera. 2009. BCL6 suppression of BCL2 via Miz1 and its disruption in diffuse large B cell lymphoma. *Proceedings of the National Academy of Sciences*. 106:11294–11299. doi:10.1073/pnas.0903854106.

Salim, K., M.J. Bottomley, E. Querfurth, M.J. Zvelebil, I. Gout, R. Scaife, R.L. Margolis, R. Gigg, C.I. Smith, P.C. Driscoll, M.D. Waterfield, and G. Panayotou. 1996. Distinct specificity in the recognition of phosphoinositides by the pleckstrin homology domains of dynamin and Bruton's tyrosine kinase. *The EMBO Journal*. 15:6241–6250.

Sancak, Y., C.C. Thoreen, T.R. Peterson, R.A. Lindquist, S.A. Kang, E. Spooner, S.A. Carr, and D.M. Sabatini. 2007. PRAS40 Is an Insulin-Regulated Inhibitor of the mTORC1 Protein Kinase. *Mol Cell*. 25:903–915. doi:10.1016/j.molcel.2007.03.003.

Sanderson, R.D., P. Lalor, and M. Bernfield. 1989. B lymphocytes express and lose syndecan at specific stages of differentiation. *Cell Regul.* 1:27–35.

Sarma, J.V., and P.A. Ward. 2010. The complement system. *Cell Tissue Res*. 343:227–235. doi:10.1007/s00441-010-1034-0.

Sarma, J.V., and P.A. Ward. 2011. The complement system. *Cell Tissue Res*. 343:227–235. doi:10.1007/s00441-010-1034-0.

Sasaki, Y., E. Derudder, E. Hobeika, R. Pelanda, M. Reth, K. Rajewsky, and M. Schmidt-Supprian. 2006. Canonical NF-kappaB activity, dispensable for B cell development, replaces BAFF-receptor signals and promotes B cell proliferation upon activation. *Immunity*. 24:729–739. doi:10.1016/j.immuni.2006.04.005.

Sato, S., H. Sanjo, K. Takeda, J. Ninomiya-Tsuji, M. Yamamoto, T. Kawai, K. Matsumoto, O. Takeuchi, and S. Akira. 2005. Essential function for the kinase TAK1 in innate and adaptive immune responses. *Nat Immunol*. 6:1087–1095. doi:10.1038/ni1255.

Savage, K.J. 2006. Primary Mediastinal Large B-Cell Lymphoma. *The Oncologist*. 11:488–495. doi:10.1634/theoncologist.11-5-488.

Schaerli, P., K. Willimann, A.B. Lang, M. Lipp, P. Loetscher, and B. Moser. 2000. CXC chemokine receptor 5 expression defines follicular homing T cells with B cell helper function. *J Exp Med*. 192:1553–1562.

Schamel, W.W., and M. Reth. 2000. Monomeric and oligomeric complexes of the B cell antigen receptor. *Immunity*. 13:5–14.

Scharenberg, A.M., L.A. Humphries, and D.J. Rawlings. 2007. Calcium signalling and cell-fate choice in B cells. *Nat Rev Immunol*. 7:778–789. doi:10.1038/nri2172.

Schatz, D.G., and Y. Ji. 2011. Recombination centres and the orchestration of V(D)J recombination. *Nat Rev Immunol*. 11:251–263. doi:10.1038/nri2941.

Schreiber, M., A. Kolbus, F. Piu, A. Szabowski, U. Möhle-Steinlein, J. Tian, M. Karin, P. Angel, and E.F. Wagner. 1999. Control of cell cycle progression by c-Jun is p53 dependent. *Genes Dev*. 13:607–619.

Sciammas, R., and M.M. Davis. 2004. Modular nature of Blimp-1 in the regulation of gene expression during B cell maturation. *J Immunol*. 172:5427–5440.

Shaffer, A.L., K.-I. Lin, T.C. Kuo, X. Yu, E.M. Hurt, A. Rosenwald, J.M. Giltnane, L. Yang, H. Zhao, and K. Calame. 2002. Blimp-1 orchestrates plasma cell differentiation by extinguishing the mature B cell gene expression program. *Immunity*. 17:51–62.

Shaffer, A.L., M. Shapiro-Shelef, N.N. Iwakoshi, A.-H. Lee, S.-B. Qian, H. Zhao, X. Yu, L. Yang, B.K. Tan, A. Rosenwald, E.M. Hurt, E. Petroulakis, N. Sonenberg, J.W. Yewdell, K. Calame, L.H. Glimcher, and L.M. Staudt. 2004. XBP1, downstream of Blimp-1, expands the secretory apparatus and other organelles, and increases protein synthesis in plasma cell differentiation. *Immunity*. 21:81–93. doi:10.1016/j.immuni.2004.06.010.

Shaffer, A.L., X. Yu, Y. He, J. Boldrick, E.P. Chan, and L.M. Staudt. 2000. BCL-6 represses genes that function in lymphocyte differentiation, inflammation, and cell cycle control. *Immunity*. 13:199–212.

Shapiro-Shelef, M., and K. Calame. 2005. Regulation of plasma-cell development. *Nat Rev Immunol*. 5:230–242. doi:10.1038/nri1572.

Shaulian, E., and M. Karin. 2002. AP-1 as a regulator of cell life and death. *Nature Publishing Group*. 4:E131–6. doi:10.1038/ncb0502-e131.

Shi-Wen, X., F. Rodriguez-Pascual, S. Lamas, A. Holmes, S. Howat, J.D. Pearson, M.R. Dashwood, R.M. du Bois, C.P. Denton, C.M. Black, D.J. Abraham, and A. Leask. 2006. Constitutive ALK5-Independent c-Jun N-Terminal Kinase Activation Contributes to Endothelin-1 Overexpression in Pulmonary Fibrosis: Evidence of an Autocrine Endothelin Loop Operating through the Endothelin A and B Receptors. *Molecular and Cellular Biology*. 26:5518–5527. doi:10.1128/MCB.00625-06.

Shinohara, H., and T. Kurosaki. 2009. Comprehending the complex connection between PKCbeta, TAK1, and IKK in BCR signaling. *Immunological Reviews*. 232:300–318. doi:10.1111/j.1600-065X.2009.00836.x.

Shinohara, H., S. Maeda, H. Watarai, and T. Kurosaki. 2007. IkappaB kinase beta-induced phosphorylation of CARMA1 contributes to CARMA1 Bcl10 MALT1 complex formation in B cells. *Journal of Experimental Medicine*. 204:3285–3293. doi:10.1084/jem.20070379.

Shinohara, H., T. Yasuda, Y. Aiba, H. Sanjo, M. Hamadate, H. Watarai, H. Sakurai, and T. Kurosaki. 2005. PKC beta regulates BCR-mediated IKK activation by facilitating the interaction between TAK1 and CARMA1. *J Exp Med*. 202:1423–1431. doi:10.1084/jem.20051591.

Siebenlist, U., K. Brown, and E. Claudio. 2005. Control of lymphocyte development by nuclear factor-κB. *Nat Rev Immunol*. 5:435–445. doi:10.1038/nri1629.

Slifka, M.K., R. Antia, J.K. Whitmire, and R. Ahmed. 1998. Humoral immunity due to long-lived plasma cells. *Immunity*. 8:363–372.

Snow, A.L., W. Xiao, J.R. Stinson, W. Lu, B. Chaigne-Delalande, L. Zheng, S. Pittaluga, H.F. Matthews, R. Schmitz, S. Jhavar, S. Kuchen, L. Kardava, W. Wang, I.T. Lamborn, H. Jing, M. Raffeld, S. Moir, T.A. Fleisher, L.M. Staudt, H.C. Su, and M.J. Lenardo. 2012. Congenital B cell lymphocytosis explained by novel germline CARD11 mutations. *Journal of Experimental Medicine*. 209:2247–2261. doi:10.1084/jem.20120831.

Sommer, K., B. Guo, J. Pomerantz, A. Bandaranayake, M. Moreno-García, Y. Ovechkina, and D. Rawlings. 2005. Phosphorylation of the CARMA1 linker controls NF-[kappa] B activation. *Immunity*. 23:561–574.

Srinivasan, L., Y. Sasaki, D.P. Calado, B. Zhang, J.H. Paik, R.A. Depinho, J.L. Kutok, J.F. Kearney, K.L. Otipoby, and K. Rajewsky. 2009. PI3 Kinase Signals BCR-Dependent Mature B Cell Survival. *Cell*. 139:573–586. doi:10.1016/j.cell.2009.08.041.

Staal, J., T. Bekaert, and R. Beyaert. 2011a. Regulation of NF-κB signaling by caspases and MALT1 paracaspase. *Nature Publishing Group*. 21:40–54. doi:10.1038/cr.2010.168.

Staal, J., Y. Driege, T. Bekaert, A. Demeyer, D. Muyllaert, P. Van Damme, K. Gevaert, and R. Beyaert. 2011b. T-cell receptor-induced JNK activation requires proteolytic inactivation of CYLD by MALT1. *The EMBO Journal*. 30:1742–1752. doi:10.1038/emboj.2011.85.

Staudt, L.M. 2010. Oncogenic activation of NF-kappaB. *Cold Spring Harbor Perspectives in Biology*. 2:a000109. doi:10.1101/cshperspect.a000109.

Staudt, L.M., K. Dunleavy, J.J. Buggy, E. Hedrick, N. Lucas, and S. Pittaluga. 2011. The Bruton's tyrosine kinase (Btk) inhibitor PCI-32765 modulates chronic active BCR signaling and induces tumor regression in relapsed/refractory ABC DLBCL. *Blood (ASH Annual ….* 118:2716.

Sun, L., L. Deng, C.-K. Ea, Z.-P. Xia, and Z.J. Chen. 2004. The TRAF6 ubiquitin ligase and TAK1 kinase mediate IKK activation by BCL10 and MALT1 in T lymphocytes. *Mol Cell*. 14:289–301.

Takata, M., and T. Kurosaki. 1996. A role for Bruton's tyrosine kinase in B cell antigen receptor-mediated activation of phospholipase C-gamma 2. *J Exp Med*. 184:31–40.

Tanner, M.J., W. Hanel, S.L. Gaffen, and X. Lin. 2007. CARMA1 coiled-coil domain is involved in the oligomerization and subcellular localization of CARMA1 and is required for T cell receptor-induced NF-kappaB activation. *J Biol Chem*. 282:17141–17147. doi:10.1074/jbc.M700169200.

Tarlinton, D.M., M. McLean, and G.J. Nossal. 1995. B1 and B2 cells differ in their potential to switch immunoglobulin isotype. *Eur. J. Immunol.* 25:3388–3393. doi:10.1002/eji.1830251228.

Tavares, G.A., E.H. Panepucci, and A.T. Brunger. 2001. Structural characterization of the intramolecular interaction between the SH3 and guanylate kinase domains of PSD-95. *Mol Cell*. 8:1313–1325.

Taylor, A., J. Verhagen, K. Blaser, M. Akdis, and C.A. Akdis. 2006. Mechanisms of immune suppression by interleukin-10 and transforming growth factor-beta: the role of T regulatory cells. *Immunology*. 117:433–442. doi:10.1111/j.1365-2567.2006.02321.x.

Thome, M., J.E. Charton, C. Pelzer, and S. Hailfinger. 2010. Antigen receptor signaling to NF-kappaB via CARMA1, BCL10, and MALT1. *Cold Spring Harbor Perspectives in Biology*. 2:a003004. doi:10.1101/cshperspect.a003004.

Toker, A., and A.C. Newton. 2000. Cellular signaling: pivoting around PDK-1. *Cell*. 103:185–188.

Tolar, P., H.W. Sohn, and S.K. Pierce. 2005. The initiation of antigen-induced B cell antigen receptor signaling viewed in living cells by fluorescence resonance energy transfer. *Nat Immunol*. 6:1168–1176. doi:10.1038/ni1262.

Trøen, G., V. Nygaard, T.-K. Jenssen, I.M. Ikonomou, A. Tierens, E. Matutes, A. Gruszka-Westwood, D. Catovsky, O. Myklebost, G. Lauritzsen, E. Hovig, and J. Delabie. 2010. Constitutive Expression of the AP-1 Transcription Factors c-jun, junD, junB, and c-fos and the Marginal Zone B-Cell Transcription Factor Notch2 in Splenic Marginal Zone Lymphoma. *The Journal of Molecular Diagnostics*. 6:297–307. doi:10.1016/S1525-1578(10)60525-9.

Turner, M., P.J. Mee, P.S. Costello, O. Williams, A.A. Price, L.P. Duddy, M.T. Furlong, R.L. Geahlen, and V.L. Tybulewicz. 1995. Perinatal lethality and blocked B-cell

development in mice lacking the tyrosine kinase Syk. *Nature*. 378:298–302. doi:10.1038/378298a0.

Uehata, T., H. Iwasaki, A. Vandenbon, K. Matsushita, E. Hernandez-Cuellar, K. Kuniyoshi, T. Satoh, T. Mino, Y. Suzuki, D.M. Standley, T. Tsujimura, H. Rakugi, Y. Isaka, O. Takeuchi, and S. Akira. 2013. Malt1-Induced Cleavage of Regnase-1 in CD4+ Helper T Cells Regulates Immune Activation. *Cell*. 153:1036–1049. doi:10.1016/j.cell.2013.04.034.

van Dam, H., S. Huguier, K. Kooistra, J. Baguet, E. Vial, A.J. van der Eb, P. Herrlich, P. Angel, and M. Castellazzi. 1998. Autocrine growth and anchorage independence: two complementing Jun-controlled genetic programs of cellular transformation. *Genes Dev*. 12:1227–1239.

Verma, I.M., J.K. Stevenson, E.M. Schwarz, D. Van Antwerp, and S. Miyamoto. 1995. Rel/NF-kappa B/I kappa B family: intimate tales of association and dissociation. *Genes Dev*. 9:2723–2735.

Victora, G.D., and M.C. Nussenzweig. 2012. Germinal Centers. *Annu Rev Immunol*. 30:429–457. doi:10.1146/annurev-immunol-020711-075032.

Vig, M., A. Beck, J.M. Billingsley, A. Lis, S. Parvez, C. Peinelt, D.L. Koomoa, J. Soboloff, D.L. Gill, A. Fleig, J.-P. Kinet, and R. Penner. 2006. CRACM1 Multimers Form the Ion-Selective Pore of the CRAC Channel. *Current Biology*. 16:2073–2079. doi:10.1016/j.cub.2006.08.085.

Vinuesa, C.G., I. Sanz, and M.C. Cook. 2009. Dysregulation of germinal centres in autoimmune disease. *Nat Rev Immunol*. 9:845–857. doi:10.1038/nri2637.

Wagner, E.F., and A.R. Nebreda. 2009. Signal integration by JNK and p38 MAPK pathways in cancer development. *Nat Rev Cancer*. 9:537–549. doi:10.1038/nrc2694.

Wang, C., L. Deng, M. Hong, G.R. Akkaraju, J. Inoue, and Z.J. Chen. 2001. TAK1 is a ubiquitin-dependent kinase of MKK and IKK. *Nature*. 412:346–351. doi:10.1038/35085597.

Wang, M., Ç. Atayar, S. Rosati, A. Bosga-Bouwer, P. Kluin, and L. Visser. 2009. JNK is constitutively active in mantle cell lymphoma: cell cycle deregulation and polyploidy by JNK inhibitor SP600125. *J. Pathol.* 218:95–103. doi:10.1002/path.2521.

Wegener, E., A. Oeckinghaus, N. Papadopoulou, L. Lavitas, M. Schmidt-Supprian, U. Ferch, T.W. Mak, J. Ruland, V. Heissmeyer, and D. Krappmann. 2006. Essential Role for IκB Kinase β in Remodeling Carma1-Bcl10-Malt1 Complexes upon T Cell Activation. *Mol Cell*. 23:13–23. doi:10.1016/j.molcel.2006.05.027.

Whittier, J.R., D.F. Klein, G. Levine, and D. Weiss. 1960. Mepazine (pacatal): Clinical trial with placebo control and psychological study. *Psychopharmacologia*. 1:280–287.

Wong, S.C. 2003. Impaired germinal center formation and recall T-cell-dependent immune responses in mice lacking the costimulatory ligand B7-H2. *Blood*. 102:1381–1388. doi:10.1182/blood-2002-08-2416.

Wright, G., B. Tan, A. Rosenwald, E.H. Hurt, A. Wiestner, and L.M. Staudt. 2003. A gene expression-based method to diagnose clinically distinct subgroups of diffuse large B cell lymphoma. *Proc Natl Acad Sci USA*. 100:9991–9996. doi:10.1073/pnas.1732008100.

Wu, C.-J., and J.D. Ashwell. 2008. NEMO recognition of ubiquitinated Bcl10 is required for T cell receptor-mediated NF-kappaB activation. *Proceedings of the National Academy of Sciences*. 105:3023–3028. doi:10.1073/pnas.0712313105.

Xu, H., X. Li, D. Liu, J. Li, X. Zhang, X. Chen, S. Hou, L. Peng, C. Xu, W. Liu, L. Zhang, and H. Qi. 2013. Follicular T-helper cell recruitment governed by bystander B cells and ICOS-driven motility. *Nature*. 496:523–527. doi:10.1038/nature12058.

Xu, Y., K.W. Harder, N.D. Huntington, and M.L. Hibbs. 2005. ScienceDirect.com - Immunity - Lyn Tyrosine Kinase: Accentuating the Positive and the Negative. *Immunity*.

Xu, Z., H. Zan, E.J. Pone, T. Mai, and P. Casali. 2012. Immunoglobulin class-switch DNA recombination: induction, targeting and beyond. *Nat Rev Immunol*. 12:517–531. doi:10.1038/nri3216.

Yasuda, T., H. Sanjo, G. Pagès, Y. Kawano, H. Karasuyama, J. Pouysségur, M. Ogata, and T. Kurosaki. 2008. Erk Kinases Link Pre-B Cell Receptor Signaling to Transcriptional Events Required for Early B Cell Expansion. *Immunity*. 28:499–508. doi:10.1016/j.immuni.2008.02.015.

Zandi, E. 1998. Direct Phosphorylation of IB by IKK and IKK: Discrimination Between Free and NF-B-Bound Substrate. *Science*. 281:1360–1363. doi:10.1126/science.281.5381.1360.

Zhang, T., F. Inesta-Vaquera, M. Niepel, J. Zhang, S.B. Ficarro, T. Machleidt, T. Xie, J.A. Marto, N. Kim, T. Sim, J.D. Laughlin, H. Park, P.V. LoGrasso, M. Patricelli, T.K. Nomanbhoy, P.K. Sorger, D.R. Alessi, and N.S. Gray. 2012. Discovery of Potent and Selective Covalent Inhibitors of JNK. *Chemistry & Biology*. 19:140–154. doi:10.1016/j.chembiol.2011.11.010.

Zhang, X., E. Deriaud, X. Jiao, D. Braun, C. Leclerc, and R. Lo-Man. 2007. Type I interferons protect neonates from acute inflammation through interleukin 10-producing B cells. *Journal of Experimental Medicine*. 204:1107–1118. doi:10.1084/jem.20062013.

Zotos, D., and D.M. Tarlinton. 2012. Determining germinal centre B cell fate. *Trends in Immunology*. 33:281–288. doi:10.1016/j.it.2012.04.003.

10. DANKSAGUNG

An dieser Stelle möchte ich mich bei allen, die mich im Laufe meiner Doktorarbeit begleitet und unterstützt haben, bedanken.

Primär möchte ich meinem Betreuer und Mentor Prof. Dr. Jürgen Ruland allergrößten Dank aussprechen, weil er mir ermöglicht hat in seinem Labor zu promovieren. In dieser Zeit war er mir immer ein gutes Vorbild und ist mir in allen Situationen mit Rat und Tat zur Seite gestanden.

Gerne möchte ich mich auch bei Prof. Dr. Küster bedanken, der sich bereit erklärt hat mein Zweitgutachter zu sein.

Außerdem möchte ich allen Kollaborationspartner danken. Zum einen PD Dr. Kremer und Prof. Dr. Alexandar Tzankov, die die Untersuchung der Histologien zu übernahmen. Ebenso Annette Wolf und Prof. Dr. Georg Lenz von der Charité Berlin, die eine große Unterstützung für dieses Projekt waren.

Auch möchte ich meinen Arbeitskollegen der Arbeitsgruppe Ruland, Haas/Poeck und Jost danken für die gute Zusammenarbeit und hilfreiche Diskussionen. Besonderer Dank geht an Christoph Vahl, Christina Groß, Monica Yabal und Susanne Roth, die mir beim Korrekturlesen dieser Arbeit geholfen haben.

Zu guter Letzt, möchte ich meiner Familie und Freunden und Christoph für ihre Liebe, Geduld und Aufmerksamkeit danken. Marc Schmidt-Supprian danke ich für seine langjährige Unterstützung und Motivation.

11. CURRICULUM VITAE

Persönliche Daten

Nathalie Knies
Thalkirchner Straße 74, 80337 München
Telefon: 017662662960
E-Mail: nathalie.knies@googlemail.com

Geboren am 24.03.1986 in Tokio, ledig
Deutsche Staatsbürgerschaft

Studium

01/2010 – 07/2014 **Promotion experimentelle Medizin, Technische Universität München**

- Klinikum rechts der Isar, Institut für klinische Chemie und Pathobiochemie, Prof. Dr. Ruland
- Titel: „Consequences of CARD11(L225LI) expression in murine B lymphocytes *in vivo"*

10/2007 – 12/2009 **Master Genetik und Molekularbiologie, Paris Lodron Universität Salzburg**

- Schwerpunktfächer: Genetik und Molekularbiologie
- **04/2009** - **12/2009** Masterarbeit
  Max Planck Institut für Biochemie Martinsried, Dr. Schmidt-Supprian
  Titel: „Generation of B cell-specific Cre-transgenic mice by BAC recombineering"

10/2005 – 06/2008 **Bachelor Genetik, Paris Lodron Universität Salzburg**

- Schwerpunktfach: Genetik
- **08/2007 – 09/2007** Bachelorarbeit
  Helmholtz Zentrum München, PD. Dr. Thalhammer
  Titel: "Virtual reaction chamber PCR optimization"

09/1995 – 07/2005 **Abitur, Kurfürst Maximilian Gymnasium Burghausen**

- Leistungskurse: Mathematik, Französisch

Publikationen

- **Knies, N**., Wolf, A., Brunner, K., Kremer, M., Lenz G., & Ruland, J. (2013). Genetically enforced CARD11 / BCL10 / MALT1 signaling drives lethal B lymphoproliferation via cooperative NF-κB and JNK activation*. Manuskript eingereicht.*
- Yabal, M., Müller, N., Adler, H., **Knies, N**., Thomas, C., Damgaard, R., et al. (2013). Deregulated TNF signaling in the absence of XIAP drives RIP3-dependent inflammasome activation. *Cell reports, 7*(6).
- Vahl, J. C., Heger, K., **Knies, N**., Hein, M. Y., Boon, L., Yagita, H., et al. (2013). NKT cell-TCR expression activates conventional T cells in vivo, but is largely dispensable for mature NKT cell biology. *PLoS Biology*, *11*(6).